

ERCOFTAC

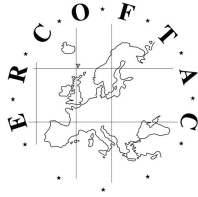
European Research Community
On Flow, Turbulence And Combustion

16th ERCOFTAC SIG 33 Workshop

Progress in Flow Instability, Transition and Control

Cagliari, Italy, June 30 - July 2, 2025





16th ERCOFTAC SIG 33 Workshop

Progress in Flow Instability, Transition and Control

Cagliari, Italy, June 30 – July 2, 2025

Organisers:

Pier Giuseppe Ledda, Giorgio Querzoli (UNICA)
Javier Sierra Ausin (ONERA)
Franco Auteri (Politecnico di Milano)
Flavio Giannetti (Università di Salerno)
Ardeشير Hanifi (KTH)



Con il patrocinio dell'Università
degli Studi di Cagliari



List of participants

Name		Affiliation	Email
Laura Denisa	Antonuzzi	Università di Salerno	lantonuzzi@unisa.it
Omid	Ashtari	EPFL	omid.ashtari@epfl.ch
Franco	Auteri	Politecnico di Milano	franco.auteri@polimi.it
Rama	Ayoub	KAUST	rama.ayoub@kaust.edu.sa
Maria Grazia	Badas	Università degli Studi di Cagliari	mgbadas@unica.it
Victor	Ballester	Imperial College London	vb824@ic.ac.uk
Hans Peter	Barth	German Aerospace Center	peter.barth@dlr.de
Pierre	Beck	EPFL	pierre.beck@epfl.ch
Riccardo	Bertoncello	Politecnico di Milano	riccardo.bertoncello@polimi.it
Daniel	Bodony	University of Illinois Urbana-Champaign	bodony@illinois.edu
Pietro Carlo	Boldini	Delft University of Technology	p.c.boldini@tudelft.nl
Luca	Boscagli	Imperial College London	l.boscagli@imperial.ac.uk
Clément	Caillaud	CEA-CESTA	clement.caillaud@cea.fr
Yifu	Chen	TU Delft	Y.Chen-20@tudelft.nl
Alessandro	Chiarini	Politecnico di Milano	alessandro.chiarini@polimi.it
Paola	Cinnella	Institut Jean Le Rond D'Alembert	paola.cinnella@sorbonne-universite.fr
Nicola	Ciola	Politecnico di Bari	n.ciola@phd.poliba.it
Simone	Cruciani	ISAE-SUPAERO	simone.cruciani@isae-supaero.fr
Simon	Demange	TU Berlin	s.demange@tu-berlin.de
Nicolas	d'Éprémesnil	CEA-CESTA	nicolas.du-val-d-epremesnil@ensma.fr
Aditya	Desai	CNRS-LISN	aditya.desai@lisn.fr
Savyaraj	Deshmukh	EPFL	savyaraj.deshmukh@epfl.ch
David	Fabre	IMFT, University of Toulouse	david.fabre@imft.fr
Marcello Augusto	Faraco de Medeiros	Universidade de São Paulo	marcello@sc.usp.br
Michel	Fournié	ISAE-SUPAERO	michel.fournie@isae-supaero.fr
Alessandro	Franchini	Arts et Metiers ParisTech	alessandro.franchini@ensam.eu
Lukas Maximilian	Fuchs	TU Berlin	l.fuchs@tu-berlin.de
François	Gallaire	EPFL	francois.gallaire@epfl.ch
Giovanni	Gelmetti	ISAE-SUPAERO	gelmetti.giovanni02@gmail.com
Niccolo	Geracitano	Gran Sasso Science Institute	niccolo.geracitano@gssi.it
Artur	Gesla	Sorbonne Université	agesla09e@gmail.com
Flavio	Giannetti	Università di Salerno	fgiannetti@unisa.it
Anton	Glazkov	KAUST	anton.glazkov@kaust.edu.sa
George	Haller	ETHZ	georgehaller@ethz.ch
Ardeshir	Hanifi	FLOW, KTH	hanifi@kth.se
Jiaao	Hao	The Hong Kong Polytechnic University	jiaao.hao@polyu.edu.hk
Stefan	Hein	German Aerospace Center	stefan.hein@dlr.de
Dan	Henningson	FLOW, KTH	henning@kth.se
Kacper	Janczuk	Imperial College London	koj19@ic.ac.uk
Peter	Jordan	Uni. Poitiers	peter.jordan@univ-poitiers.fr
Antoine	Jouin	ONERA	antoine.jouin@onera.fr
Johann Simon	Kern	DynFluid, Arts et Metiers Institute of Technology	johann-simon.kern@ensam.eu
Markus	Kloker	IAG, University of Stuttgart	markus.kloker@iag.uni-stuttgart.de
Marios	Kotsonios	TU Delft	m.kotsonis@tudelft.nl
Pier Giuseppe	Ledda	Università degli Studi di Cagliari	PierGiuseppe.Ledda@unica.it
Lutz	Lesshafft	LadHyx	lutz.lesshafft@polytechnique.edu
Paolo	Luchini	Università di Salerno	luchini@unisa.it
Luca	Magri	Imperial College London	l.magri@imperial.ac.uk
Igor	Maia	Instituto Tecnológico de Aeronáutica	igoriam@ita.br
Matteo	Mancinelli	Università Roma Tre	matteo.mancinelli@uniroma3.it
Riccardo	Maranelli	ONERA/CNAM	riccardo.maranelli@onera.fr
Nicolas	Matheou	Imperial College London	nm1420@ic.ac.uk

Mohammad	Moniripiri	FLOW, KTH	momp@kth.se
Aimee	Morgans	Imperial College London	a.morgans@imperial.ac.uk
Jens S.	Müller	TU Berlin	jens.mueller@tu-berlin.de
Pierre	Penet	ONERA-LadHyx	pierre.penet@polytechnique.edu
Victoria	Prieto	ONERA	vmprieturueda@gmail.com
Giorgio	Querzoli	Università degli Studi di Cagliari	querzoli@unica.it
Cédric	Raibaud	University of Orléans	cedric.raibaud@univ-orleans.fr
Georgios	Rigas	Imperial College London	g.rigas@imperial.ac.uk
Jean-Clément	Ringebach	EPFL	jean-clement.ringebach@epfl.ch
Ulrich	Rist	IAG, University of Stuttgart	ulrich.rist@iag.uni-stuttgart.de
Aliénor	Rivière	EPFL	alienor.riviere@epfl.ch
Jean-Christophe	Robinet	DynFluid, Arts et Metiers Institute of Technology	Jean-Christophe.Robinet@ensam.eu
Daniel	Rodríguez	Universidad Politécnica de Madrid	daniel.rodriguez@upm.es
Taraneh	Sayadi	Conservatoire National Arts et Métiers	taraneh.sayadi@lecnam.net
Peter J.	Schmid	KAUST	peter.schmid@kaust.edu.sa
Oliver	Schmidt	UC San Diego	oschmidt@ucsd.edu
Tobias	Schneider	EPFL	Tobias.schneider@epfl.ch
Javier	Sierra-Ausin	ONERA	javier.sierra_ausin@onera.fr
Ziming	Song	The Hong Kong Polytechnic University	ziming.song@connect.polyu.hk
Antonios-Lykourgos	Synodinos	TU Delft	a.l.synodinos@tudelft.nl
Donato	Variale	Politecnico di Bari	d.variale@phd.poliba.it
Yongxiang	Wu	IAG, University of Stuttgart	yongxiang.wu@iag.uni-stuttgart.de
Tian	Yang	EPFL	tian.yang@epfl.ch
Eunok	Yim	EPFL	eunok.yim@epfl.ch
Zhenyang	Yuan	FLOW, KTH	zhenyang@kth.se
Usama Muhammad	Zahid	University of Genova	usama.muhammad.zahid@edu.unige.it
Zheng	Zheng	EPFL	zheng.zheng@epfl.ch

16TH ERCOFATC SIG33 WORKSHOP

Progress in Flow Instability, Transition and Control

June 30- July 2, 2025

Cagliari, Sardinia, Italy

Monday, June 30			
08:30		Registration	
08:45		Welcome	
09:00	Peter Schmid	Quantitative analysis of fluid systems - tools and approaches	Chair: D. Henningson
09:45	Anton Glazkov	An acceleration technique for modal flow analysis	
10:05	Daniel Rodriguez	A time-frequency mode decomposition for the analysis of non-stationary separated flow	
10:25	Simon Demange	Gradient-augmented Bayesian shape optimization for flow instability control using linearized Navier-Stokes models	
10:45	Aditya Desai	Reduced order modeling and control of a fluidic pinball wake: An experimental investigation	
11:05	coffee		
11:25	Jens S. Müller	Linear stability and shape sensitivity analysis with a linearized turbulence model for shape optimization	Chair: G. Rigas
11:45	Yifu Chen	Stabilization of stationary crossflow instability by wall cooling	
12:05	Mohammad Moniripiri	Direct numerical simulation of the effects of a smooth surface hump on instabilities and transition in swept-wing boundary layers	
12:25	Yongxiang Wu	Control of streak-induced laminar-turbulent transition by a crossbar	
12:45	Victoria Prieto	Impact of distributed roughness on instabilities in boundary layers under pressure gradient	
13:05	Lunch		
14:35	George Haller	Modeling nonlinear dynamics from data	Chair: T. Sayadi
15:20	Oliver Schmidt	Predicting Complex Flows via Space-Time POD: A Data-Driven Forecasting Approach	
15:40	Rama Ayoub	A family of physics-constrained data-driven quadratic roms	
16:00	Coffee		
16:20	Jean-Clement Ringenbach	Tracking invariant solutions of rotating magneto-hydrodynamics in a channel geometry	Chair: F. Gallaire
16:40	Artur Gesla	From annular cavity to rotor-stator flow: nonlinear dynamics of axisymmetric rolls	
17:00	Pierre Beck	The induced latent dynamics of an autoencoder	
19:00	Reception		
Tuesday, July 1			
08:30	Paola Cinnella	Learning transition from data with high-fidelity simulations and machine learning	Chair: J.-C. Robinet
09:15	Luca Boscagli	Transition control of hypersonic boundary layer with spanwise non-uniform surface temperature	
09:35	Ziming Song	Transition mechanism of shock-wave/boundary-layer interaction at Mach 4	
09:55	Clément Caillaud	Resonant waves in transitional hypersonic separated flows	
10:15	Nicolas d'Eprémesnil	Moderate nose bluntness effects on transition instabilities: a resolvent analysis	
10:35	Coffee		
10:55	Javier Sierra	Interplay between transonic buffeting and flutter	Chair: P. Jordan
11:15	Laura Antonuzzi	An experimental investigation of the installation effects of a flat plate on screech generation	
11:35	Jean-Christophe Robinet	Instabilities in subsonic installed jet	
11:55	Zhenyang Yuan	Sensitivity of impinging jet noise to flow conditions inside the nozzle	
12:15	Matteo Mancinelli	Experimental control of jet-surface interaction noise	
12:35	Riccardo Maranelli	Ensemble variational-based optimization for resolvent analysis	
12:55	Lunch		

14:25	Daniel Bodony	Simulation and physics-based modeling for controlling shock-laden flows	Chair: A. Morgans
15:10	Lukas Maximilian Fuchs	Linear Modeling and Control of Standing-Wave Low-Frequency Dynamics of a Turbulent Separation Bubble	
15:30	Kacper Janczuk	Slow active control of road vehicle wakes: a strategy for drag reduction in varying flow conditions	
15:50	Cédric Raibaud	Sweeping jets actuators for flow separation control: characterisation and application on a canonical ramp	
16:10	Antonios-Lykourgos Synodinos	Effect of base flow modifications on the growth of instabilities in laminar channel flows	
16:30	Social event		
Wedensda, July 2			
09:00	Alessandro Franchini	Global stability analysis of turbulent screeching jets via automatic differentiation	Chair: L. Lesshaft
09:20	Pierre Penet	Perturbed eddy-viscosity approach in resolvent analysis of a turbulent boundary layer	
09:40	Antoine Jouin	Resolvent stability analysis of turbulent mean flows: an application to aeroacoustics	
10:00	Francois Gallaire	Noise-induced transitions after a steady symmetry-breaking bifurcation: the case of the sudden expansion	
10:20	David Fabre	Is the transition to unsteadiness in strongly convective wakes and jets an artefact of boundary conditions?	
10:40	Edouard Boujo	Imperfect bifurcations in a laminar 3-D bluff body wake: effect of yaw and pitch	
11:00	Coffee		
11:20	Igor Mala	Low-frequency unsteadiness in rotating plane Couette flow	Chair: P. Luchini
11:40	Simon Kern	Stability of large-amplitude pulsatile flow in a torus	
12:00	Eunok Yim	Stability of turbine draft tube vortex	
12:20	Nicola Ciola	Detuned streak instabilities originate large-scale flows in transitional channel	
12:40	Simone Cruciani	Stability of the flow past a flexible cylinder	
13:00	Lunch		
14:30	Pietro Carlo Boldini	Widom-line effect on the boundary-layer transition with a highly non-ideal fluid	Chair: M. Kotsonis
14:50	Víctor Ballester Ribó	Flow transition over gaps	
15:10	Marcello Medeiros	A fast and accurate method to simulate the effect of a bump on a TS wave	
15:30	Hans Peter Barth	Crossflow-Dominated Laminar-Turbulent Transition Downstream of an Isolated Roughness Element of Small Height	
15:50	Riccardo Bertoincello	Optimal perturbations in a Blasius boundary layer	
16:10	Coffee		
16:10	Pier Giuseppe Ledda	Linear stability analysis of freely falling annular disks	Chair: S.Hein
16:30	Usama Muhammad Zahid	Interface stability of a ferrofluid coated channel flow subject to collinear magnetic field	
16:50	Aliénor Rivière	Competition between deformation and drift in uniaxial straining flows	
17:10	Niccolò Geracitano	Stability of Quantum Fluid Wakes	
17:30	Closing		

QUANTITATIVE ANALYSIS OF FLUID SYSTEM – TOOLS AND APPROACHES

Peter J. Schmid¹

¹Department of Mechanical Engineering, King Abdullah University of Science and Technology (KAUST), Saudi Arabia

Numerical simulations of multiphysics and multiscale fluid systems have reached an impressive level of maturity and precision and have complemented an equally impressive development of high-resolution experimental techniques. In light of these new capabilities, the analysis of complex fluid systems requires a commensurate level of sophistication to detect and extract key mechanisms responsible for the bulk of mass, momentum and energy transport. In this talk, we will introduce a set of tools that venture beyond the common standards to model intrinsic fluid behavior and that lay the foundation for optimization, control, and a reduced description of essential subprocesses. Both model-based and data-driven techniques will be covered. Transfer operators [1] (see figure 1 for an example from regime-switching Rayleigh-Bénard convection), enhanced autoencoders [2], agent-based optimization, and sequential compression schemes [3] will be demonstrated on a range of fluid applications.

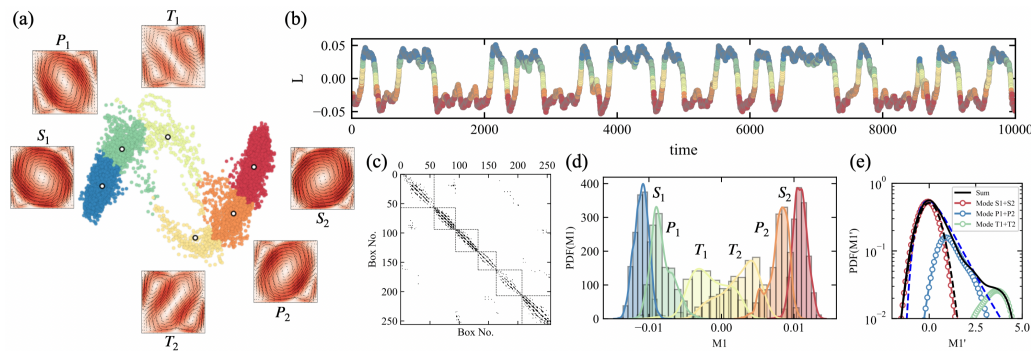


FIGURE 1. Flow analysis of regime-switching in Rayleigh-Bénard convection using transfer operators and graph-clustering techniques.

References

- [1] R. Yang, and P. J. Schmid. Complex-network modeling of reversal events in turbulent thermal convection. *J. Fluid Mech.*, 1011:A30, 2025.
- [2] P. Gupta, T. Sayadi, D. Sipp, P. J. Schmid, and G. Rigas. Mori-Zwanzig latent-space Koopman closure for nonlinear autoencoders. *Proc. Roy. Soc. A*, 481:20240259, 2025.
- [3] A. Glazkov, and P. J. Schmid. Dynamic-preserving compression for modal flow analysis. *J. Fluid Mech.*, 1001:A48, 2024.

AN ACCELERATION TECHNIQUE FOR MODAL FLOW ANALYSIS

Anton Glazkov¹, Bhargav Mantravadi¹, Peter Schmid¹

¹*Department of Mechanical Engineering, Division of Physical Sciences and Engineering (PSE), King Abdullah University of Science and Technology (KAUST), Thuwal 23955, Saudi Arabia*

Dynamics-rich, large-scale flows are becoming increasingly common and important in engineering and scientific applications. This makes them prime candidates for in-depth analysis, but a key difficulty in achieving this is that common algorithms reach the limits of their performance at scales that are a few orders of magnitude below realistic resolutions. Despite this, these flows tend to be structure-sparse, and so not all degrees of freedom are required to extract and reproduce all of the underlying information. For this reason, the information contained within the flow may be considered to be compressive, and so a strategy that is able to compress the spatial information implicitly stored within the experimental or numerical snapshots, while minimally distorting the temporal relationships in the snapshot sequence, would be of great practical use.

In this work [1], we borrow approaches from locality-sensitive hashing, which we apply to a random sampling problem applied to the snapshot vectors. A rigorous mathematical foundation for this arises from the Johnson-Lindenstrauss lemma [2], which determines a user-selectable distortion factor between any two snapshots in a sequence in compressed space. This enforces a dynamics-preserving relationship on the temporal trajectory in phase space, thus maintaining the temporal dynamics. Work by Ailon and Chazelle [3] in the form of the Fast Johnson Lindenstrauss Transform is integrated into this method to create a flexible and high-performance algorithm for a range of practical problems.

To demonstrate the utility of this technique, we present two cases. The first case is a model flow through a linear representation of a turbomachinery compressor cascade, and the second is a Rayleigh-Bénard convection in a spherical shell, for super-critical Rayleigh numbers. In these cases, we achieve compression rates of over $12\times$, with fewer than 8% of degrees of freedom retained, while maintaining distortion factors below 1%, and achieving speed-ups of over $15\times$ relative to uncompressed snapshot sequences.

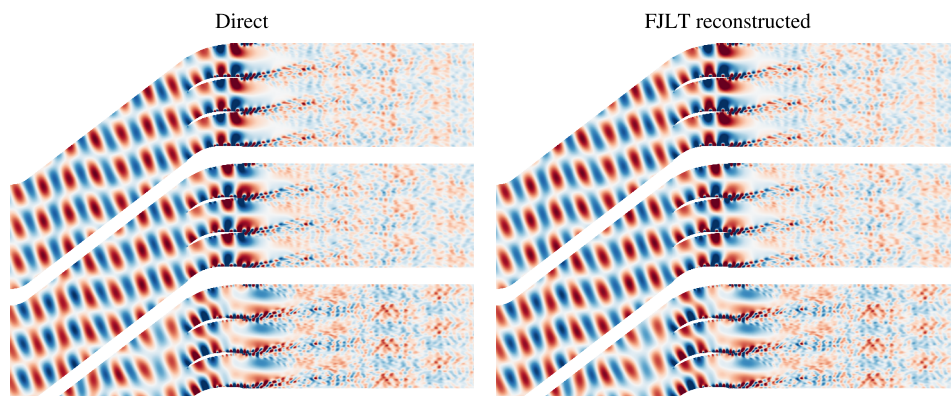


FIGURE 1. Leading POD modes for a linear blade cascade computed with unmodified and FJLT-compressed snapshot sequences. The resulting modes are visualised for the horizontal flow velocity component.

References

- [1] A. Glazkov and P. J. Schmid. Dynamics-preserving compression for modal flow analysis. *Journal of Fluid Mechanics*, 1001:A48, 2024.
- [2] W.B. Johnson and J. Lindenstrauss. Extensions of Lipschitz mappings into a Hilbert space. *Contemp. Math.*, 26:189–206, 1984.
- [3] N. Ailon and B. Chazelle. The fast Johnson-Lindenstrauss transform and approximate nearest neighbors. *SIAM J. Comput.*, 39(1):302–322, 2009.

A TIME-FREQUENCY MODE DECOMPOSITION FOR THE ANALYSIS OF NON-STATIONARY SEPARATED FLOW

Himpu Marbona¹, Daniel Rodríguez^{1,†}, Alejandro Martínez-Cava¹, Eusebio Valero¹

¹ School of Aeronautics (ETSIAE/UPM), Universidad Politécnica de Madrid, Spain

[†] daniel.rodriquez@upm.es

Understanding the physical processes underlying the dynamics of the separated flow and its reattachment is a crucial step in improving the aerodynamic efficiency. Popular mode decomposition techniques in fluid dynamics like POD, SPOD and DMD have demonstrated their potential in extracting large-scale dynamic phenomena when the underlying dynamics are stationary, but are not well suited to accurately decompose non-stationary or transient phenomena in an interpretable manner. Recently, a time-frequency approach has been proposed to effectively decompose non-stationary phenomena [1]. Variational Mode Decomposition (VMD) decomposes dynamic signals into amplitude-modulated and frequency-modulated modes by solving a variational optimization problem that minimizes the resulting bandwidth associated to each signal component. Its application to non-stationary flows has demonstrated superior modelling capabilities compared to existing methods [2]: the ability of each mode to recover dynamics contained in bandwidths rather than discrete frequencies adapts to the nature of non-stationary dynamics better than DMD, while the lack of imposed orthogonality in the modal spatial structures is aligned with the non-normality of the Navier-Stokes equations. However, the method was found to be sensitive to user-defined input parameters and small-scale noise, and does not explicitly ensure orthogonality (either temporal or spatial) between the modes, which ultimately leads to over-segmentation: overlapping modes recovering the same dynamics and partially cancelling each other as an unphysical destructive interference. Here we introduce an extension to VMD which explicitly enforces temporal orthogonality between the modes, leading to an enhanced robustness of the decomposition and avoiding over-segmentation. We apply the new method (referred to as Orthogonalized VMD) to separated flows subjected to a temporal evolution of the boundary conditions. The dynamics of the separated flow are then non-stationary and follow the inflow changes, but are not necessarily synchronized to them [3]. The novel technique allows to decompose the flow fluctuations into modes representing transient and time-localized dynamics, including the low-frequency evolution of the underlying flow and high-frequency dynamics appearing transiently. Figure 1 illustrates a pair of non-stationary modes describing the modulation of the shear-layer vortex shedding due to the harmonic change in inflow velocity.

Acknowledgements: This work has received funding from the European Union’s Horizon 2020 research and innovation programme under the Marie Skłodowska Curie grant agreement No 955923-SSECOID and by the Government of the Community of Madrid within the multi-annual agreement with Universidad Politécnica de Madrid through the Program of Excellence in Faculty (V-PRICIT line 3).

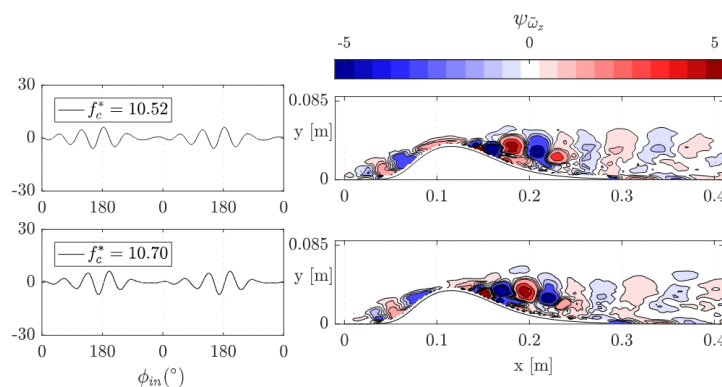


FIGURE 1. *Non-stationary mode pair in transient separation over wall-bounded bump geometry due to a change in the inflow. Left: temporal evolution of the amplitude coefficient. Right: spanwise vorticity field.*

References

- [1] K. Dragomiretskiy & D. Zosso. Variational Mode Decomposition. *IEEE T. on Signal Processing*, **62** (3), 531544, 2014.
- [2] Z.-M. Liao, Z. Zhao, L.-B. Chen, Z.-H. Wan, N.-S. Liu and X.-Y. Lu. Reduced-order variational mode decomposition to reveal transient and non-stationary dynamics in fluid flows. *J. Fluid Mech.* **966**, A7, 2023.
- [3] H. Marbona, D. Rodríguez, A. Martínez-Cava, E. Valero. Impact of harmonic inflow variations on the size and dynamics of the separated flow over a bump. *Phys. Rev. Fluids*, **Vol. 9**, p. 053901, 2024.

GRADIENT-AUGMENTED BAYESIAN SHAPE OPTIMIZATION FOR FLOW INSTABILITY CONTROL USING LINEARIZED NAVIER-STOKES MODELS

Demange, S.¹, Reumschüssel, J. M.¹, Müller, J. S.¹, Knechtel, S. J.¹, Oberleithner, K.¹

¹Laboratory for Flow Instabilities and Dynamics, Technische Universität Berlin

The control of flow instabilities is a crucial aspect in many industrial applications, whether for the reduction of drag, noise or the enhancement of mixing. However, identifying the optima of costly objective functions, whether by simulation or experiment, is often a prohibitively expensive process. We aim to overcome this challenge by combining physics-based models of flow instabilities, here the linearized Navier-Stokes equations, with Bayesian optimization (BO) augmented with adjoint-based gradient information. In this work we consider a passive control method based on the deformation of a parametrized geometry.

BO provides an optimization technique that is known to identify global minima in a sample-efficient manner. It builds on a probabilistic surrogate model of the objective function, which is derived from Gaussian process regression. In the proposed framework, the model predictions are informed through data from linearized base flow analysis. Furthermore, we leverage the adjoint operator to obtain the gradient information of the cost function with respect to changes of the shape parameters at reasonable computational cost [1]. By extending the BO method accordingly, we significantly accelerate the convergence compared to classical BO. Therefore, the methodology (shown in fig 1a) provides a highly efficient tool for the reduction of flow instabilities in technical devices.

In this presentation, the approach will be illustrated for two laminar cases in order to provide a proof of concept. The first one considers the flow around a hydrofoil similar to [2], and uses the growth rate from linear stability analysis as an objective function to suppress the global wake mode. As shown in fig 1b, BO with gradients (d-BO) outperforms classical BO and BFGS-B methods for this case. The second case considers a backward-facing ramp similar to [3] and uses the leading gain from resolvent analysis to dampen convective instabilities downstream of the ramp. Gradient-augmented BO of the ramp geometry shows an effective reduction of the leading gain (see figs. 1c and 1d).

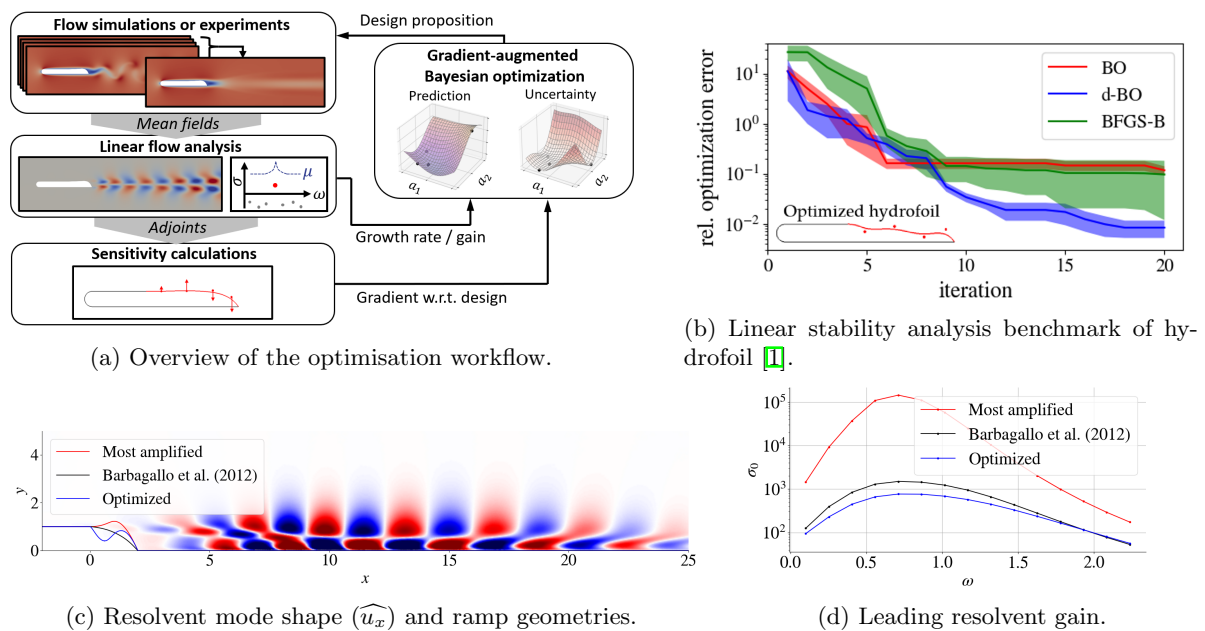


Figure 1: Illustration of methodology and preliminary results.

References

- [1] Jens S. Müller, Johann Moritz Reumschüssel, Thomas L. Kaiser, Sophie Knechtel, and Kilian Oberleithner. Combining Bayesian optimization with adjoint-based gradients for efficient control of flow instabilities. In *Proceedings of the Summer Program*, pages 143–152, Center for Turbulence Research, Stanford University, 2024.
- [2] Alison L. Marsden, Meng Wang, John E. Dennis, Jr., and Parviz Moin. Optimal Aeroacoustic Shape Design Using the Surrogate Management Framework. *Optimization and Engineering*, 5(2):235–262, June 2004.
- [3] Alexandre Barbagallo, Gregory Dergham, Denis Sipp, Peter J. Schmid, and Jean-Christophe Robinet. Closed-loop control of unsteadiness over a rounded backward-facing step. *Journal of Fluid Mechanics*, 703:326–362, July 2012.

REDUCED MODELING AND CONTROL OF A FLUIDIC PINBALL WAKE: AN EXPERIMENTAL INVESTIGATION

Aditya Desai¹, Luc Pastur², Onofrio Semeraro³ and François Lusseyran⁴

¹CNRS, Laboratoire Interdisciplinaire des Sciences du Numérique (LISN), Université Paris-Saclay, Orsay, France

²Unité de mécanique, ENSTA-Paris, Institut Polytechnique de Paris, Palaiseau, France

Over the past ten years, the fluidic pinball has become a valuable benchmark for studying flow control strategies [1]. The fluidic pinball comprises of three independently rotating cylinders positioned at the vertices of an equilateral triangle, with the flow directed perpendicularly to one of its sides. The cylinder rotation rates serve as the control inputs, while velocity sensors located in the wake provide the outputs. This configuration enables the investigation of both steady and unsteady actuation strategies over a wide range of parameters. Fig. 1 presents a snapshot of the near-field wake captured using smoke visualization.

Despite its geometric simplicity, the wake behind the fluidic pinball displays complex interactions of multiple frequencies and nonlinear dynamics, making it an excellent test case for the development and evaluation of control laws. While numerous numerical studies have been performed at low Reynolds numbers[1], experimental literature is limited, mainly due to the associated engineering challenges [2].

This study presents the findings from low-speed wind tunnel experiments conducted on the fluidic pinball. The Reynolds number based on the cylinder diameter and free-stream velocity, is $Re = 1333$, indicating a turbulent regime [1]. Planar two-component particle image velocimetry (PIV) is employed to capture the velocity field, while hot-wire anemometry provides high-resolution velocity time traces at three distinct spatial locations. Complete characterization of the coherent structures and their dynamics in the wake is proposed for both the stationary pinball and the flow with open-loop control. This includes modal decompositions such as proper orthogonal decomposition (POD) and dynamic mode decomposition (DMD) [3], along with an examination of the associated temporal dynamics, low-order modeling, and physical implications. Preliminary results on closed-loop control will also be presented.

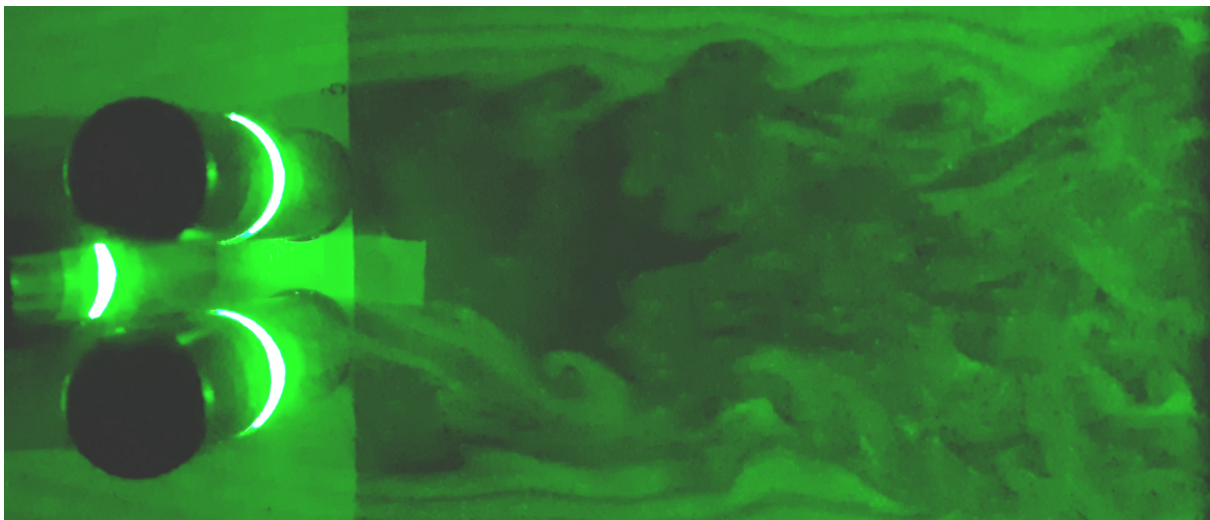


FIGURE 1. *Smoke visualization of the fluidic pinball wake at $Re = 1333$.*

References

- [1] N. Deng, B. R. Noack, M. Morzyński, and L. R. Pastur. *Low-order model for successive bifurcations of the fluidic pinball*. *Journal of Fluid Mech.*, 884, A37, 2020.
- [2] C. Raibaud, P. Zhong, B. R. Noack and R. J. Martinuzzi. Machine learning strategies applied to the control of a fluidic pinball. *Physics of Fluids*, 32(1), 015108, 2020.
- [3] Schmidt, P. J. Dynamic mode decomposition of numerical and experimental data. *Journal of Fluid Mech.*, 656, 5-28, 2010

LINEAR STABILITY AND SHAPE SENSITIVITY ANALYSIS WITH A LINEARIZED TURBULENCE MODEL FOR SHAPE OPTIMIZATION

Jens S. Müller¹, Sophie J. Knechtel¹, Kilian Oberleithner¹

¹Laboratory for Flow Instabilities and Dynamics, Technische Universität Berlin, Müller-Breslau-Straße 8, 10623 Berlin

Mean-flow-based linear stability analysis (LSA) and shape sensitivity analysis are performed in a turbulent draft tube flow of a Francis turbine model. The significance of including a linearized turbulence model and its implications for shape optimization are discussed.

Self-excited global instabilities often possess narrow regions which are highly sensitive to small perturbations or changes to the flow. These changes can be induced by minor modifications of the shape of a body associated with the flow instability that can have a large impact on the instability itself. In LSA, this property can be exploited using shape optimization to suppress the global instability by minimizing its growth rate towards marginal stability, using adjoint-based shape sensitivity as gradient information [1]. The LSA of fully turbulent flows requires the inclusion of additional turbulence models in order to close the otherwise unknown turbulent-coherent interaction term. Eddy viscosity models are widely spread in usage. However, it is often assumed that the eddy viscosity is ‘frozen’ and does not fluctuate with the coherent field. In this work, this assumption is suspended and a linearized turbulence model equation is added to the linear stability and shape sensitivity analysis to account for the changes of the turbulent field when changes to the shape are made.

For demonstrating the relevance of including a linearized turbulence model, the precessing vortex rope instability in a fully turbulent swirling flow is considered. The vortex rope is located at the downstream end of a centerbody in the draft tube of a Francis turbine model. This technically highly relevant setup has already been studied intensively in the past, both experimentally and numerically such as in [2, 3]. In the current work, steady 2D Reynolds-averaged Navier–Stokes (RANS) simulations are performed using a k - ϵ turbulence model (see figure 1(a)). The intricate inlet conditions are tuned against 3D unsteady RANS fields that include a complex duct upstream of the centerbody. The 2D RANS simulations are conducted at sub- and supercritical conditions for Reynolds numbers between $Re \approx 20000$ and 30000. The mean flow fields serve as the input for the LSA (see figures 1(b,c)) and shape sensitivity computations. The influence of the linearized turbulence model on the shape sensitivity and the physical mechanisms that stabilize the flow are discussed.

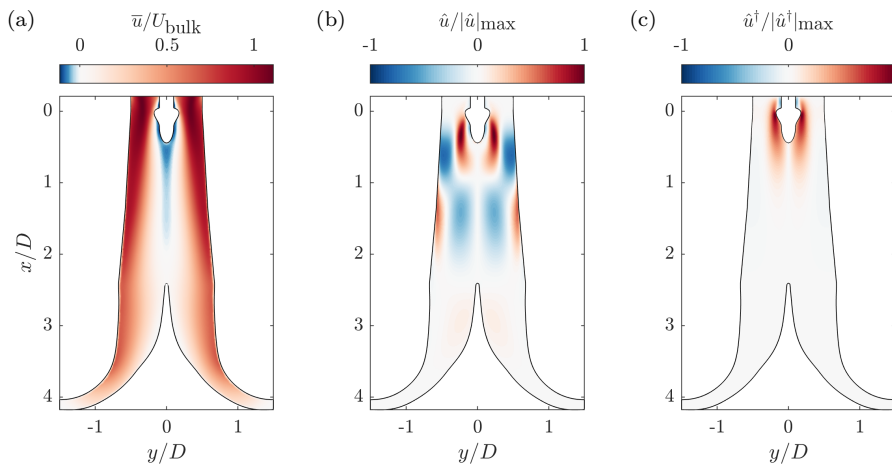


FIGURE 1. Swirling flow in a Francis turbine draft tube at supercritical conditions ($Re \approx 20000$): (a) mean axial velocity field, (b) axial velocity of vortex rope eigenmode, (c) axial velocity of vortex rope adjoint eigenmode.

References

- [1] J. S. Müller, J. M. Reumschüssel, T. L. Kaiser, S. J. Knechtel and K. Oberleithner. Combining Bayesian optimization with adjoint-based gradients for efficient control of flow instabilities. *Proceedings of the Summer Program*, Center for Turbulence Research, Stanford University, 143–152, 2024.
- [2] J. S. Müller, F. Lückoff, T. L. Kaiser, and K. Oberleithner. On the relevance of the runner crown for flow instabilities in a Francis turbine. *IOP Conference Series: Earth and Environmental Science*, 1079(1):012053, 2022.
- [3] F. Lückoff, M. Naster, J. S. Müller, M. Sieber, I. Litvinov, and K. Oberleithner. Impact of runner crown shape modifications on the onset of the precessing vortex core. *IOP Conference Series: Earth and Environmental Science*, 1079(1):012051, 2022.

STABILIZATION OF STATIONARY CROSSFLOW INSTABILITY BY WALL COOLING

Yifu Chen¹, Davide Modesti², Marios Kotsonis¹

¹ Department of Flow Physics and Technology, Faculty of Aerospace Engineering, Delft University of Technology, Delft, Netherlands

² Gran Sasso Science Institute, 67100 L'Aquila, Italy

With hydrogen technologies playing an increasingly important role towards a more sustainable aviation, the concept of cryogenic aircraft has found a renewed interest for improving aerodynamic performance. By leveraging the cooling capability of cryogenic liquid hydrogen, the laminar-to-turbulent transition can be delayed, leading to a reduction in friction drag [1, 2]. In this work, the effect of active wall cooling on the stationary crossflow instability (SCFI) is studied by compressible nonlinear parabolized equations (CNPSE) and direct numerical simulations (DNS). A three dimensional boundary layer on a swept flat plate with swept angle $\phi=45^\circ$ is considered. On the top boundary of DNS, a favourable pressure gradient is imposed to achieve a Falkner-Skan-Cooke velocity distribution. The cooling ratio is $T_w/T_\infty = 0.8$, starting from $x = 50\delta_0$ where δ_0 is the inflow boundary layer thickness, in order to make the upstream history of perturbations consistent to the adiabatic reference case. The steady solution of the DNS is used to perform linear stability analysis to search the most critical unstable spanwise wavelength which is $\lambda_z = 11.12\delta_0$ in this case. Modal crossflow perturbations are introduced at the inflow of the numerical domain. The time-invariant DNS solution is also used as the baseflow for running CNPSE. Figure 1 shows the streamwise velocity evolution of SCFI at $z/\delta_0 = 0$. The stabilization effect on CFI is qualitatively evident as the crossflow vortices in the wall cooling case are weaker than in the adiabatic case. Meanwhile, the amplitude development predictions from DNS and CNPSE are in good agreement. Both methods predict a delay of SCFI saturation by wall cooling control.

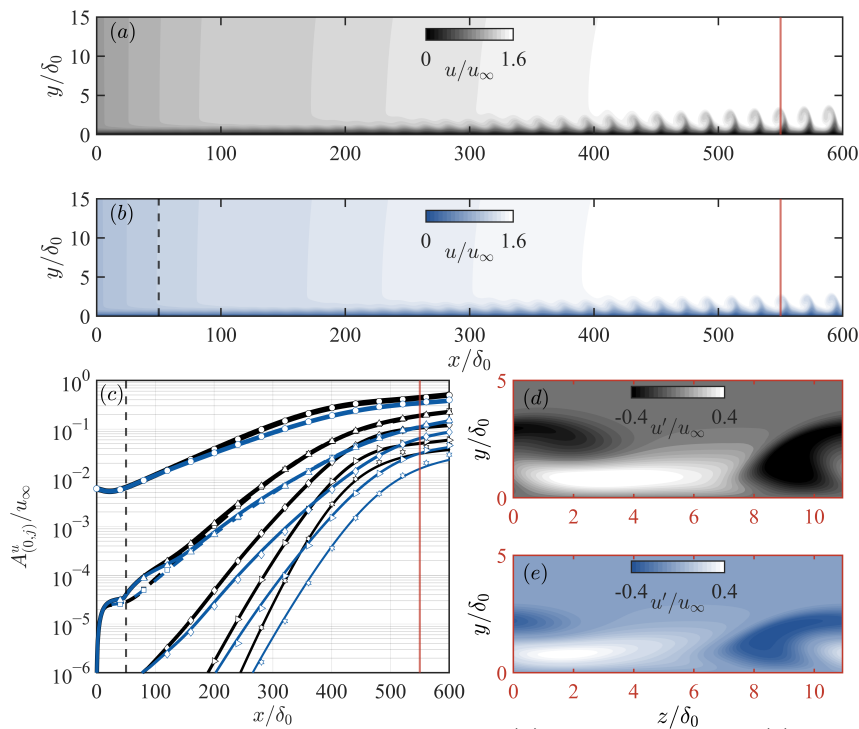


FIGURE 1. Streamwise evolution of normalized u velocity for (a) adiabatic case and (b) cooling case where the wall is cooled down to $T_w/T_\infty = 0.8$ downstream of $x = 50\delta_0$ (dashed lines in (b) and (c)) for cooling case. (c) Streamwise evolution of amplitudes of SCFI from CNPSE (symbols) and DNS (solid lines). Black: adiabatic. Blue: cooling. Fourier modes $j=1-5$ (thick-to-thin) and $j=0$ (dashed). Spanwise distribution of total u perturbation fields at $x = 550\delta_0$ (red lines in (a), (b) and (c)) is depicted for (d) adiabatic case and (e) cooling case.

References

- [1] Eli Reshotko. Drag reduction by cooling in hydrogen-fueled aircraft. *Journal of Aircraft*, 16(9):584–590, 1979.
- [2] J Theisen, G Brewer, and L Miranda. Laminar flow stabilization by surface cooling on hydrogen fueled aircraft. In *Aircraft Systems and Technology Meeting*, page 1863, 1979.

DIRECT NUMERICAL SIMULATION OF THE EFFECTS OF A SMOOTH SURFACE HUMPS ON INSTABILITIES AND TRANSITION IN SWEEPED-WING BOUNDARY LAYERS

Mohammad Moniripiri¹, Alberto F. Rius-Vidales², Marios Kotsonis², Ardeshir Hanifi¹

¹*FLOW, Department of Engineering Mechanics, KTH Royal Institute of Technology, Stockholm, Sweden*

²*Department of Flow Physics and Technology, Faculty of Aerospace Engineering, Delft University of Technology, The Netherlands*

Recent experiments by Rius-Vidales *et al.* [1] have shown the great potential of using a smooth surface hump as a passive control device for transition delay on swept-wings. When the amplitude of incoming Crossflow (CF) vortices was *relatively* low, a transition delay of approximately 14% of the chord (with respect to the clean case with no surface hump) was achieved. In the same experiments, when the amplitude of incoming CF vortices was increased, the hump exhibited a supercritical behaviour with transition location shifted to the vicinity of the hump. This study aims to numerically model the experiments of [1] using Direct Numerical Simulations (DNS), in order to understand the mechanisms underlying transition delay/advancement in the experiments of Rius-Vidales *et al.* [1].

The numerical results for both *low* and *high* amplitudes of incoming CF vortices are validated against experimental data, and a close agreement between DNS and experimental results is achieved. Downstream of the hump, a region with reversal of CF velocity component of the meanflow is identified. For the *low* amplitude case, linear mechanisms are still dominant. Within the CF reversal region, the shape and orientation of the CF perturbations change, especially near the wall. It is shown that CF perturbations recovers their original orientation after a short distance downstream of the hump within a so-called *recovery region*. During recovery, linear production weakens due to reduced *lift-up* effect. This leads to a reduced growth rate, and stabilisation of steady CF perturbations. As a result, the neutral point for type II secondary instability is shifted more downstream (compared to the clean case with no surface hump), while type I secondary instability is found to become stable. In contrast, when the amplitude of incoming CF perturbation is relatively *high*, a pair of counter-rotating vortices (marked in Figure 1) forms downstream of the hump due to interactions between fundamental and higher harmonics of CF perturbation within the CF reversal region. The growth of secondary instabilities arising from the vortex-system results in transition at $\approx 25\%$ of the chord in the hump case, compared to at $\approx 43\%$ of the chord in the clean case.

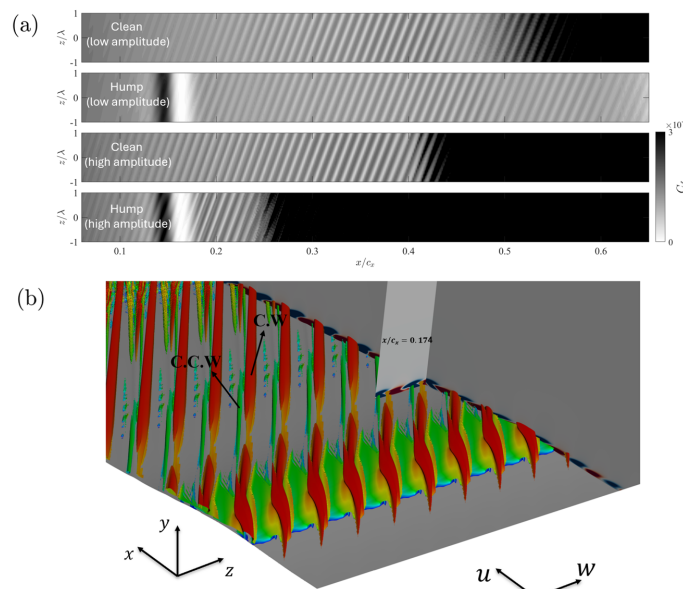


FIGURE 1. (a) Time-averaged skin friction coefficient at the wall for different cases. (b) λ_2 visualization of the time-averaged meanflow, coloured by spanwise velocity component. in panel (b), C.C.W and C.W labels correspond to counter-clock wise and clock-wise vortices, respectively.

References

- [1] A. F. Rius-Vidales, L. Morais, S. Westerbeeck, J. Casacuberta, M. Soyler, M. Kotsonis . *Delay of Swept-Wing Transition using a Surface Hump*. Under review in *Journal of Fluid Mechanics*, 2025.

CONTROL OF STREAK-INDUCED LAMINAR-TURBULENT TRANSITION BY A CROSSBAR

Yongxiang Wu¹, Ulrich Rist¹, Christoph Wenzel¹

¹*Institute of Aerodynamics and Gas Dynamics, University of Stuttgart, Wankelstraße 3, D-70563 Stuttgart, Germany*

Boundary layer streaks are featured by streamwise elongated alternating high- and low-speed fluids and are the primary coherent structure of both turbulent and transitional boundary layers. Free-stream turbulence (FST) intensities of 1% or higher can induce streaks in a laminar boundary layer and hence trigger bypass transition. The mechanism of streak generation is denoted by Landahl as the “lift-up” effect, where very weak streamwise vortices can push high-speed fluid towards the wall and low-speed fluid in the opposite direction. Streaks can also be created by surface roughness. The difference is that surface roughness-induced streaks are steady while those induced by FST are unsteady.

Controlled streaks can have positive effects on instability attenuation and delay laminar-turbulent transition. Boiko *et al.* [1] observed the stabilization effect of unsteady streaks on the primary boundary layer instability, i.e. the Tollmien-Schlichting waves. With properly chosen parameters, Fransson *et al.* [2] eventually obtained a full transition delay with cylindrical roughness elements induced streaks. In our previous experimental investigation [3], we found that a horizontal circular crossbar can homogenize the steady streaks created by roughness elements positioned ahead and eventually delay the laminar-turbulent transition. The mechanism revealed by a linear stability analysis is the reduction of the sinuous instability. The objective of this study is to numerically investigate the ability of a crossbar to homogenize the freestream-induced unsteady streaks and its potential for controlling the laminar-turbulent transition through direct numerical simulations. Figure 1 shows the comparison of wall-parallel slices of streamwise velocity u_x between the flat-plate reference case and a case with static crossbar. As expected, the streak behind the crossbar is homogenized. However, the presented case shows a negative effect of the method that a fast transition is observed. The unsteady nature of the incoming streak renders the above-mentioned mechanism invalid. We then examined the impact of a rotating crossbar with the objective of energizing the boundary layer. The results indicate that an unexpected new shear layer is induced whose instability arises when the bar is positioned at a specific distance from the wall and rotates at an optimal rate.

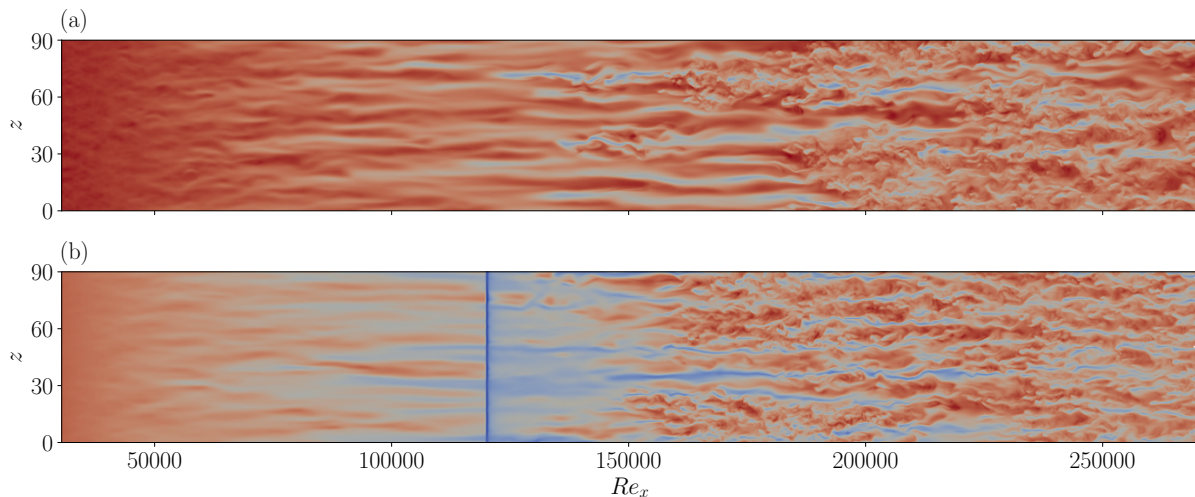


FIGURE 1. Comparison of the instantaneous streamwise velocity u_x in a plane parallel to the wall at (a): $y = 2.5$ for Reference flat-plate case and (b): $y = 1.553$ for case with a crossbar (diameter $d/\delta_0^* = 0.3$) placed at the same height.

References

- [1] A. Boiko, K. Westin, B. Klingmann, V. Kozlov, P. Alfredsson. Experiments in a boundary layer subjected to free stream turbulence. Part 2. The role of TS-waves in the transition process. *J. Fluid Mech.* 281, 219–245, 1994
- [2] J.H. Fransson, A. Talamelli, L. Brandt, C. Cossu. Delaying transition to turbulence by a passive mechanism. *Phys. Rev. Lett.* 96(6), 064501, 2006
- [3] D.K. Puckert, Y. Wu, U. Rist. Homogenization of streaks in a laminar boundary layer. *Exp. Fluids*, 61, 1–15, 2020

IMPACT OF DISTRIBUTED ROUGHNESS ON INSTABILITIES IN BOUNDARY LAYERS UNDER PRESSURE GRADIENT

Victoria Prieto^{1,2}, Erwin R. Gowree², Maxime Forte¹

¹DMPE, ONERA, Université de Toulouse, 31000, Toulouse, France

²DAEP, ISAE-SUPAERO, 31000, Toulouse, France

The effectiveness of control strategies aimed at extending the laminar boundary layer is highly dependent on the condition of the aerodynamic surfaces, which can deteriorate over time. It is well known that the presence of distributed roughness can shift the onset of the transition upstream [1], although the underlying reasons for such an enhancement of the transition are varied. For instance, Corke et al. demonstrated through experiments on a flat plate that this phenomenon can result from an increase in the linear amplification of modal instabilities, a process known as over-amplification [2]. In an effort to quantify this transition advance, some studies have adopted a semi-empirical approach using the e^N method, which combines Linear Stability Theory (LST) with experimentally measured transition onsets [3]. Despite these advances, there is a lack of predictive models that can accurately determine the onset of transition in the presence of randomly distributed roughness under different aerodynamic conditions. The present work aims to further investigate the influence of stochastically distributed roughness on a two-dimensional incompressible boundary layer developing over a profile where modal instabilities are expected. This approach will not only allow the study of the amplification as a function of different roughness parameters but will also provide a ΔN model to predict transition under such conditions.

An experimental campaign was carried out in the SaBRé subsonic wind tunnel at ISAE-SUPAERO. The study was conducted on an unswept wing with a span of 1.2 m and a symmetric ONERA-D airfoil with a chord length of 0.35 m for Reynolds numbers ranging from 3.5×10^5 to 5.5×10^5 , and at two angles of attack: 0.5° and 1° . In terms of roughness, two types of sandpaper with average roughness heights of $S_a = 18 \mu\text{m}$ and $28 \mu\text{m}$ were studied. These rough strips were placed on the upper surface of the wing from 30% of the chord up to 38.5% and 44.2% for two roughness extensions, L_R , of 30 and 50 mm respectively. The results of these experiments have so far allowed us to prove the effect of the average roughness height on the amplification of Tollmien-Schlichting instabilities. Figure 1a shows the spectra obtained at $y = \delta_1$ for different roughness heights at $x/c=0.55$, showing a hump at around 700 Hz with increasing energy as the roughness increases, which is a strong indicator of TS instabilities. This figure also illustrates the appearance of secondary modes at the same position for the highest roughness height. By integrating the spectra around the most amplified frequency, $f = 750$ Hz, we obtain the velocity fluctuations presented in Figure 1b. This figure indicates that, although the shape of the experimental fluctuation profiles remains unchanged, the presence of roughness leads to a non-negligible overamplification. Moreover, the eigenfunction obtained from the LST performed on the smooth case presents excellent agreement with the experimental fluctuation profiles, even when roughness is present. Further results on the impact of other roughness parameters on this overamplification phenomenon will be presented at the workshop.

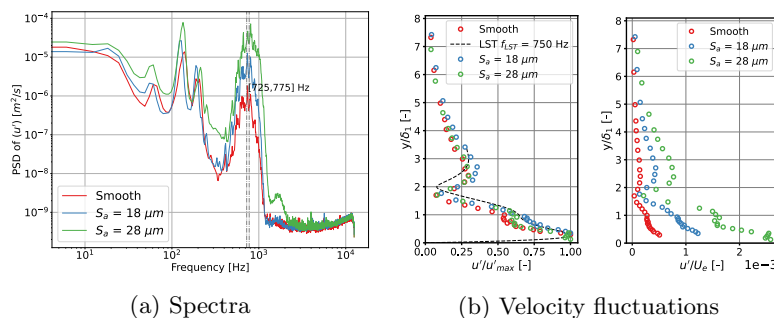


Figure 1: Spectra and velocity fluctuations profiles for different roughness heights S_a at a given roughness extent $L_R = 30\text{mm}$. $Re = 4.5 \times 10^5$ and $\alpha = 0.5^\circ$

References

- [1] A. E. von Doenhoff and A. L. Braslow. *The Effect of Distributed Surface Roughness on Laminar Flow*. In *Boundary Layer and Flow Control*, pages 657-681. Pergamon, 1961.
- [2] T. C. Corke, A. Bar-Sever, and M. V. Morkovin. *Experiments on Transition Enhancement by Distributed Roughness*. *The Physics of Fluids*, 29(10):3199-3213, October 1986.
- [3] F. Ducaffy. *Étude expérimentale de l'influence de la rugosité de surface sur la transition laminaire/turbulent d'une couche limite 2D en écoulement incompressible*. PhD thesis, ISAE-SUPAERO, July 2022.



MODELING NONLINEAR DYNAMICS FROM DATA

George Haller

Institute for Mechanical Systems, ETH Zürich

I discuss a dynamical systems alternative to neural networks in the data-driven reduced-order modeling of nonlinear phenomena. Specifically, I show that the recent concept of spectral submanifolds (SSMs) provides very low-dimensional attractors in a large family of mechanics problems ranging from wing oscillations to transitions in shear flows. A data-driven identification of the reduced dynamics on these SSMs gives a mathematically justified way to construct accurate and predictive reduced-order models for solids, fluids and controls without the use of governing equations. I illustrate this on physical problems including the accelerated finite-element simulations of large structures, prediction of transitions to turbulence, reduced-order modeling of fluid-structure interactions, extraction of reduced equations of motion from videos, and model-predictive control of soft robots. The recently published introduction [?] to the theory and applications of SSMs contains more detail and references.

References

- [1] G. Haller. *Modeling Nonlinear Dynamics from Equations and Data – with Applications to Solids, Fluids and Controls*. SIAM, Philadelphia, 2025.

PREDICTING COMPLEX FLOWS VIA SPACE-TIME POD: A DATA-DRIVEN FORECASTING APPROACH

Oliver T. Schmidt

Department of Mechanical and Aerospace Engineering, University of California San Diego, La Jolla, CA 92093, USA

This work introduces an extension of space-time Proper Orthogonal Decomposition (ST-POD, [1]) for data-driven prediction of complex flows. The proposed method leverages ensemble realizations spanning a specified prediction horizon to compute a set of space-time modes over the hindcast horizon. By extending these modes into the forecast horizon, we capture key dynamical correlations without requiring additional hyperparameters—rank truncation is the sole tuning parameter. Figure 1 illustrates our approach on the challenging case of high-speed flow over an open cavity, highlighting its ability to reproduce the dominant coherent structures over short-term forecasts. We demonstrate the robustness of space-time POD-based prediction with two large-scale datasets: numerical simulations of supernova shell expansions in a turbulent interstellar medium [2], and experimental particle image velocimetry (PIV) measurements of an open cavity flow [3]. The supernova data present strongly anisotropic, rapidly evolving shock structures, while the cavity flow features broadband turbulence with prominent resonance tones. In both scenarios, the method shows predictive skill up to meaningful time horizons, accurately capturing spatiotemporal evolution even in the presence of nonuniform time steps (supernova) or noisy experimental data (cavity). The key to this performance lies in projecting new hindcast snapshots onto the precomputed mode basis. This approach yields prediction fields by balancing the latent correlations uncovered during training with the unique features of the new input data. Our results highlight the flexibility and accuracy of space-time POD-based forecasting for distinct flow regimes, offering a baseline methodology for forecasting of complex flows.

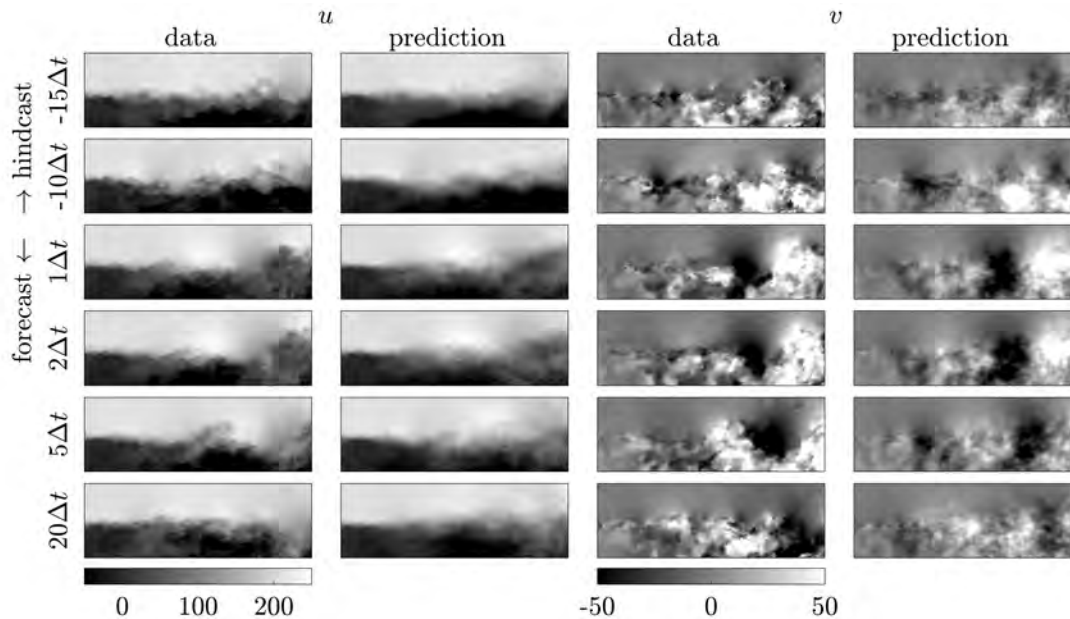


FIGURE 1. Prediction of the cavity flow using a hindcast horizon of 15 and a forecast horizon of 20. The prediction is based on the leading 100 modes retained from the space-time POD decomposition of 1593 realizations. The prediction horizon was placed in the middle of the test dataset.

References

- [1] O. T. Schmidt and P. J. Schmid. A conditional space-time pod formalism for intermittent and rare events: example of acoustic bursts in turbulent jets. *Journal of Fluid Mechanics*, 867:R2, 2019.
- [2] K. Hirashima, K. Moriwaki, M. S. Fujii, Y. Hirai, T. R. Saitoh, and J. Makino. 3d-spatiotemporal forecasting the expansion of supernova shells using deep learning towards high-resolution galaxy simulations. *Monthly Notices of the Royal Astronomical Society*, 526(3):4054–4066, 2023.
- [3] Y. Zhang, L. N. Cattafesta, and L. Ukeiley. Spectral analysis modal methods (samms) using non-time-resolved piv. *Experiments in Fluids*, 61(11):1–12, 2020.



A FAMILY OF PHYSICS-CONSTRAINED DATA-DRIVEN QUADRATIC ROMS

Rama Ayoub¹, Mourad Oulghelou², Peter Schmid³

^{1,3} *Mechanical Engineering, King Abdullah University of Science and Technology, Thuwal, Saudi Arabia.*

² *Institute of Computing and Data Sciences, Sorbonne University, Paris, France.*

² *Jean Le Rond D'Alembert Institute, Sorbonne University, Paris, France.*

We introduce a framework for constructing physics-constrained, data-driven reduced order models (ROMs) for discrete latent dynamical systems. Our methodology is based on a quadratic discrete evolution equation,

$$v^{n+1} = A v^n + \mathbf{Q} (v^n \otimes I_r) v^n, \quad n \geq 0,$$

where the linear operator A and the quadratic part $\mathbf{Q} = [Q_1 \ Q_2 \ \dots \ Q_r]$ jointly describe the dynamics of the system. Models relying solely on the linear operator A can capture primary behavior in some settings. However, many complex physical systems, like those governed by the Navier–Stokes equations, require the inclusion of non-linear effects. Quadratic interactions are often the most significant. The quadratic model was previously proposed in the studies on the GILD (Greedy Identification of Latent Dynamics) and the improved version I-GILD methods [1], [2]. In these approaches, the non-linear operator is typically obtained using a greedy resolution technique. To ensure that the reduced models adhere to fundamental physical laws, our framework incorporates structural constraints derived from principles such as energy conservation, dissipation, damping, etc. In particular, we enforce conditions including symmetry, skew-symmetry, bounded spectral norms, positive semidefiniteness, and Hurwitz stability in the identification of both A and \mathbf{Q} . In addition, we develop efficient numerical algorithms for the systematic estimation of these constrained models. The goal of this work is to demonstrate through numerical examples that the proposed models provide a robust, data-driven pathway for modeling complex nonlinear dynamical systems while rigorously preserving essential mathematical and physical properties.

References

- [1] Ayoub, R. and Oulghelou, M. and Schmid, P. Improved Greedy Identification of Latent Dynamics with Application to Fluid Flows. *Computer Methods in Applied Mechanics and Engineering*, 2025.
- [2] Oulghelou, M. and Ammar, A. and Ayoub, R. Greedy identification of latent dynamics from parametric flow data. *Computer Methods in Applied Mechanics and Engineering*, 2024.

TRACKING INVARIANT SOLUTIONS OF ROTATING MAGNETO-HYDRODYNAMICS IN A CHANNEL GEOMETRY

Jean-Clément Ringenbach¹, Steven M. Tobias², Tobias M. Schneider¹

¹*École Polytechnique Fédérale de Lausanne (EPFL), ECPS, Lausanne, Switzerland*

²*University of Leeds, School of Mathematics, Leeds Institute for Fluid Mechanics, Leeds, United-Kingdom*

Invariant solutions are the building blocks of the dynamics and underlie chaotic motions in non-linear dynamical systems. Finding and tracking invariant solutions for specific systems, such as the Navier-Stokes or Rayleigh-Bénard equations, allows to comprehend the mechanistic dependence of given properties onto the control parameters of their governing equations. This has notoriously been achieved by Nagata [1] for plane Couette flows, paving the way to the finding of more invariant solutions and to a better understanding of non-linear dynamical systems.

Reetz et al. [2] found exact invariant solutions in the context of inclined layer convection in a channel geometry, where the gravity vector is tilted with respect to the vertical direction of the geometry. In this case, the turbulence feeds on convection, which is thermally-driven. Expanding upon this model, we add rotation as well as magnetic fields in the system and study the resulting rotating magneto-hydrodynamics (MHD) problem. More specifically, we aim at investigating heat transfer changes compared to inclined layer convection when rotation and magnetic driving are present.

In order to perform this investigation, we study a channel geometry, periodic in the x and z directions as depicted in Figure 1. The fluid considered is an electrically conductive Boussinesq fluid whose convection is driven by thermal forcing, subject to inclined rotation and gravity. Using an extension to the C++ ChannelFlow software, we perform parametric continuations in the Lorentz force's intensity and Rayleigh number to explore different bifurcation branches. Doing so, we attempt to characterize differences in heat transport and their parameter dependence.

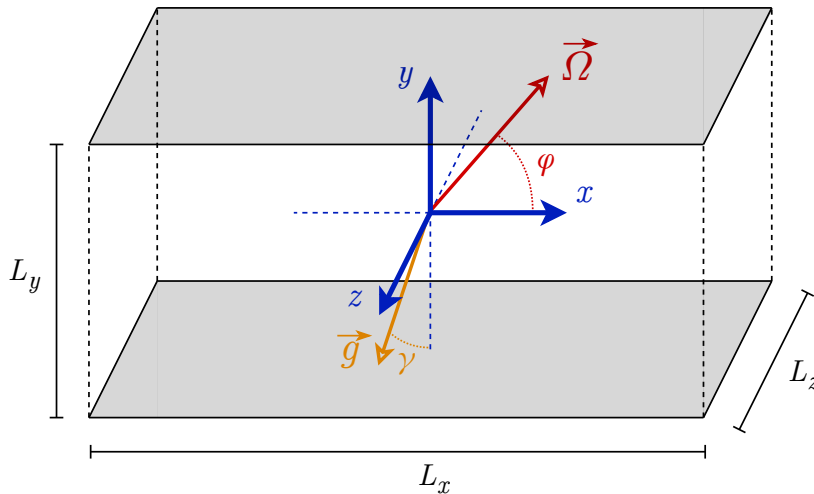


FIGURE 1. Geometry of the x, z -periodic box used, with gravity and rotation inclined in the (x, y) -plane.

References

- [1] M. Nagata. *Three-dimensional finite-amplitude solutions in plane Couette flow: bifurcation from infinity*. J. Fluid Mech. **217** (1990).
- [2] F. Reetz, R. Kreilos, and T. M. Schneider *Exact invariant solution reveals the origin of self-organized oblique turbulent-laminar stripes*. Nat. Commun. **10** (2019)

FROM ANNULAR CAVITY TO ROTOR-STATOR FLOW: NONLINEAR DYNAMICS OF AXISYMMETRIC ROLLS

Artur Gesla^{1,2}, Patrick Le Quéré², Yohann Duguet², Laurent Martin Witkowski³

¹*Sorbonne Université, F-75005 Paris, France*

²*LISN-CNRS, Université Paris-Saclay, F-91400 Orsay, France*

³*Université Claude Bernard Lyon 1, CNRS, Ecole Centrale de Lyon, INSA Lyon, LMFA, UMR5509, 69622 Villeurbanne, France*

Spatio-temporally complex flows are found at the onset of unsteadiness in (axisymmetric) rotor-stator turbulence in the shape of concentric rolls [1, 2]. The emergence of these rolls is rationalised using a homotopy approach, where the original flow configuration is continuously deformed into a simpler, better understood configuration. We deform here rotor-stator flow into an annular flow, thereby controlling curvature effects, and we investigate numerically the transition scenarios as functions of the Reynolds number. In the low curvature regime the transition scenario is supercritical. Modal selection rests on a specific radial localisation property of all eigenmodes (figure 1 left), linked to the space-dependent convective radial velocity which intensifies as curvature is increased. A new nonlinear mechanism for the pairing of rolls is proposed based on multiple resonances of the eigenmodes of the base flow. Increasing curvature reveals a clear path towards a subcritical scenario as a function of the Reynolds number. As the rotor-stator configuration is approached, supercritical branches shift to increasing Reynolds number while a subcritical branch of chaotic states takes over, effectively changing the transition scenario from supercritical to subcritical. For the whole family of annular configurations, ranging from the planar limit to rotor-stator flow, the linear stability of the base flow is governed by two branches of eigenvalues (figure 1 right) with one branch dominating the limiting low and high curvature configurations and the other one pronounced in the intermediate curvature set-up.

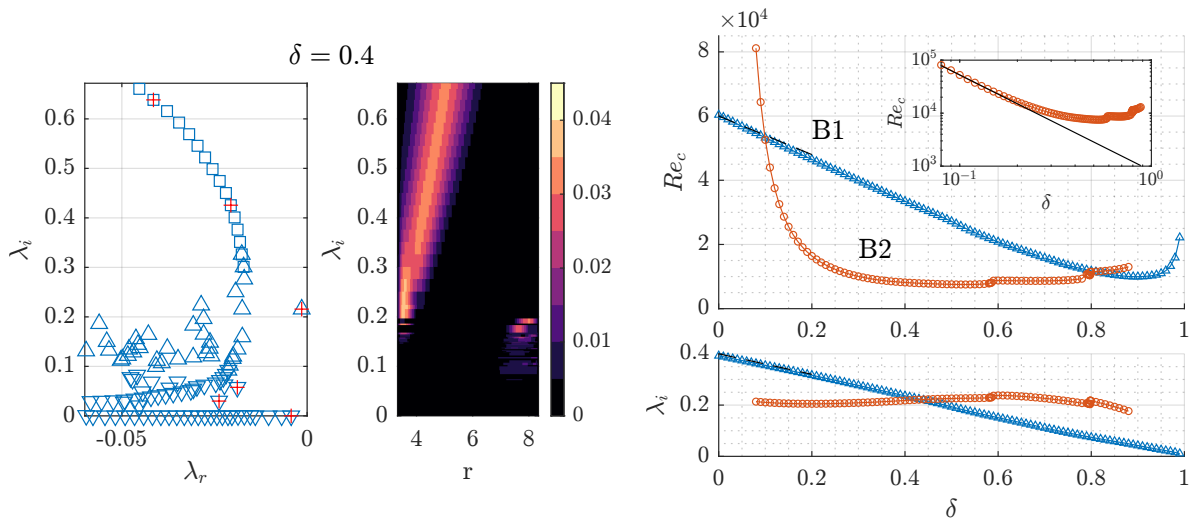


FIGURE 1. Spectrum of the linearised Navier–Stokes operator in an annular rotor-stator configuration with the resonating modes responsible for the pairing events marked by red crosses together with the amplitude of the eigenmode as a function of the radial direction (left) and competition of two branches of unstable modes responsible for the linear instability of the base flow as a function of a curvature parameter δ ($\delta = 0$ rotor-stator flow, $\delta \rightarrow 1$ planar case) (right).

References

- [1] G. Gauthier, P. Gondret, and M. Rabaud. Axisymmetric propagating vortices in the flow between a stationary and a rotating disk enclosed by a cylinder. *J. Fluid Mech.*, 386:105–126, 1999.
- [2] A. Gesla, Y. Duguet, P. Le Quéré, and L. Martin Witkowski. On the origin of circular rolls in rotor-stator flow. *J. Fluid Mech.*, 1000:A47, 2024.

THE INDUCED LATENT DYNAMICS OF AN AUTOENCODER

Pierre Beck^{1,†}, Tobias M. Schneider¹

¹ *Emergent Complexity in Physical Systems Laboratory, EPFL, Switzerland*

[†] pierre.beck@epfl.ch

Invariant solutions, such as equilibria, travelling waves or unstable periodic orbits (UPOs), have helped with explaining recurrent patterns in chaotic fluid flows [1, 2]. In particular, in the dynamical systems point of view of chaotic fluid flows, UPOs are believed to be the underlying dynamical building blocks of spatio-temporal chaos. The identification of UPOs remains challenging though, as fluid flows are usually spatially discretized with many thousand or million degrees of freedom. However, in chaotic driven dissipative systems, the dynamics collapse on a chaotic attractor, and this attractor can be embedded in a manifold of far lower dimension. Recently, autoencoder neural networks (a nonlinear model order reduction technique) have been successful in approximating these embeddings. The standard approach for defining the dynamics in the autoencoder's latent space has been to use a second purely data-driven approach, such as recurrent neural networks or neural ODEs [3], discarding previous knowledge of the exact PDE.

We obtain an approximation of the manifold coordinates via an autoencoder, and by an application of the chain rule, we pull the physical dynamics into the latent space, giving us an induced latent dynamics, without recourse to a second data-driven approximation. Evaluating the induced latent dynamics reveals multiple challenges in correctly training the autoencoder, such as spectral bias - the learning bias towards low frequency modes. By adding a physics loss to the autoencoder's loss function, as well as a first order directional derivative condition, we alleviate these challenges and obtain accurate temporal derivatives and latent dynamics. We investigate these induced latent dynamics by searching for their invariant solutions, most importantly UPOs, and compare them to those of the full physical system. We discover the UPOs of the latent dynamics with an implementation of loop convergence algorithms [4, 5] based on automatic differentiation, and find a correspondence between the solutions of the latent space and the physical space. We show applications of our methods to the 1D Kuramoto-Sivashinsky equation and the 2D Navier-Stokes equation with Kolmogorov forcing.

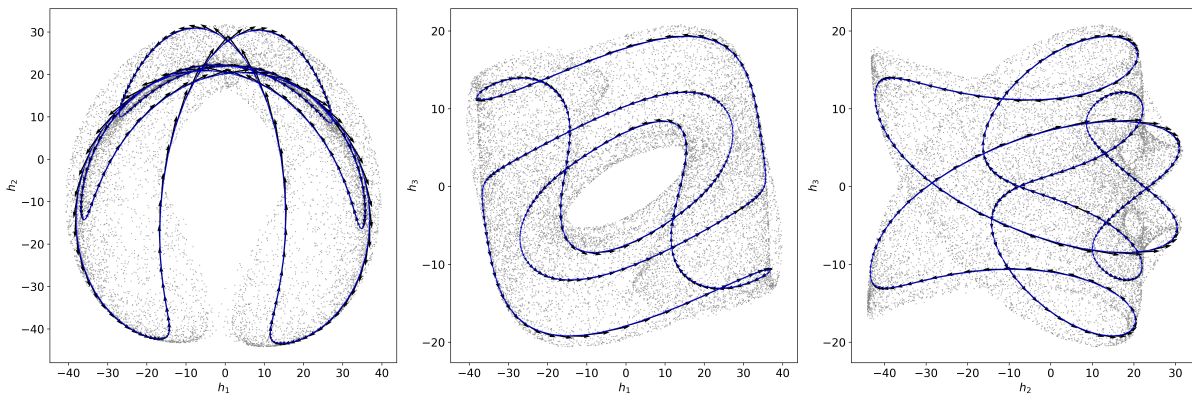


FIGURE 1. 2D projections of the latent chaotic attractor of the Kuramoto-Sivashinsky equation (grey) with one of its periodic orbits (blue). The latent dynamics (black arrows) are tangent everywhere to the periodic orbit.

References

- [1] G. Kawahara, and S. Kida. *Periodic motion embedded in plane Couette turbulence: regeneration cycle and burst.* *Journal of Fluid Mechanics*, 449, pp291–300, 2001.
- [2] F. Reetz, T. Kreilos, and T. M. Schneider. *Exact invariant solution reveals the origin of self-organized oblique turbulent-laminar stripes.* *Nature Communications*, volume 10, 2277, 2019.
- [3] A. J. Linot, M. D. Graham. *Dynamics of a data-driven low-dimensional model of turbulent minimal Couette flow.* *Journal of Fluid Mechanics*, 973, A42, 2023.
- [4] Y. Lan, and P. Cvitanović. *Variational method for finding periodic orbits in a general flow.* *Phys. Rev. E*, 69, 016217, 2004.
- [5] S. Azimi, O. Ashtari, and T. M. Schneider. *Constructing periodic orbits of high-dimensional chaotic systems by an adjoint-based variational method.* *Phys. Rev. E*, 105, 014217, 2022.

LEARNING TRANSITION FROM DATA WITH HIGH-FIDELITY SIMULATIONS AND MACHINE LEARNING

Paola Cinnella

Sorbonne Université, Institut Jean Le Rond D'Alembert

Advances in high-performance computing and high-order numerical methods have enabled the simulation of complex transitional flows across a wide range of conditions, scales, and geometries. These simulations not only complement classical approaches based on linear and nonlinear stability theory, but also generate rich datasets that can inform transition modeling in coarse-grained frameworks. The resulting availability of high-fidelity data opens new opportunities for applying machine learning techniques to analyze transitional flow physics and develop improved predictive models.

In this talk, I will first provide an overview of recent progress in direct numerical and large-eddy simulations of transitional flows—ranging from free-stream-turbulence-induced transition in incompressible regimes to second-mode instabilities in high-enthalpy hypersonic flows. I will then discuss how unsupervised and supervised machine learning methods can support physical understanding and enable the data-driven discovery of transition models. A particular focus will be placed on transition models used to supplement Reynolds-Averaged Navier-Stokes (RANS) simulations, which remain the workhorse of industrial flow prediction. I will review widely used transition correlations, highlight their limitations and uncertainties, and introduce recent developments in open-box machine learning—such as Bayesian symbolic regression [3]—that allow for the automated discovery of interpretable, analytically tractable transition models grounded in data.

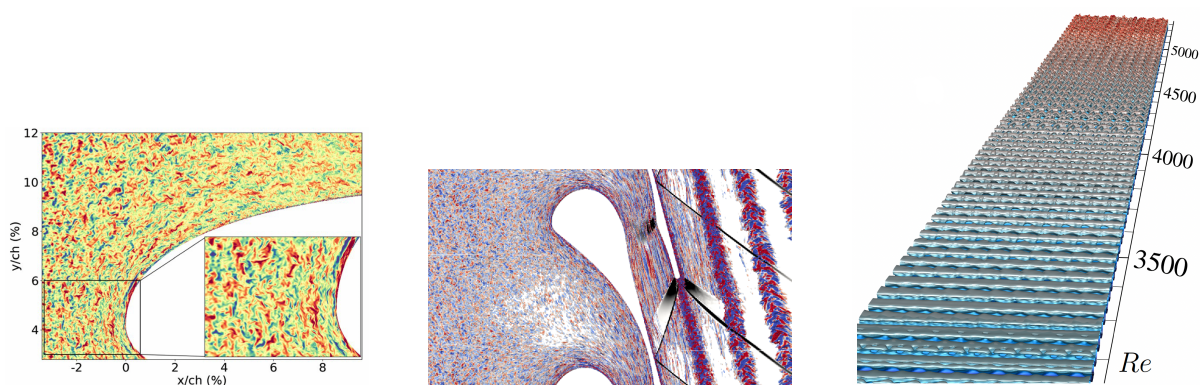


FIGURE 1. *Left: Freestream transition in transonic flow of an organic vapor past a leading edge [2]. Middle: effects of freestream turbulence on the flow of an organic vapor through a supersonic turbine cascade [4]. Right: subharmonic second-mode transition in a chemically reacting hypersonic boundary layer at Mach 10. [5].*

References

- [1] Bienner, A., Gloerfelt, X., & Cinnella, P. (2024). Influence of large-scale free-stream turbulence on bypass transition in air and organic vapour flows. *Journal of Fluid Mechanics*, **997**, A56.
- [2] Bienner, A., Gloerfelt, X., & Cinnella, P. (2024). Leading-edge effects on freestream turbulence induced transition of an organic vapor. *Flow, Turbulence and Combustion*, **112**(1), 345–373.
- [3] Cinnella, P. (2024). Data-driven turbulence modeling. In *Machine Learning for Fluid Dynamics*. Editors: M.A. Mendez, A. Parente. Von Karman Institute, 2025. To appear. Also arXiv preprint arXiv:2404.09074.
- [4] Matar, C., Gloerfelt, X., & Cinnella, P. (2024). Influence of free-stream turbulence on real-gas flows through a supersonic turbine cascade. In *Proceedings of DLESXIV*, Erlangen, Germany, April 10–12, 2024.
- [5] Passiatore, D., Gloerfelt, X., Sciacovelli, L., Pascazio, G., & Cinnella, P. (2024). Direct numerical simulation of subharmonic second-mode breakdown in hypersonic boundary layers with finite-rate chemistry. *International Journal of Heat and Fluid Flow*, **109**, 109505.

TRANSITION CONTROL OF HYPERSONIC BOUNDARY LAYER WITH SPANWISE NON-UNIFORM SURFACE TEMPERATURE

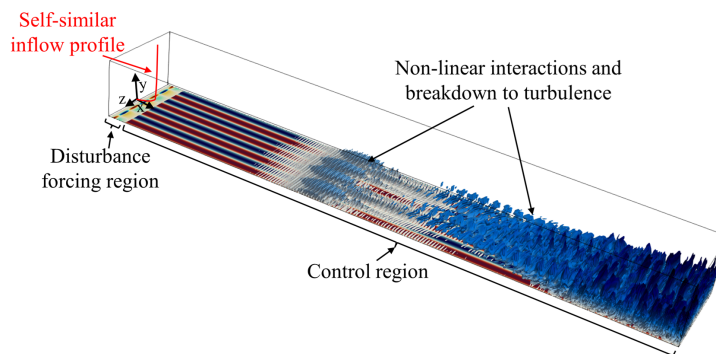
Luca Boscagli¹, Georgios Rigas¹, Olaf Marxen², Paul Bruce¹

¹*Department of Aeronautics, Imperial College London, London, SW7 2AZ, UK*

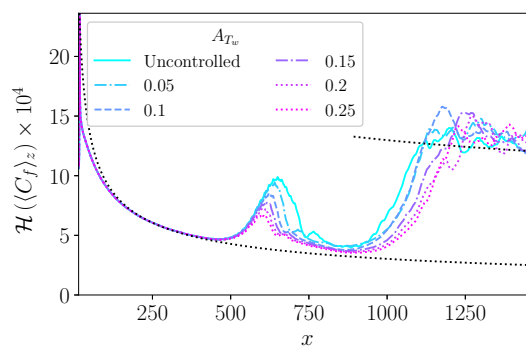
²*School of Mechanical Engineering Sciences, University of Surrey, Guildford, GU2 7XH, UK*

The location of laminar to turbulent transition in hypersonic boundary layers has a significant influence on viscous drag and aerodynamic heating of external surfaces of hypersonic vehicles. Boundary layer stabilization and transition delay via optimally growing streaks is a well established control mechanism for low and high-speed flows [1, 2]. Recently, we have proposed a novel control method for generation of streaks in hypersonic boundary layers through a spanwise non-uniform surface temperature distribution [3]. Direct Numerical Simulations (DNS) showed that the control method can stabilize the second Mack mode. A highly-tuneable, practical implementation of this control method has been proposed and experimentally tested [4], and it promises significant improvement on the aero-thermal-structural efficiency of hypersonic vehicles.

In this work, DNS studies of a Mach 6 boundary layer over a flat plate are used to assess the effect of spanwise non-uniform surface temperature on breakdown to turbulence under deterministic forcing (Fig. 1a). The effect of spanwise surface temperature variation (A_{T_w}) and streak wavelength is parametrically investigated (Fig. 1b), and primary aero-thermodynamic mechanisms identified. Our results extend previous findings by showing how spatially non-uniform thermal conditions can delay transition to turbulence. The insights gained here provide guidelines for further optimization of this control strategy and its integration into future hypersonic vehicle designs.



(a)



(b)

Figure 1: (a) Schematic of the computational domain. (b) Effect of control method on transition location; grey dotted lines in (b) indicate the laminar and turbulent correlations.

References

- [1] C. Cossu, and L. Brandt. *Phys. Fluids*, 14(8), L57-L60, 2002.
- [2] J. Ren and S. Fu and A. Hanifi. *Phys. Fluids*, 28(2): 024110, 2016.
- [3] K. Ozawa and X. Chengwei and G. Rigas and P. Bruce. *AIAA J.*, Under review.
- [4] K. Ozawa and P. Bruce. *AIAA SCITECH 2025 Forum*, AIAA 2025-0262.

TRANSITION MECHANISM OF SHOCK-WAVE/BOUNDARY-LAYER INTERACTION AT MACH 4

Ziming Song¹, Jiaao Hao¹, Ismaïl Ben Hassan Saïdi², Jean-Christophe Robinet²

¹*Department of Aeronautical and Aviation Engineering, The Hong Kong Polytechnic University*

²*DynFluid laboratory, Arts et Métiers Institute of Technology*

The laminar-turbulent transition in high-speed boundary layers remains a challenging problem in both fundamental research and engineering applications, further complicated by the commonly encountered shock-wave/boundary-layer interactions (SWBLIs). SWBLIs can promote transition through multiple mechanisms, including global instability and convective instabilities [1]. One of the characteristic features of the SWBLIs induced transition is the breakdown of streaks, which has been observed both experimentally [2] and numerically [3]. However, the underlying mechanism driving this breakdown is still unclear. Two primary explanations are proposed for globally stable flows: nonlinear interaction of a pair of oblique modes [3] and the secondary instability of streaks. Therefore, this paper aims to identify the dominant mechanism responsible for the breakdown of streaks using resolvent analysis and direct numerical simulation (DNS).

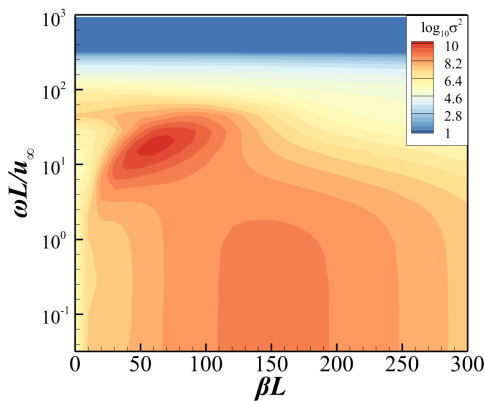


Figure 1: The gain contour from resolvent analysis.

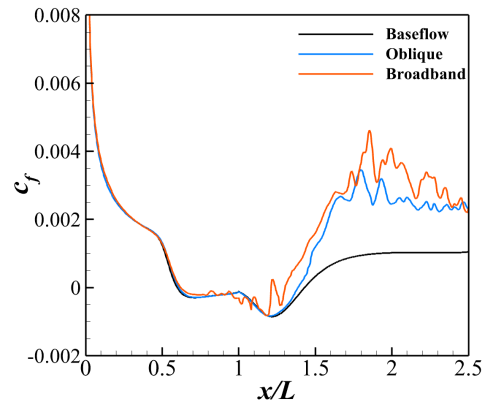


Figure 2: The distributions of spanwise averaged skin friction coefficient.

A compression ramp configuration is considered under the flow conditions from the experiment of [2], with a Mach number of 4 and a Reynolds number of 3.66×10^5 based on flat plate length L . In DNS, free-stream forcing is introduced in the form of slow acoustic waves to simulate the noise in wind tunnels. Correspondingly, resolvent analysis with slow acoustic forcing is used to determine the dominant frequency and wavenumber. As shown in Figure 1, the optimal gain is located at $\omega_r L/u_\infty = 15$ ($f = 16$ kHz) and $\beta L = 60$ (wavelength $\lambda = 10.5$ mm), corresponding to oblique acoustic waves. Based on the resolvent results, high-fidelity DNS is conducted with a seventh-order spatial scheme and a three-stage Runge–Kutta time marching method. An initial test is performed on a coarse grid with a λ spanwise length at 10° ramp angle. The first wall-normal height y^+ is 0.3, while the streamwise spacing x^+ and spanwise spacing z^+ are 6. Forcing is applied from the farfield, including a pair of dominant oblique waves and broadband disturbances. The distributions of spanwise averaged skin friction coefficient in Figure 2 demonstrate that acoustic waves trigger transition efficiently and the broadband forcing advances transition onset.

In the formal simulation, a finer grid with a wider spanwise domain will be employed, along with additional ramp angle cases. The intensity of broadband disturbances will be reduced to ensure that transition occurs near the reattachment point. Spectral proper orthogonal decomposition and Fourier mode decomposition will be applied to gain deeper insights into the breakdown mechanism leading to turbulence.

References

- [1] V. Tsakagiannis, C. Hader and H. F. Fasel Numerical Investigations of the Linear and Nonlinear Transition Stages for a Hollow Cylinder Flare at Mach 5. *AIAA AVIATION FORUM AND ASCEND 2024*.
- [2] G. Zhao, T. Ma, Z. Chen, Z. Zhang, J. Hao, and C.-Y. Wen. Investigation of streamwise streak characteristics over a compression ramp at Mach 4. *Physics of Fluids*, 36(10): 104121, 2024.
- [3] M. Lugrin, S. Beneddine, C. Leclercq, E. Garnier, and R. Bur. Transition scenario in hypersonic axisymmetrical compression ramp flow. *Journal of Fluid Mechanics*, 907: A6, 2021.

RESONANT WAVES IN TRANSITIONAL HYPERSONIC SEPARATED FLOWS

Clément Caillaud¹, Mathieu Lugin², Sébastien Esquieu¹

¹ CEA-DAM, CESTA, 15 Avenue des Sablières, 33114, Le Barp, France,

² DAAA, ONERA, Institut Polytechnique de Paris, F-92190 Meudon - France

This research highlights new results in transitional separated flows found in a combined experimental and numerical investigation of hypersonic boundary layer transition. The study is carried on a Cone-Cylinder-Flare geometry with a flare angle of $\theta_f = 12^\circ$. The wind tunnel operates at a Mach number of $M_\infty = 7$ and Reynolds numbers ranging from the laminar to the fully turbulent regime. Among the different routes to turbulence existing on such geometries, a complex transition scenario involving multiple modes is observed for large to moderate separation length. Specifically, the interplay of upcoming boundary-layer disturbances produced by the growth of convective instabilities and the laminar separated flow on the cylinder-flare region is studied. For such coupled dynamics between the disturbance environment and the separated region, our experimental and numerical results show that the Mack second-mode wave, which is usually deemed to remain neutral in the separated region, follows a nontrivial mode exchange mechanism with successive acoustic resonant waves within the separated region, leading to the growth of multiple frequency peaks. This scenario is contrasting with previous results, where the first Mack-mode was deemed to be the only relevant unsteady waves in the separated region.

In order to discuss these dynamics, experiments are probed by using high-speed Schlieren imagery and spectral methods (Spectral Proper Orthogonal Decomposition & Bispectral Mode Decomposition). The optical diagnostics are also coupled to high-frequency wall pressure measurements to further probe the flow response to wind-tunnel disturbances. The experimental observations are complemented by global stability analyses using the Resolvent framework to identify linear mechanisms at play within the separation region. In the separated region, the primary instability mechanisms are numerically and experimentally identified, and their subsequent evolution are quantified in order to clarify the leading energy transfer in the mean flow region. Using these tools, the acoustic resonance of hypersonic instabilities is measured in the separated region for the first time. This study highlights the advantages of combining data-driven methods and global stability tools to draw a clearer picture of the transition scenarios on such separated flows under wind tunnel conditions.

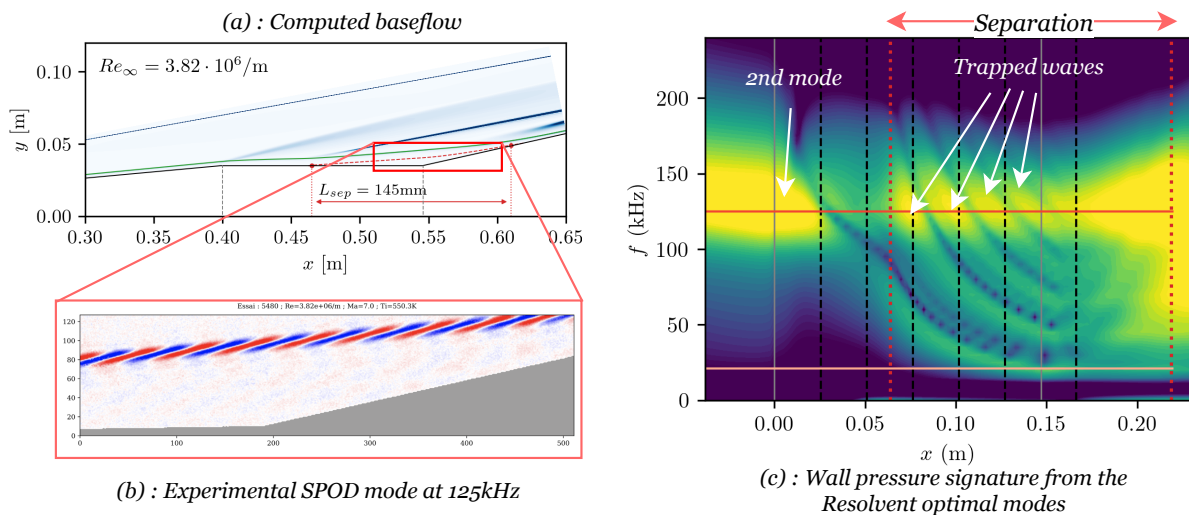


FIGURE 1. Summary of the computed and experimentally measured data along the separation region on the CCF12 geometry

MODERATE NOSE BLUNTNESS EFFECTS ON TRANSITION INSTABILITIES: A RESOLVENT ANALYSIS

N. d'Éprémesnil¹, C. Caillaud¹, G. Lehnasch², M. Olazabal¹, P. Jordan²

¹CEA-CESTA, 15 Avenue des Sablières, Le Barp, France

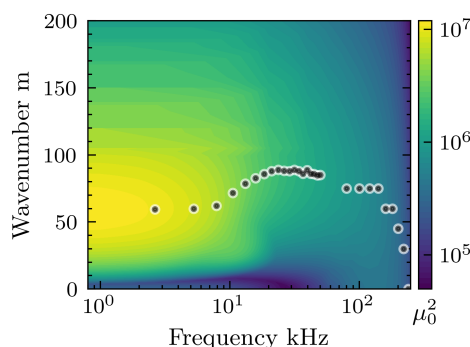
²Département Fluides, Thermique, Combustion, Institut PPRIME CNRS UPR 3346, ISAE-ENSMA, 86036 Poitiers, France

This research presents global stability analysis using the resolvent operator on a moderately blunt cone at Mach number $M = 6$ and nose-radius base Reynolds number $Re_{R_n} = 90\,000$ with half angle 7° . The nose-tip bluntness introduces a bow shock detached in front of the tip, followed by a subsonic region and an entropy layer above the boundary layer which substantially changes the base flow compared to a canonical sharp-nose geometry. Such changes in the flow lead to a strong attenuation of the Mack modes, responsible for transition in the canonical sharp case. In this study, we investigate other linear mechanisms possibly leading to transition.

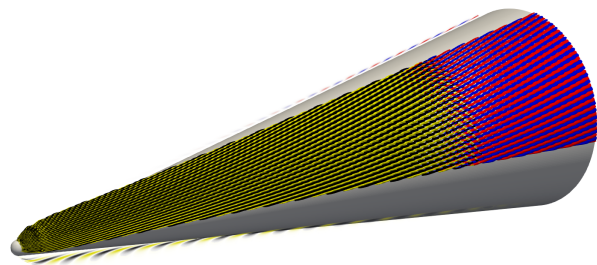
Optimal growth theory associated with the Harmonic Linearised Navier-Stokes Equations (HLNSE) and Parabolised Stability Equation (PSE) has shown non-negligible N-factor growth associated with streak and entropy layer modes, [3]. These mechanisms have been shown to produce transition in Direct Numerical Simulation (DNS), with an initial perturbation located in the entropy layer far from the boundary layer, [1]. Additionally, schlieren visualisations, have shown elongated wisp structures in the entropy layer, [2], providing further credibility to the role of entropy layer modes in transition.

Although these studies highlight a possible key role of the entropy layer modes in the laminar-turbulent transition process, a more comprehensive analysis of the receptivity and growth mechanisms at play is still lacking. The present research tackles this issue by using a global linear stability framework and Resolvent operator analysis. The aim is to extend past studies by providing a comprehensive cartography of all the linear instabilities that can exist on a moderately blunt cone baseflow considering the global flow structure, as well as providing insight into the receptivity support. Resolvent analysis is used to produce optimal gain maps, see figure a, for both isothermal and adiabatic wall conditions in comparison to a sharp isothermal cone reference. It reveals the presence of multiple growing mechanisms for isothermal, and adiabatic walls, such as : streaks ; entropy layer modes, or 1st Mack unstable modes. The streak mode is the most amplified in the isothermal case, followed of entropy layer modes. These entropy layer modes present force almost only kinetic energy that correspond to a very strong wall-normal velocity forcing located high in the entropy layer, see figure b. The associated response is dominated by a strong temperature response in the entropy layer that peaks slightly before the end of the domain. At iso-azimuthal wavenumber, these modes have the same forcing and response structure, independent of frequency.

Our study shows that streaks are the most amplified, followed by entropy layer modes, whose forcing structure extends away from the cone. This suggests that environmental perturbations could more easily trigger the growth of entropy layer modes, potentially leading to turbulence.



(a) Map of optimal gain for the isothermal case, ● most amplified mode at given f



(b) 3D representation of the isothermal entropy layer mode at $m = 88$, $f = 35\text{kHz}$, the forcing is in black-yellow and the response in red-blue

- [1] Hartman et al. “Nonlinear transition mechanism on a blunt cone at Mach 6: oblique breakdown”.
- [2] Kennedy et al. “Characterization of instability mechanisms on sharp and blunt slender cones at Mach 6”.
- [3] Paredes et al. “Nonmodal Growth of Traveling Waves on Blunt Cones at Hypersonic Speeds”.

INTERPLAY BETWEEN TRANSONIC BUFFETING AND FLUTTER

Javier Sierra-Ausin¹, Flavio Giannetti²

¹ONERA/DMPE, Université de Toulouse, 31055 Toulouse, France

²Dipartimento di Ingegneria Industriale, Università degli studi di Salerno, 84084 Fisciano (SA), Italy

Shock buffeting on wings is a phenomenon caused by the strong interaction between the shock wave and the boundary layer, in turn inducing a self-sustained feedback mechanism which is usually detrimental to the structural integrity. Previous studies using global stability analysis have shown the existence of two instability branches, a two-dimensional mode of low frequency when the sweep angle Λ is null, and a high frequency mode with increasing Λ . In the case of a NACA0012 airfoil Crouch et al. [1, 2] evidenced the existence of a low-frequency unstable global mode responsible of the two-dimensional buffeting mode. Sartor et al. [3] obtained a good comparison with experiments carried out by [4] in the case of the OAT15a airfoil using the Spallart-Allmaras turbulence model. More recently, in swept wings, Paladini et al. [5] obtained a global unstable mode whose frequency grows as $\omega \propto \tan(\Lambda)$.

In this study, we focus on a simplified structural model, and we aim to understand the interplay between the aerodynamic buffeting instability and the structural degrees of freedom. In transonic conditions, a sharp decrease of the onset flutter in terms of the dynamic pressure is known as the transonic dip. Karnick et al. [6] studied the transonic dip in a similar simplified model, and they attributed the early appearance of flutter to the shock-induced separation, which is known to be also one of the major causes of the buffeting phenomenon. In order to determine the interplay between the buffeting instability and the transonic dip, we restrict the analysis to the simplest flutter scenario; that is, we consider an aeroelastic model with only two degrees of freedom: heaving and pitching, which account for the first two flutter modes, an sketch is depicted in fig. 1 (left). In this configuration, we analyse the unstable branches and we determine the possible existence of an exceptional point, i.e., a degenerate eigenmode where both instability two or more branches of modes collapse, in the space of parameters that is responsible for the earlier onset of aeroelastic phenomena in transonic conditions.

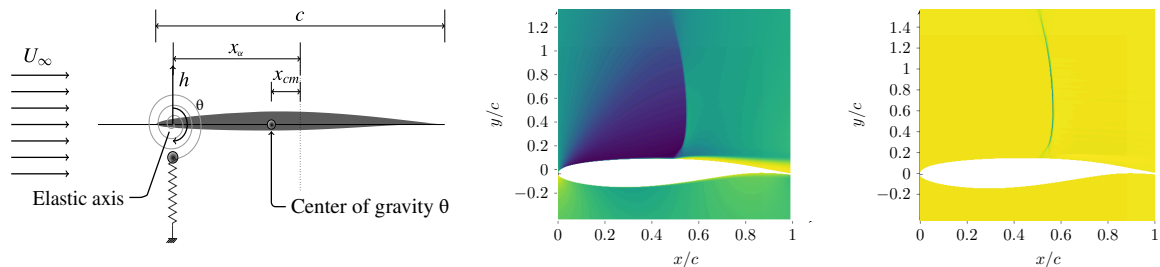


FIGURE 1. (Left) Sketch of the spring-mounted airfoil. (Middle) Steady-state of the OAT15a airfoil computed using Spallart-Allmaras model. (Right) Real part of the temperature component of the unstable two-dimensional global mode.

References

- [1] J. D. Crouch, A. Garbaruk, and D. Magidov, “Predicting the onset of flow unsteadiness based on global instability,” *Journal of Computational Physics*, vol. 224, no. 2, p. 924, 2007.
- [2] J. D. Crouch, A. Garbaruk, D. Magidov, and A. Travin, “Origin of transonic buffet on aerofoils,” *Journal of Fluid Mechanics*, vol. 628, p. 357, 2009.
- [3] F. Sartor, C. Mettot, and D. Sipp, “Stability, receptivity, and sensitivity analyses of buffeting transonic flow over a profile,” *AIAA Journal*, vol. 53, no. 7, p. 1980, 2015.
- [4] L. Jacquin, P. Molton, S. Deck, B. Maury, and D. Soulevant, “Experimental study of shock oscillation over a transonic supercritical profile,” *AIAA Journal*, vol. 47, no. 9, p. 1985, 2009.
- [5] E. Paladini, S. Beneddine, J. Dandois, D. Sipp, and J.-C. Robinet, “Transonic buffet instability: from two-dimensional airfoils to three-dimensional swept wings,” *Physical Review Fluids*, vol. 4, no. 10, p. 103906, 2019.
- [6] P. T. Karnick and K. Venkatraman, “Shock–boundary layer interaction and energetics in transonic flutter,” *Journal of Fluid Mechanics*, vol. 832, pp. 212–240, 2017.

AN EXPERIMENTAL INVESTIGATION OF THE INSTALLATION EFFECTS OF A FLAT PLATE ON SCREECH GENERATION

Laura Denisa Antonuzzi^{1,3}, Matteo Mancinelli², Flavio Giannetti¹, Francesco Petrosino³

¹ DIIN, Università degli Studi di Salerno, 84084 Fisciano (SA), Italy

e-mail: lantonuzzi@unisa.it, fgiannetti@unisa.it

² Dipartimento di Ingegneria civile, informatica e delle tecnologie aeronautiche, Università degli Studi Roma Tre, 00146 Roma, Italy

e-mail: matteo.mancinelli@uniroma3.it

³ CIRA, Centro Italiano Ricerche Aerospaziali, 81043 Capua (CE), Italy

e-mail: fpetrosino@cira.it

This study investigates the effect of a flat plate on screech generation using an experimental approach. Several configurations in which the plate is located at different radial distances from the axis of a converging nozzle were studied: $H = 0.7D$, $H = 0.85D$, $H = 1D$, $H = 1.5D$, $H = 2D$, $H = 2.5D$ and $H = 3D$. Acoustic measurements were performed to evaluate the effect of the plate on the jet aeroacoustics. Power spectral density maps obtained from the acoustic measurements, illustrated in Fig. 1, show that when the plate is located at a distance less than one diameter ($H < 1D$), the staging mechanism of the axisymmetric modes A1 and A2 is altered, since mode A2 is suppressed and mode A1 is extended to flow conditions for which mode A2 is usually active in the free-jet case [1]. Under the same conditions, modes B and C also exhibit modified dynamics, with mode C being suppressed and mode B being extended to M_j for which mode C is usually active in free-jet conditions. Additionally, a frequency splitting is exhibited by mode B for the radial distance $H = 0.7D$. The plate effect on screech generation was found to be robust with respect to variations of the jet-plate alignment, that is, roll and pitch angles and slight translations of the surface along both the streamwise and transverse directions. Wavelet analysis was explored to study the staging dynamics of screech and to assess whether modes A2 and C appear intermittently. Schlieren measurements were also carried out to determine whether the changes observed in the screech behaviour are correlated with changes in the jet shock-cell structure.

(Acknowledgements: L. D. Antonuzzi' works is cofinanced by NRRP, (Mission 4 "Education and Research").

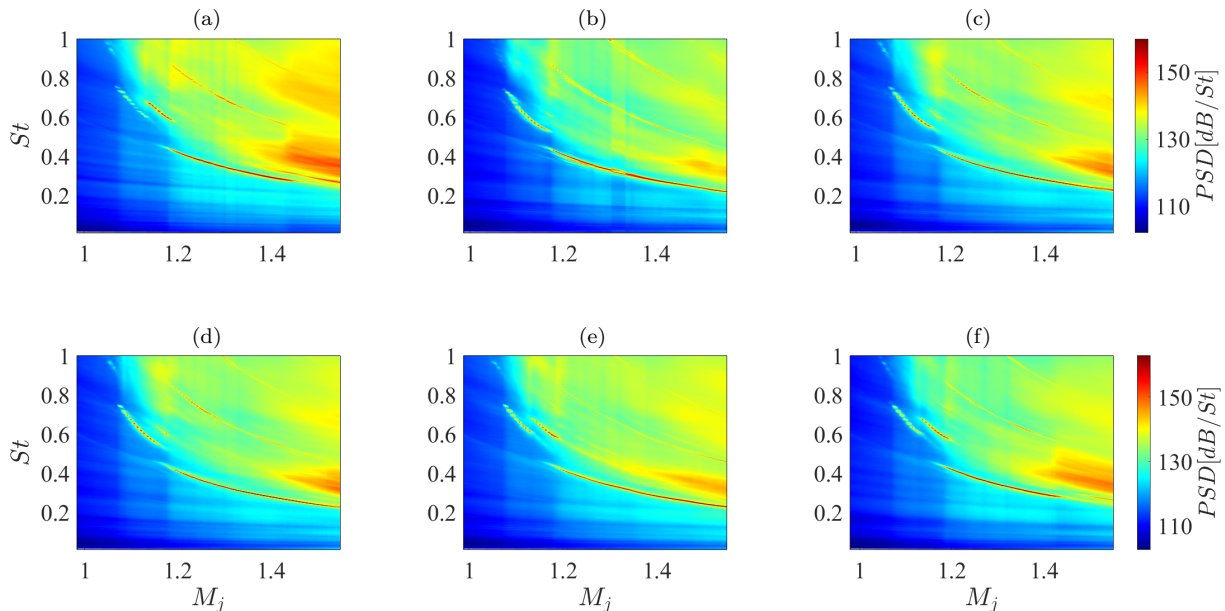


FIGURE 1. Power Spectral Density maps as a function of Strouhal number and fully expanded jet Mach number, measured by the far-field microphone at $\psi = 120^\circ$ and $\theta = 0^\circ$, for the following configurations: (a) free jet, (b) jet-plate with radial distance of $H = 0.7D$, (c) $H = 0.85D$, (d) $H = 1D$, (e) $H = 1.5D$ and (f) $H = 2.5D$.

References

- [1] M. Mancinelli, S. Meloni and R. Camussi. *AIAA*. Jet-plate interaction in a supersonic screeching jet.

INSTABILITIES IN SUBSONIC INSTALLED JET

Alessandro Franchini¹, Mateus Avanci¹, Nicolas Alferez², Jean-Christophe Robinet¹

¹*DynFluid Laboratory, Arts et Métiers Institute of Technology, Paris, France*

²*DynFluid Laboratory, CNAM, Paris, France*

In recent times, jet noise during takeoff has become a significant concern for commercial aircraft manufacturers. To mitigate the health impacts of jet noise in densely populated areas, stringent regulations on aircraft noise have been implemented [2]. This, along with the need to reduce fuel consumption and green house gas emissions, has driven to substantial modifications of turbofan engines. Specifically, the jet diameter is increased, introducing installation noise, which arises from the interaction between the jet flow and solid surfaces such as wings and flaps. In order to understand these groups of phenomena, many studies are being pursued within the aeroacoustics community from many different perspectives: experimental studies, mathematical models and CFD simulations.

Some studies [1] looked at the installed jet problem by exploring the interaction between large coherent turbulent structure and the aircraft wing, by means of geometrically complex CFD simulations with hybrid RANS/LES models. Recent experimental studies held in anechoic room with wind tunnel by Institut Pprime [3] explored a vast range of different parameters, generating a large database and insights on the fundamental structure of the interactions. In this work, the interaction between a subsonic and adiabatic jet and a flat plate is studied as a function of physical and geometric parameters (see Fig. 1). The experiments show that when the jet interacts strongly with the plate, a tonal dynamic appears, characteristic of a resonance mechanism between two waves propagating respectively upstream and downstream. The aim of this study is to analyse the nature of the instabilities developing in the installed jet. To do this, the global stability of the flow is studied in order to determine the resonance conditions and the modes associated with them (Fig. 2a, 2b). On the other hand, when the flow is convectively stable, the study is completed by a 3D PSE analysis extracting the dominant convective modes and showing that the non-linear dynamics (by SPOD) is multimodal in nature (Fig. 2c).

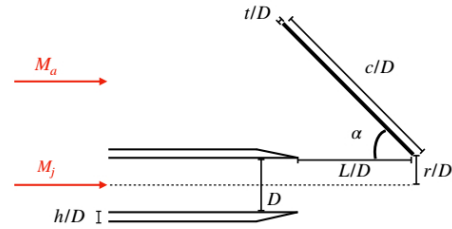
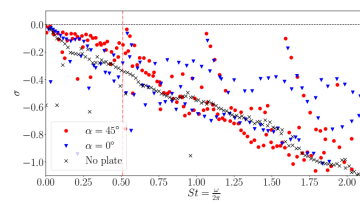
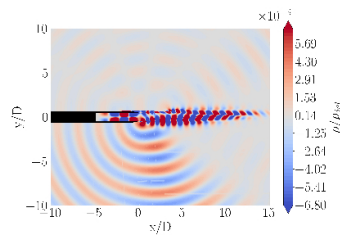


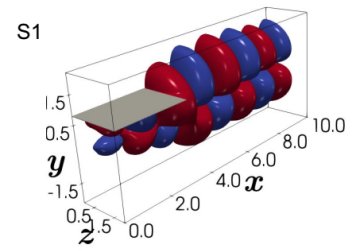
Figure 1: Sketch of the jet plate interaction with important geometrical parameters



(a) Global eigenspectrum: $\lambda = \sigma + i\omega$ for: (x): free jet; \bullet : $\alpha = 0^\circ$; \bullet : $\alpha = 45^\circ$



(b) Eigenfunction: $\Re [\tilde{p}(x, y)/\rho_{jet}]$



(c) Dominant 3-D PSE mode, $\Re [\tilde{p}(x, y, z)]$

Figure 2: (a) and (b): Global Stability analysis; (c) 3D-PSE

References

- [1] Huber, J., Pont, G., Jordan, P. et al. Wavepacket Modelling of Jet-Flap Interaction Noise: from Laboratory to Full-Scale Aircraft. *Flow Turbulence Combust*, 113, 773–802., 2024.
- [2] Pepper, C.B., Nascarella, M.A., Kendall, R.J. A review of the effects of aircraft noise on wildlife and humans, current control mechanisms, and the need for further study. *Environ Manage.*, 32(4):418-32, 2003.
- [3] Amaral, F.R., Lebedev, A., Jordan, P. Experiments on installed jet noise. *AIAA AVIATION*, 32(4):418-32, 2023.

SENSITIVITY OF IMPINGING JET NOISE TO FLOW CONDITIONS INSIDE THE NOZZLE

Zhenyang Yuan¹, Vincent Jaunet², Peter Jordan², André V. G. Cavalieri³, Ardeshir Hanifi¹

¹*FLOW, Department of Engineering Mechanics, KTH Royal Institute of Technology, Stockholm, Sweden*

²*Département FTC, Institut Pprime, CNRS-Université de Poitiers-ISAE-ENSMA, Poitiers, France*

³*Divisão de Engenharia Aeronáutica, Instituto Tecnológico de Aeronáutica, São José dos Campos, Brazil,*

In this work, we investigate the tonal noise generation from an impinging jet. Several high fidelity implicit large eddy simulations are performed, focusing on a high subsonic ($M_j = 0.9$), axisymmetric round jet with a geometry and operating conditions aligned with experiment [1]. Cases with $Re = 1 \times 10^5$ with/without forced boundary layer tripping and $Re = 2 \times 10^5$ without forced boundary layer tripping are investigated. The results suggest that at the lower Reynolds number, the boundary layer within the nozzle is laminar, and thus Kelvin-Helmholtz coherent structures, or wavepackets, in the jet have low amplitude. A boundary layer tripping is a necessary condition for significant amplitudes of Kelvin-Helmholtz wavepackets, which eventually leads to tonal noise generation by a feedback loop with the acoustic waves generated at the impinging plate [2]. At the higher Reynolds number case, the untripped boundary layer status is found to be sensitive: above a critical Reynolds number Re_{cr} , the upstream travelling guided jet wave could force the transition of the boundary layer, and below Re_{cr} , the boundary layer re-laminarize naturally. The pressure fluctuation fields visualization can be found in figure 1.

This shows that the feedback loop in impinging jets is also affected by the nozzle boundary layer conditions. This is further analysed by stability analyses of the Kelvin-Helmholtz and acoustic waves involved in the feedback loop, which extract growth rates at relevant flow locations and allow the determination of corresponding amplitudes for each configuration studied in this work.

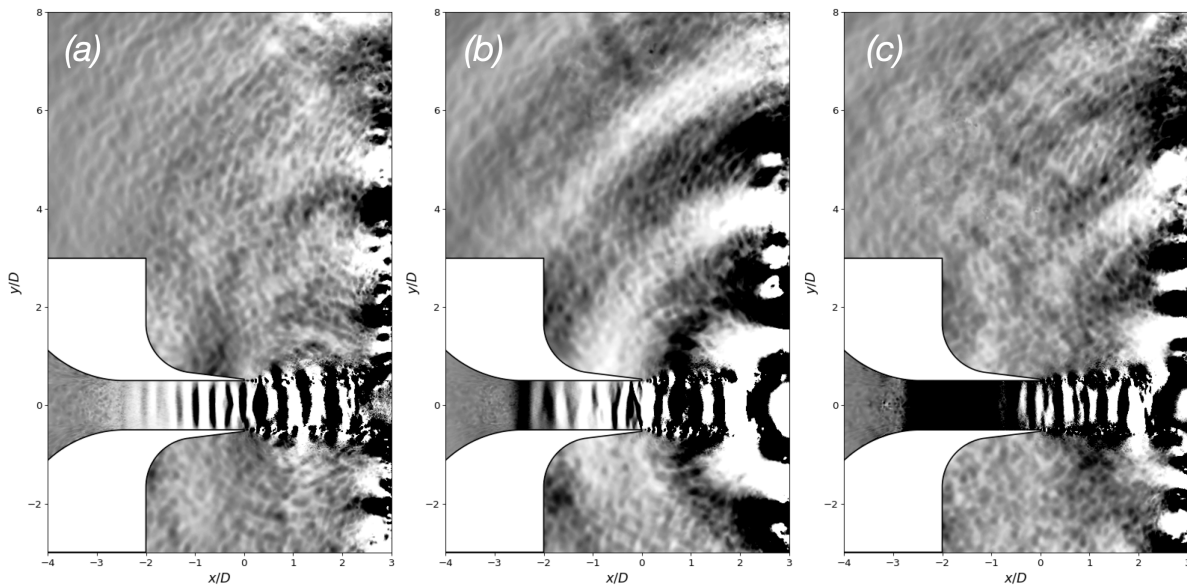


FIGURE 1. *The visualization of the pressure fluctuation field of three cases: (a) $Re = 1 \times 10^5$ untripped, (b) $Re = 1 \times 10^5$ tripped and (c) $Re = 2 \times 10^5$ untripped. The case (c) is still under the transition phase.*

References

- [1] P. Beltra and V. Jaunet and G. Lehnasch and M. Mancinelli. Surrounding effects and hysteretical behavior of impinging jets resonances. *57th 3AF International Conference on Applied Aerodynamics*, pp:1-7, 2023.
- [2] D. Edgington-Mitchell. Aeroacoustic resonance and self-excitation in screeching and impinging supersonic jets – A review *Int. J. Aeroacoustics*, 18(2-3):118-188, 2019.

EXPERIMENTAL CONTROL OF JET-SURFACE INTERACTION NOISE

M. Mancinelli¹, D. Audiffred², E. Martini³, P. Jordan³, A.V.G. Cavalieri², A. Lebedev³

¹Department of Civil Engineering, Computer Science and Aeronautical Technologies, Università Roma Tre, Rome, Italy

²Department of Aeronautical Engineering, Instituto Tecnológico de Aeronáutica, São José dos Campos, Brazil

³Department of Fluids, Thermal Science and Combustion, Institut Pprime, Poitiers, France

This paper presents an experimental application of reactive control to jet installation noise based on destructive interference. The work is motivated by the success of previous studies in applying this control approach to several flow systems, among which turbulent jets [1, 2, 3]. We exploit the fact that jet-surface interaction (JSI) noise is underpinned by wavepackets that can be modelled in a linear framework and develop a linear control strategy where piezoelectric actuators situated at the edge of a scattering surface are driven in real time by sensor measurements in the near field of the jet, the objective being to reduce noise radiated in the acoustic field at a given observer position. The control mechanism involves imposition of an anti-dipole at the trailing edge to cancel the scattering dipole that arises due to an incident wavepacket perturbation, as schematically described in figure 1(a). We explore two different control strategies: (i) the inverse feed-forward approach (IFFC), where causality is imposed by truncating the control kernel, and (ii) the Wiener-Hopf (WH) approach, where causality is optimally enforced in building the control kernel. We show that the Wiener-Hopf approach has better performance than that obtained using the truncated inverse feed-forward kernel. Broadband noise reductions of up to 75% (corresponding to ≈ 6 dB) are achieved, as shown in figure 1(b).

For the Wiener-Hopf approach, we explore the directivity pattern of the noise modifications achieved along a polar arc. Specifically, the control reduces the radiated noise for all the upstream polar positions, where JSI noise has its preferential propagation direction, and amplifies the intensity of the acoustic emissions for downstream polar positions. This result is consistent with the physics of installed jet noise radiation, given that JSI is not the dominant noise source for downstream polar positions where, on the contrary, 'direct' jet noise dominates over the installed one. We, finally, explore robustness features of the controller to changes of the flow conditions. Specifically, we calculate the control kernel for a given jet Mach number, M^* and explore control effectiveness for M variations in the range $M^* \pm 50\%M^*$. We show that control remains still effective and the control authority monotonically reduces as the Mach number moves away from M^* . Specifically, noise reductions achieved decreases of $\approx 60\%$ for $M = M^* + 50\%M^*$.

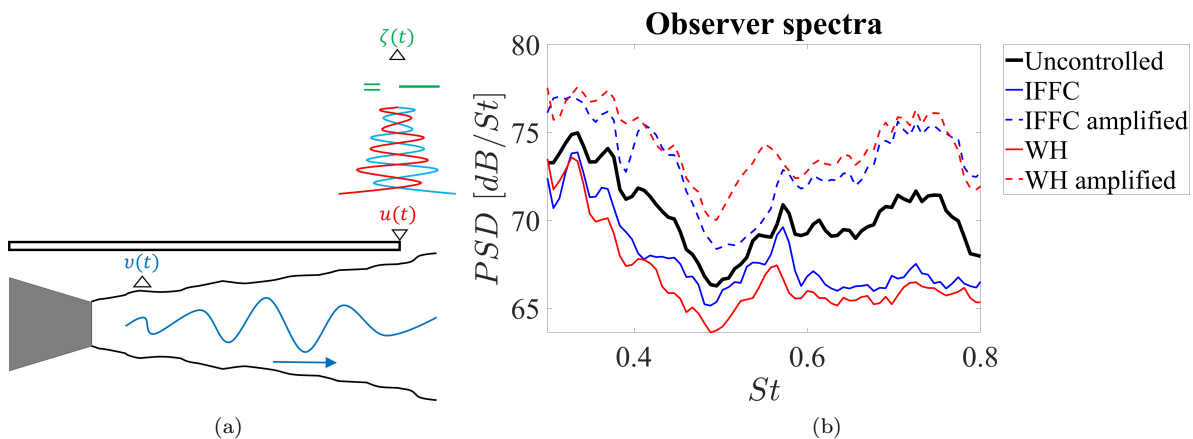


FIGURE 1. (a) Schematic representation of the wave-cancellation strategy for the JSI noise control. v denotes the near-field sensor, u the actuator and ζ the observer in the acoustic field. (b) Power spectral densities at the observer position ζ .

References

- [1] Maia, I. A., Jordan, P., Cavalieri, A. V. G., Martini, E., Sasaki, K. and Silvestre, F. J. Real-time reactive control of stochastic disturbances in forced turbulent jets. *Phys. Rev. Fluids*, 6(12), 123901, 2021.
- [2] Maia, I. A., Jordan, P. and Cavalieri, A. V. G. Wave cancellation in jets with laminar and turbulent boundary layers: The effect of nonlinearity. *Phys. Rev. Fluids*, 7(3), 033903, 2022.
- [3] Audiffred, D. B. S., Cavalieri, A. V. G., Maia, I. A., Martini, E. and Jordan, P. Reactive experimental control of turbulent jets. *J. Fluid Mech.*, 994, A15, 2024.

ENSEMBLE VARIATIONAL-BASED OPTIMIZATION FOR RESOLVENT ANALYSIS

Riccardo Maranelli^{1,2}, Vincent Mons¹, Jean-Camille Chassaing³, Taraneh Sayadi²

¹DAAA, ONERA, Institut Polytechnique de Paris, 92190 Meudon, France

²M2N, Conservatoire National Arts et Métiers, Paris, France

³Sorbonne Université, CNRS, Institut Jean Le Rond d'Alembert, UMR 7190, Paris, France

Understanding the worst-case scenario that leads to the most amplified energy growth is key to predicting flow instability. In a linear setting, resolvent analysis provides a powerful framework for this assessment, helping to inform and design effective flow control strategies. This study aims to recover the forcing mode that leads to the largest energy amplification in the flow, using the resolvent operator. It focuses on reconstructing the resolvent forcing mode of a system at a given frequency using ensemble-based variational techniques (EnVar) [1, 3]. This approach provides an alternative to methodologies that involve performing the eigenvalue decomposition of an operator formed by the composition of the resolvent operator and its adjoint [4], and could be extended to other applications for identifying conditions that lead to energy growth. In fact, while developing adjoint models can be a complex task, the EnVar method is non-intrusive, making it easier to formulate and implement. The search for an optimal forcing term takes place within a subspace defined by an ensemble of realizations, each representing a simulation with a different forcing. The iterative procedure aims to determine the optimal forcing by linearly combining ensemble members based on their evaluations.

We apply this methodology to perform the optimization on the energy gains (amplification magnitude) of the frequency response in a two-dimensional cavity flow [2]. The ensembles are generated using Gaussian processes. The control vectors that result successfully approximate the forcing given by a more standard eigenvalue analysis that involves the adjoint of the resolvent operator, as illustrated in Figure 1. While the computational benefits of the EnVar optimization method for resolvent analysis may become more apparent in complex applications, we emphasize its ease of implementation and computational efficiency in studying flow instability (with potential extension to a nonlinear framework), supporting the development of control strategies in complex and unstable scenarios that we aim to address, such as rotor-stator cavities.

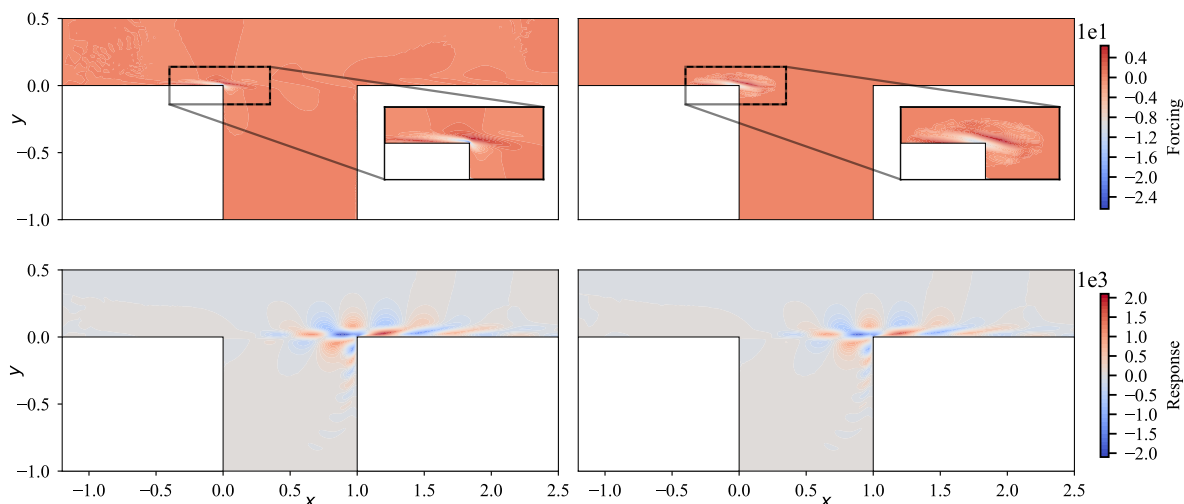


Figure 1: Forcings (top row) and responses (bottom row) derived from eigenvalue analysis (left column) and through the EnVar methodology for an approximation of the forcing (right column).

References

- [1] V. Mons, Y. Du, and T. Zaki. Ensemble-Variational Assimilation of Statistical Data in Large-Eddy Simulation. *Phys. Rev. Fluids*, 6(10):104607, 2021.
- [2] C. Leclercq, F. Demourant, C. Poussot-Vassal, and D. Sipp. Linear iterative method for closed-loop control of quasiperiodic flows. *J. Fluid Mech.*, 868:26–65, 2019.
- [3] R. Jahanbakhshi and T. A. Zaki. Nonlinearly most dangerous disturbance for high-speed boundary-layer transition. *J. Fluid Mech.*, 876:87–121, 2019.
- [4] L. V. Rolandi, J. H. M. Ribeiro, C.-A. Yeh, and K. Taira. An Invitation to Resolvent Analysis. *Theor. Comput. Fluid Dyn.*, 38(5):603–639, 2024..

SIMULATION AND PHYSICS-BASED MODELING FOR CONTROLLING SHOCK-LADEN FLOWS

Daniel Bodony, Alberto Padovan, and Sandeep Murthy

*Department of Aerospace Engineering
University of Illinois at Urbana-Champaign*

Shocks are frequently present in high-speed flows of fundamental and applied interest, possibly as a dynamically-important flow feature. While many numerical methods exist to simulate shock-laden flows [1], only recently have they been modified such that their linearizations also provide accurate forward and adjoint sensitivities [2, 3] and verification analytical solutions available [2].

With numerical methods for non-linear simulations and linearized analysis of flows with shocks available, it is natural to consider how to develop low-rank representations of the flows, usually from data, for use in rapid, approximate analysis, parameter surveys, and/or controller design. Flows with shocks are characterized by mixtures of sharp features, possibly in motion, embedded within an otherwise smooth flow field. The presence of one or more nearly discontinuous features challenges rank-reduction methods, making low-rank models elusive.

In this work, we present recent developments focused on low-rank methods suitable for shock-laden flows. Borrowing from our prior work on rank-reduction of multiphase flows [4, 5, 6, 7], we develop a ‘pull-back’ mapping that seeks to identify a coordinate transformation $\xi = \Xi(x, t)$ to increase the dominance of the first singular value of the data matrix $\hat{X} = [u(\xi, t_1), u(\xi, t_2), \dots]$ relative to the original data $X = [u(x, t_1), u(x, t_2), \dots]$. The time rate-of-change of the mapping minimizes the objective $J = \sum_{k=0}^{m-1} \sqrt{\sigma_k^2(\hat{X}) + \varepsilon}$, where σ_k is the k th singular value of \hat{X} and $\varepsilon \ll 1$ is a very small number to ensure $J > 0$. A sample outcome is shown in Figure 1 for Burgers’ equation with a shock formation.

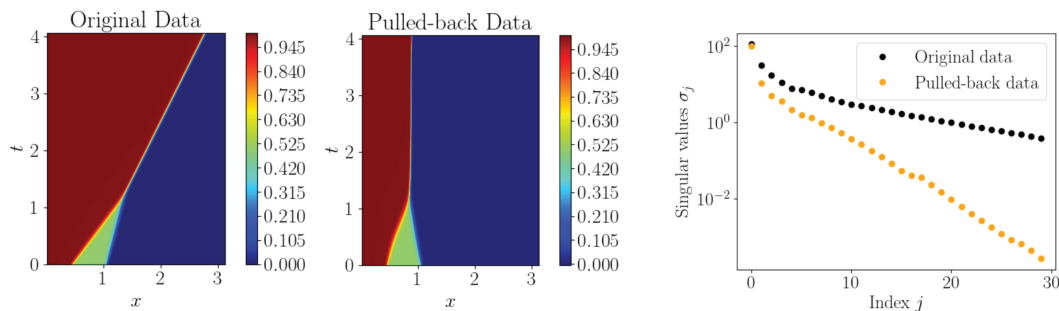


FIGURE 1. Example of data transform of shock-laden flow to enable low-rank reduction.

References

- [1] S. Pirozzoli. Numerical methods for high-speed flows. *Annual Review of Fluid Mechanics*, 43:163–194, 2011.
- [2] S. R. Murthy and D. J. Bodony. Resolvent analysis of shock-laden flows. *Journal of Fluid Mechanics*, Under revision, 2025.
- [3] Kamil Dylewicz, Rômulo Bessi, Pedro Paredes, Leonardo Alves, and Vassilis Theofilis. On shock-capturing schemes for the linear stability analysis of high-speed flows. *Proceedings of the Royal Society of London-A*, 481(2311), 2025.
- [4] A. Fikl and D. J. Bodony. Jump relations of certain hypersingular Stokes kernels on regular surfaces. *SIAM J. Appl. Math.*, 80(5):2226–2248, 2020.
- [5] A. Fikl and D. J. Bodony. Adjoint-based interfacial control of viscous drops. *Journal of Fluid Mechanics*, 911(A39), March 2021.
- [6] P. Sashittal, R. Chiodi, T. B. Morgan, O. Desjardins, T. J. Heindel, and D. J. Bodony. Modal analysis and interface tracking of multiphase flows using dynamic mode decomposition. *International Journal of Multiphase Flow*, 157(104198), 2022.
- [7] A. Fikl and D. J. Bodony. Adjoint-based control of three dimensional stokes droplets. *Journal of Computational Physics*, 494(112532), 2023.

LINEAR MODELING AND CONTROL OF STANDING-WAVE LOW-FREQUENCY DYNAMICS OF A TURBULENT SEPARATION BUBBLE

Lukas M. Fuchs¹, Jakob G.R. von Saldern¹, Ben Steinfurth², Julien Weiss², Kilian Oberleithner¹

¹Laboratory for Flow Instabilities and Dynamics, Institute of Fluid Dynamics and Technical Acoustics, Technical University Berlin

²Institute of Aerodynamics, Technical University Berlin

Turbulent separation bubbles (TSBs) exhibit complex dynamics with significant implications across various engineering applications. Despite advances in both experimental [1] and numerical [2, 3] research, the understanding of the low-frequency breathing motion of TSBs (i.e., the low-frequency expansion and contraction of the bubble) remains incomplete. This phenomenon is known to induce detrimental effects, including structural vibrations, noise, mechanical fatigue, and fluctuations in thermal loads.

In this presentation, we report on recent experimental investigations conducted in a half-diffuser configuration, providing empirical evidence of large-scale standing wave patterns governing the breathing motion. We present a low-dimensional model of this motion based on resolvent analysis, considering three-dimensional perturbations on the two-dimensional mean flow. This model, which consists of the superposition of left- and right-traveling resolvent modes resonating via the channel sidewalls, is consistent with data-driven modes obtained through modal decomposition of velocity field measurement data.

Furthermore, we aim to uncover the physical mechanism driving the low-frequency breathing motion. Preliminary analysis of the resolvent model in cross-sections reveals an interaction between streamwise streaks and cross-stream vortices which is characteristic of the lift-up effect [4].

To further investigate the dominant stability mechanisms, we complement the resolvent analysis with a global linear stability analysis. Additionally, we will examine the sensitivity of these dominant modes to external forcing through an experimental campaign, in which we excite spanwise coherent structures to actively regulate the low-frequency breathing motion. This work advances the understanding of TSB dynamics and provides new perspectives on mitigating the adverse effects of this phenomenon in practical applications.

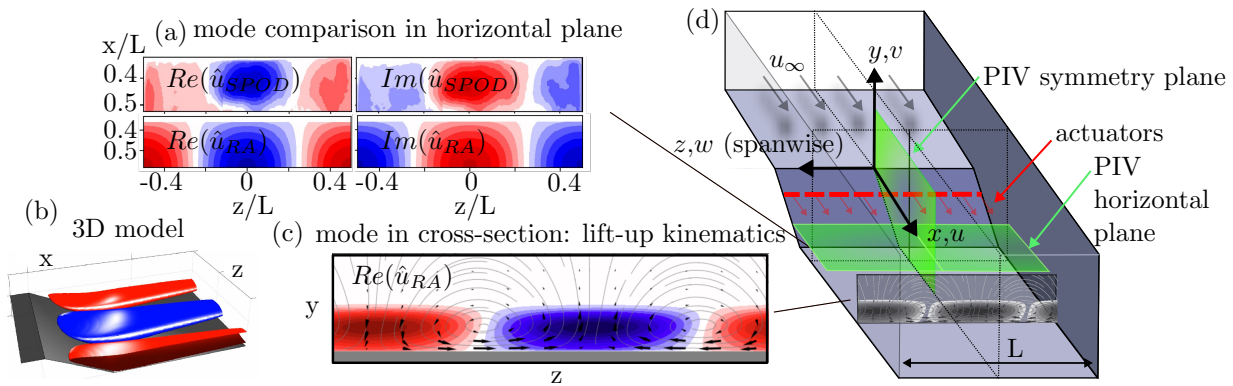


FIGURE 1. (a) Mode comparison in horizontal plane showing leading SPOD mode for $St = 0.01$ and standing wave Resolvent model for $St = 0.01$ and $\beta \frac{L}{2\pi} = 1$; (b) Iso-surface of real part of streamwise component of the standing wave Resolvent model at $St = 0.01$, $\beta \frac{L}{2\pi} = 1$; (c) Real part of streamwise Resolvent response mode (travelling wave) as blue-red contours and real part of span- and crosswise response mode as streamline and vector plots at $St = 0.01$ and spanwise wavenumber $\beta \frac{L}{2\pi} = 1$; (d) Experimental setup showing the position of the two PIV planes, the jet actuation used for control studies and the cross-section.

References

- [1] A. Mohammed-Taifour, and J. Weiss. Unsteadiness in a large turbulent separation bubble. *Journal of Fluid Mechanics*, 799, 2016.
- [2] W. Wu, et al. Spatio-Temporal dynamics of turbulent separation bubbles. *Journal of Fluid Mechanics*, 883, 2019.
- [3] C. Cura, et al. On the low-frequency dynamics of turbulent separation bubbles. *Journal of Fluid Mechanics*, 991, 2024.
- [4] P. J. Schmid, and D. S. Henningson. *Stability and Transition in Shear Flows*. Springer, New York, 2001.

SLOW ACTIVE CONTROL OF ROAD VEHICLE WAKES: A STRATEGY FOR DRAG REDUCTION IN VARYING FLOW CONDITIONS

Kacper Janczuk¹, Adrian Gaylard², Aimee S. Morgans¹

¹Department of Mechanical Engineering, Imperial College London, London SW7 2AZ, UK

²Vehicle Engineering, Jaguar Land Rover, Coventry CV3 4LF, UK

Aerodynamic drag significantly influences vehicle performance at speeds exceeding 70km/h , with wake dynamics being a primary contributor for bluff-body designs such as SUVs. These vehicles exhibit highly non-streamlined geometries, where the wake structure is sensitive to both design parameters and environmental factors such as crosswinds. Addressing this challenge requires adaptive aerodynamic solutions beyond conventional passive control strategies.

This study investigates a benchmark road vehicle geometry, the squareback Windsor body with wheels, using high-fidelity Wall-Resolved Large Eddy Simulation (WRLES). A Gaussian process-based surrogate modelling coupled with Bayesian optimisation (Kriging) is employed to develop a control strategy for varying flow conditions. The study builds upon prior work that optimised a rear roof extension at zero yaw to minimise drag, parametrising its length, angle of incidence, and penetration distance (see Figure 1). The optimisation identified six distinct drag reduction mechanisms, namely diffuser-induced pressure recovery, base size reduction, vertical wake balance modification, separation bubble effects, recirculation region core relocation, and spanwise re-symmetrisation.

The next phase of this research extends the optimisation to nonzero yaw conditions, aiming to develop a control policy for slow, active wake adaptation. By optimising the roof extension geometry across a range of yaw angles, the study will establish a framework for dynamically adjusting aerodynamic elements in response to changing flow conditions. Crucially, we aim to provide extensive analysis of both time-averaged and dynamic features, which provides detailed insight into each parameter's effect on the flow field. While the study at zero yaw angle offered valuable insights into drag reduction mechanisms, we expect the yaw angle study to yield similarly promising physical insights.

This ongoing work contributes to the development of adaptive aerodynamic strategies, offering new insights into the physics of drag reduction mechanisms.

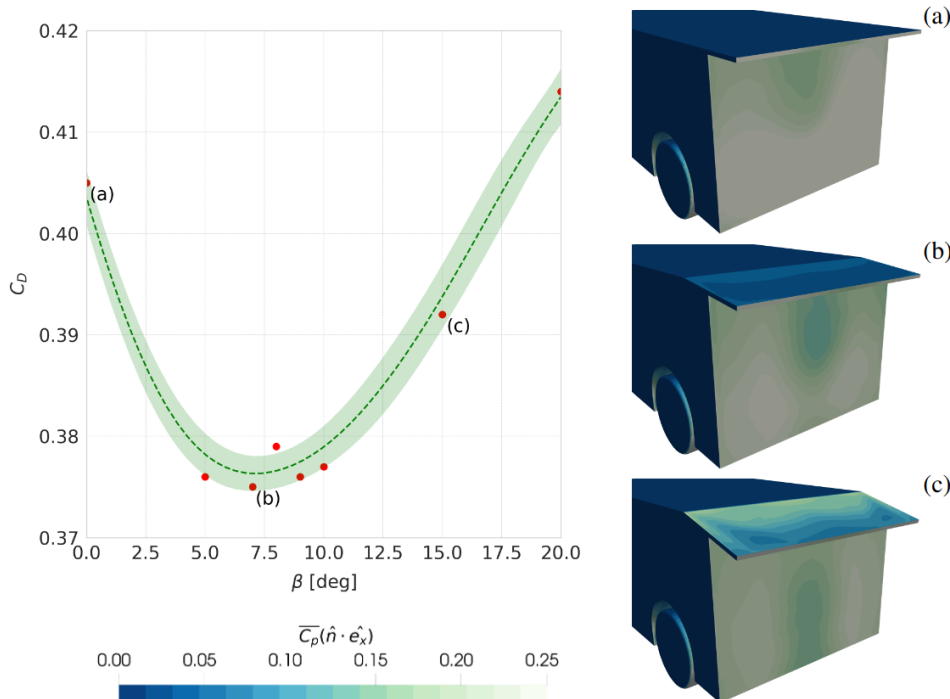


FIGURE 1. Partial dependency study of the angle of incidence, identified as the most influential parameter in the optimisation study at zero yaw. Left: Response surface plot with penetration distance and extension length at their maximum values. Right: Conditionally time-averaged pressure field superimposed on the dot product of the surface normal vector and the streamwise direction for selected simulations, illustrating wake structure modifications.

SWEEPING JETS ACTUATORS FOR FLOW SEPARATION CONTROL: CHARACTERISATION AND APPLICATION ON A CANONICAL RAMP

Mathieu Tocquer¹, Cédric Raibaudo¹, Azeddine Kourta¹

¹Univ. Orléans, INSA-CVL, PRISME UR 4229, F45072, France

Controlling flow separation to enhance aerodynamic performance is still a difficulty to achieve. Separated flows have their own dynamics, with multiple time and space scales, making the optimal actuation difficult to be applied. The purpose of this work is to investigate the efficiency of the sweeping jet actuators (SWJ) to control separated flows. It was demonstrated that SWJs could produce high-frequency oscillations with a moderate pressure supply and high-momentum injection [1], corresponding to the expected requirements for control applications. The flow generated by the SWJ was characterized using hot-wire experiments to estimate its dynamics (oscillation frequency), spatial distribution (length, width, angle), and the generated turbulence. More details can be found here [2].

The performance of SWJs is assessed using a canonical ramp geometry with a 25° slope. A previous work [3] has thoroughly examined this configuration, corresponding to a fundamental separated region, representative of flows downstream an airfoil or a car. Eight SWJ actuators are positioned upstream of the separation. Three jet angles (α) have been tested: 30°, 45° and 90°. The S2 open wind-tunnel of the PRISME laboratory is used for the experimental campaign. Coupled measurements using PIV in the center of the geometry and wall pressure are acquired. Various inlet pressures of the actuators from 0 kPa to 18 kPa, corresponding to momentum coefficients from $C_\mu = 0\%$ to $C_\mu = 20\%$, with $C_\mu = N_j \rho_j U_j^2 S_j / (\frac{1}{2} \rho_\infty U_\infty^2 h w_{ramp})$. More details can be found here [4, 5].

Using the actuators with $\alpha = 30^\circ$, the recirculation region (with length without control $L_R = 4.3h$) is shown to be completely suppressed starting at a minimal momentum coefficient of $C_\mu = 8\%$ (see Fig. 1a). For lower control pressures, the recirculation length is progressively reduced. The drag coefficient C_D , estimated from the wall pressure distribution, is decreasing 30° and 45° actuation angles α of the jets (see Fig. 1b). It proved the capacity of the sweeping jets to be used for the control of separated flows, and to be adapted depending of the incoming flow conditions. The physical mechanisms of the flow under sweeping jet control will also be explained during the conference.

Acknowledgements: Laboratory of Excellence CAPRYSES framework, financial support from Grant No. ANR-11-LABX-0006-01 of the Investissements d'Avenir LabEx CAPRYSES.

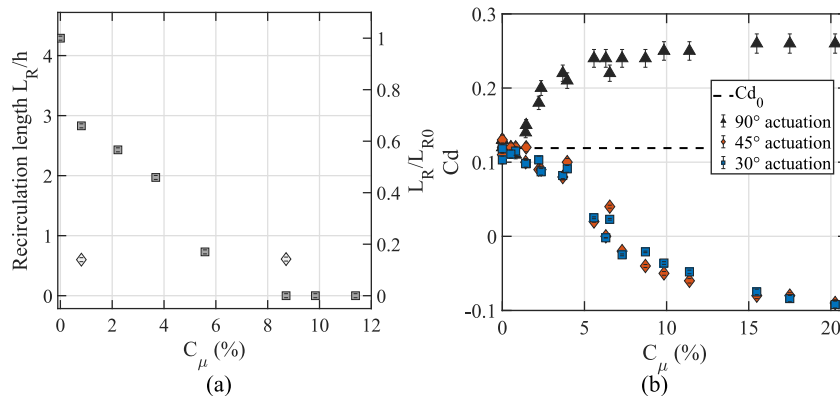


FIGURE 1. Performances of the sweeping jets actuators on the canonical ramp: evolution of (a) recirculation length L_R/h , (b) estimated drag coefficient C_D , with respect to the actuators momentum coefficient C_μ .

References

- [1] D. Hirsch and M. Gharib. Schlieren visualization and analysis of sweeping jet actuator dynamics. *AIAA Journal*, 56(8), 2947-2960, 2018.
- [2] M. Tocquer, C. Raibaudo, and A. Kourta. Experimental hot-wire characterisation of the turbulent jet produced by a sweeping jet actuator in a quiescent environment. *Sensors and Actuators A: Physical*, 377(May), 115739, 2024.
- [3] F. Stella, M. Mazellier, and A. Kourta. Scaling of separated shear layers: an investigation of mass entrainment. *Journal of Fluid Mechanics*, 826, 851-887, 2017.
- [4] M. Tocquer, C. Raibaudo, and A. Kourta. Experimental characterisation of controlled separated flows using high-frequencies sweeping jets. *58th 3AF International Conference on Applied Aerodynamics*, Orléans, France, March 7-29, 2024.
- [5] M. Tocquer, C. Raibaudo, and A. Kourta. Experimental characterisation of a sweeping jet actuator to control turbulent separated flows. *13th International Symposium on Turbulence and Shear Flow Phenomena*, Montreal, Canada, June 25-28, 2024.

EFFECT OF BASE FLOW MODIFICATIONS ON THE GROWTH OF INSTABILITIES IN LAMINAR CHANNEL FLOWS

A.L. Synodinos¹, T. Michelis², M. Kotsonis³

¹*Department of Flow Physics and Technology, Faculty of Aerospace Engineering, Delft University of Technology, 2629 HS Delft, The Netherlands.*

In the study of elastic and acoustic waves, engineered structures known as phononic crystals (PC) can attenuate the amplitude of waves with particular wavelengths (λ) [1]. The fundamental concept of PC relies on a periodic modulation of the propagation medium, with a wavelength λ_{cr} . The dispersive properties of propagating waves are found to strongly depend on the ratio λ_{cr}/λ . In transitional flows, hydrodynamic instabilities possess a wave-like character, however they exhibit fundamental differences from the aforementioned hyperbolic waves, such as their inherent growth or attenuation behavior (a_i). Nevertheless, a periodic medium of propagation can potentially alter their dispersive properties by attenuating their growth (a_i).

This work investigates the application of a fluidic PC in a two-dimensional channel flow (plane Poiseuille flow). The supporting instability modes possess a viscous character (i.e., Tollmien–Schlichting waves). A controlled periodic modulation of the medium is leveraged through stationary modifications of the base flow state vector $[U_{BF}, V_{BF}, 0]$. In this study, base-flow modifications are analytically imposed and parameterized by the modulation amplitude (A) and wavelength (λ_{cr}). Figure 1 illustrates a representative base with a modulated region extending from $x = 100$ to $x = 410$, for $A = 0.05$ and $\lambda_{cr} = 9.94$.

In the modulated region, the streamwise gradient of the velocity components gives rise to highly non-parallel features, necessitating fully elliptical stability solutions. In particular, the in-house Delft Harmonic Navier-Stokes Solver (DeHNSSo) [3] is used to solve the linear harmonic Navier-Stokes equations. In the region of base flow modification (i.e. the "crystal") the modulated growth rate of the propagating instability ($a_{i,mod}$), is extracted for a range of wavelength ratios ($\lambda_{cr}/\lambda_{TS}$). To facilitate comparison among different modes, a change in growth rate is introduced relative to the non-modified clean channel flow ($a_{i,mod} - a_i$). The corresponding stability parameter is illustrated in figure 2 for fifteen crystal cases and twenty instability waves of varying frequency. A clear wavelength dependence of the stability characteristics is found, which diminishes as larger crystal wavelengths are approached. In particular, for $\lambda_{cr}/\lambda_{TS} < 1.3$, a strong destabilization effect is observed, while for $1.3 < \lambda_{cr}/\lambda_{TS} < 2.4$, stabilization is maximized. In conclusion, stationary periodic modulation of the base-flow is found to effectively attenuate the growth rate of incoming instabilities, depending on the specific wavelength ratio between fluidic crystal and instability ($\lambda_{cr}/\lambda_{TS}$).

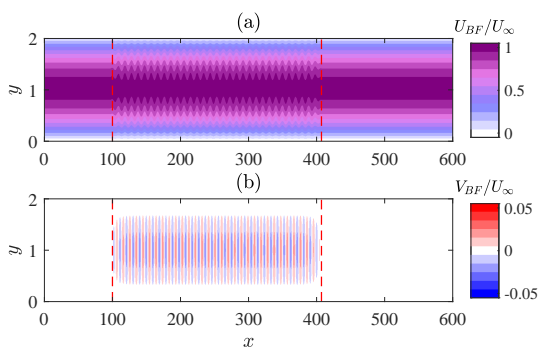


FIGURE 1. (a) streamwise (u) velocity component, (b) wall normal (v) velocity component. Dashed lines indicate the corresponding regions of homogeneous and modulated base flow. $\lambda_{cr} = 9.94$ and $A = 0.05$.

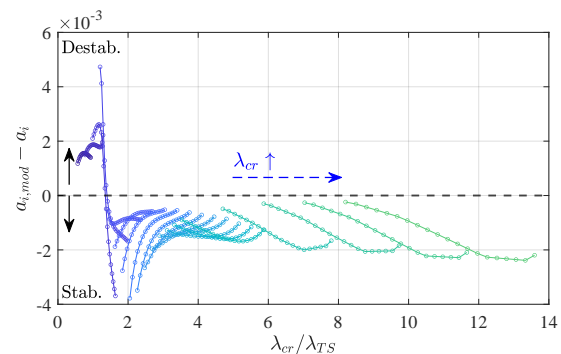


FIGURE 2. $a_{i,mod} - a_i$ as a function of the wavelength ratio $\lambda_{cr}/\lambda_{TS}$. Each color corresponds to a different crystal wavelength. Markers indicate individual discrete modes (i.e. TS waves).

References

- [1] M. I. Hussein, M. J. Leamy, and M. Ruzzene. Dynamics of Phononic Materials and Structures: Historical Origins, Recent Progress, and Future Outlook. *Applied Mechanics Reviews*, 66(4):040802, July 2014.
- [2] S. A. Orszag. Accurate solution of the Orr–Sommerfeld stability equation. *Journal of Fluid Mechanics*, 50(4):689–703, December 1971.
- [3] S. H. Westerbeek, S. Hulshoff, H. Schuttelaar, and M. Kotsonis Dehnssso: The Delft Harmonic Navier-Stokes Solver for Nonlinear Stability Problems with Complex Geometric Features, 2023.

GLOBAL STABILITY ANALYSIS OF TURBULENT SCREECHING JETS VIA AUTOMATIC DIFFERENTIATION

Alessandro Franchini¹, Nicolas Alferez², Jean Christophe Robinet¹

¹*DynFluid Laboratory, Arts et Métiers, 151, boulevard de l'hôpital, 75013 Paris
alessandro.franchini@ensam.eu, jean-christophe.robinet@ensam.eu*

²*DynFluid Laboratory, CNAM, Arts et Métiers, 151, boulevard de l'hôpital, 75013 Paris
nicolas.alferez@lecnam.net*

Imperfectly expanded jets can be divided into two main categories, under-expanded and over-expanded. If the pressure of the exhaust leaving the nozzle exit is still above ambient pressure, then a nozzle is said to be under-expanded, resulting in a shock-cell structure developing outside the nozzle. Jets in these conditions generate various types of noise and, for particular temperatures and velocities, they generate discrete tones, called screech tones. This acoustic phenomenon was first discovered by Powell [1] in 1952, who gave a preliminary explanation of the mechanism as an acoustic feedback loop between the disturbances generated in the lips of the nozzle and the structure of the shock cells formed downstream. Since then, the problem has been extensively studied experimentally [2], analytically [3] and numerically [4]. In recent years, stability theory has been central in obtaining a more refined explanation of the feedback mechanism, based on the interaction between shock and acoustic modes traveling upstream in the potential core of the jet [5]. However, in the context of stability analysis, it is still difficult to formulate a consistent modeling that is capable of addressing the problem of a fully turbulent three-dimensional jet. This work focuses on this particular question, trying to study the screech phenomenon by means of global stability analysis using RANS models. This is made possible by using a source transformation automatic differentiation tool Tapenade [7] to extract the linearised solver, then a matrix-free time-stepping approach to solve the global stability analysis problem by passing memory problems of the matrix forming approaches. The high performance finite difference solver dNami [8] is used to discretize the compressible URANS equations (k- ω SST and Spalart Allmaras models). We will present an investigation of different regimes of the screech phenomenon (round and rectangular jets), comparing different turbulence models and nozzle pressure ratios (NPR). Then a three-dimensional global stability analysis is performed, analyzing the structure of the various three-dimensional modes (axisymmetric, flapping, helical) and their coexistence for specific NPRs.

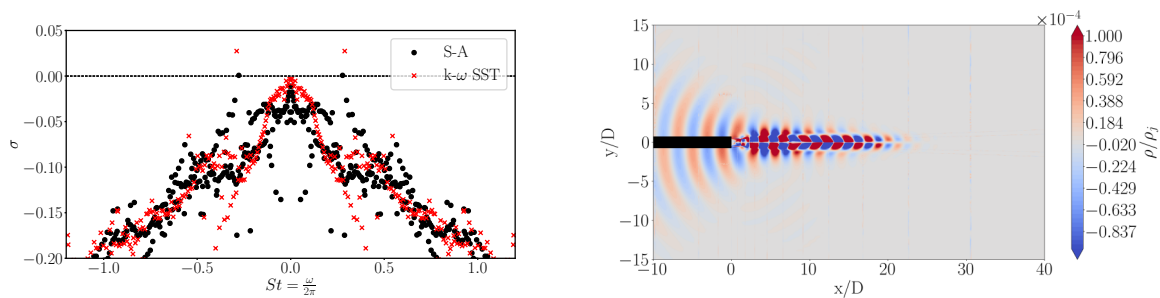


FIGURE 1. Left: Comparison of the spectra calculated at $M_j = 1.2$ with Spalart-Allmaras and k- ω SST turbulence models, an unstable mode is present. Right: The real part of the density distribution of the most unstable mode for the k- ω SST model is shown. Upstream acoustic typical of screech is visible.

References

- [1] Powell Alan. *On the noise emanating from a two-dimensional jet above the critical pressure*. Aeronautical Quarterly, 4, 2, 103–122, 1953, Cambridge University Press.
- [2] Norum, T. D., Screech suppression in supersonic jets, AIAA Journal, 21, 2, 235-240, 1983
- [3] C.K.W. Tam and H.K. Tanna. Shock associated noise of supersonic jets from convergent-divergent nozzles, Journal of Sound and Vibration, 81, 3, 337-358, 1982
- [4] Berland, Julien and Bogey, Christophe and Bailly, Christophe, Numerical study of screech generation in a planar supersonic jet, Physics of Fluids, 19, 7, 075105, 2007
- [5] Edgington-Mitchell, Daniel and Jaunet, Vincent and Jordan, Peter and Towne, Aaron and Soria, Julio and Honnery, Damon Upstream-travelling acoustic jet modes as a closure mechanism for screech, 855 Journal of Fluid Mechanics 2018
- [6] S. Beneddine, C. Mettot, D. Sipp. *Global stability analysis of underexpanded screeching jets*. European Journal of Mechanics-B/Fluids, 49, 392–399, 2015, Elsevier.
- [7] L. Hascoet and V. Pascual. *The Tapenade automatic differentiation tool: Principles, model, and specification*. ACM Trans. Math. Softw. 39:3, 2013.
- [8] N. Alferez, E. Touber, S. Winn, Y. Ali. *dNami: a framework for solving systems of balance laws using explicit numerical schemes on structured meshes*. <https://doi.org/10.5281/zenodo.6720593>, 2022, Zenodo.

PERTURBED EDDY-VISCOSITY APPROACH IN RESOLVENT ANALYSIS OF A TURBULENT BOUNDARY LAYER

P. Penet^{1,2}, O. Marquet², L. Lesshafft¹

¹LadHyX, CNRS, École polytechnique, IPParis, F-91120 Palaiseau, France

²DAAA, ONERA, Université Paris Saclay, F-92190 Meudon, France
pierre.penet@polytechnique.edu

Linear resolvent analysis has proven to be a successful approach for the identification of coherent structures in shear flows. Recent studies of turbulent wall-bounded flows have shown the importance of including the mean eddy viscosity $\bar{\nu}_T$ in the resolvent operator. In many cases the addition of eddy viscosity allowed to model empirically obtained SPOD modes more accurately, balancing the high non-normality of the resolvent operator [1].

Eddy viscosity depends on the flow variables, and if its inclusion in the linear model is pertinent, it would be consistent to account also for its unsteady fluctuations. We investigate the effect of including a perturbed eddy viscosity ν'_T in the resolvent analysis of turbulent boundary layers. A similar model coupled to data-assimilation has yielded promising results in the linear stability analysis of the flow around an airfoil [2]. We consider a spatially developing turbulent boundary layer flow and derive the mean-flow field $(\bar{u}, \bar{p}, \bar{\nu}_T)$ using the RANS equations closed with the Spalart-Allmaras turbulence model. Analogous to the velocity and pressure fields, we denote $\nu_T = \bar{\nu}_T + \nu'_T$ to account for an unsteady eddy viscosity perturbation. Linearizing the RANS equations and the Spalart-Allmaras transport equation around the mean-flow solution, we obtain a "perturbed eddy viscosity" ν'_T -resolvent in addition to the simple ν -resolvent and "frozen eddy viscosity" $\bar{\nu}_T$ -resolvent.

The ν'_T -resolvent correctly identifies the stationary streaks at $\omega = 0$ as the most energetic structures, for which the spanwise wavenumber dependency is shown in Figure 1. By comparing with the $\bar{\nu}_T$ -resolvent, we show that accounting for a perturbation in eddy viscosity leads to a reduction in the amplification of streaks. The smaller scale structures developing in the inner layer are more affected and the inner amplification maximum is shifted to smaller wavelengths. The velocity perturbations, seen in Figure 2, also extend further from the wall. Following Symon et al. [3], we will discuss this damping effect from a Reynolds-Orr energy-budget analysis.

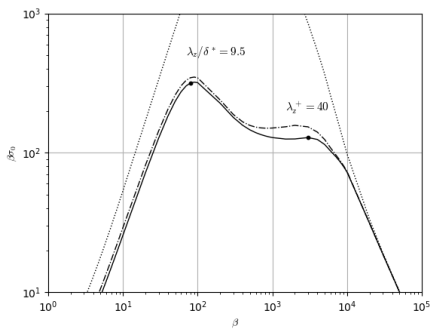


Figure 1: Scaled optimal resolvent gain at $\omega = 0$ as a function of the spanwise wavenumber β : ν -resolvent (\cdots), $\bar{\nu}_T$ -resolvent ($-\cdot-$), ν'_T -resolvent ($-$).

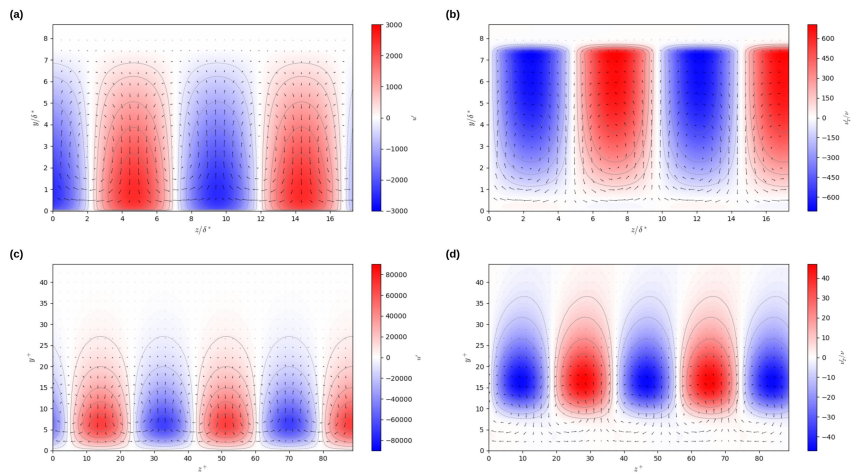


Figure 2: Cross-stream view of the ν'_T -resolvent optimal response, colored by streamwise velocity [eddy viscosity perturbation] for outer peak $\lambda_z/\delta^* = 9.5$ (a) [(b)] and inner peak $\lambda_z^+ = 40$ (c) [(d)].

References

- [1] P. Morra, O. Semeraro, D. S. Henningson and C. Cossu. Resolvent Analysis: With or Without Eddy Viscosity? *ERCOFTAC Bulletin*, 118, pp.20, 2019.
- [2] K. Sarras, C. Tayeh, V. Mons and O. Marquet. Linear stability analysis of turbulent mean flows based on a data-consistent Reynolds-averaged Navier–Stokes model: prediction of three-dimensional stall cells around an airfoil. *J. Fluid Mech.*, vol. 1001, A41, 2024.
- [3] S. Symon, S. J. Illingworth and I. Marusic. Energy transfer in turbulent channel flows and implications for resolvent modelling. *J. Fluid Mech.*, vol. 911, A3, 2021.

RESOLVENT STABILITY ANALYSIS OF TURBULENT MEAN FLOWS: AN APPLICATION TO AEROACOUSTICS

Antoine Jouin¹, Benjamin Cotté², Vincent Mons¹, Olivier Marquet¹, Lutz Lesshafft³

¹DAAA, ONERA, Université Paris Saclay, 8 rue des Vertugadins, Meudon, France

²ENSTA Paris, Institute of Mechanical Sciences and Industrial Applications, Palaiseau, France

³LadHyX, CNRS, Ecole Polytechnique, Institut Polytechnique de Paris, Palaiseau, France

A number of engineering applications, such as micro-wind blade turbines or small unmanned air vehicles, operate at low to moderate Reynolds number flow conditions, and present a significant potential for noise pollution. The most significant and well-understood source of noise at small angles of incidence is trailing edge noise, which results from the diffraction of pressure waves at the trailing edge. However, in the case of a NACA0012 profile, Sandberg *et al.* [1] observed the presence of an additional secondary noise source, located on the suction surface near the reattachment point of the boundary layer and possessing a markedly different directivity pattern.

Both these acoustic radiations can be linked to the presence of flow structures in the boundary layer, spatiotemporally coherent over distances far exceeding the integral scales of the turbulence. Furthermore, these coherent structures were found to agree well with predictions of a linearized input-output stability analysis applied on the turbulent mean flow field [2]. Still, application of the resolvent framework to turbulent mean flows is not straightforward and several difficulties arise, especially on the choice of a meaningful mean flow [3]. A consistent framework for the application of resolvent analysis to compressible turbulent flows is thus proposed. It is based on the linearization of the RANS equations closed with a Spalart-Allmaras turbulence model. A modification of the usual Chu norm is also proposed to better account for turbulence-related energy transfers.

The framework is then used to better characterize the secondary, separation-related acoustic source. First, the effect of the profile geometry and thickness is investigated by considering two separate configurations: a NACA0012 profile at various angles of incidence and a compressor blade. Some light is also shed on the noise generation mechanism underlying the secondary acoustic source. It was found that the separation-related acoustic radiation appears as a byproduct of the vortex deformation associated with the Orr mechanism in the vicinity of the recirculation bubble.

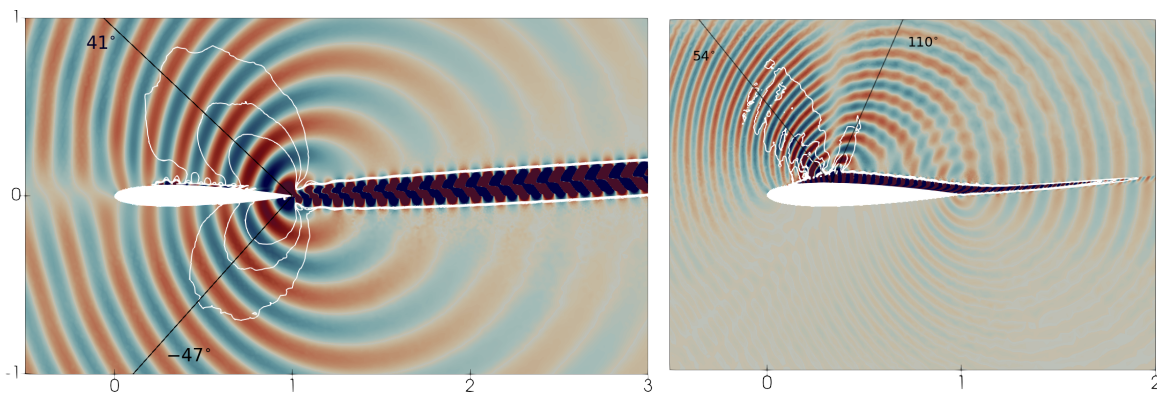


FIGURE 1. Acoustic radiation corresponding to the two most amplified responses generated by the flow over a NACA0012 profile at $Re = 2 \times 10^5$, $Ma = 0.4$, $\alpha = 5^\circ$. Coloured contours represent the density component of the optimal response while white isocontours denotes the pressure magnitude. Preferential directions of propagation are also indicated as black lines. Left: $St = 8.3$ corresponding to trailing edge noise. Right: $St = 23.4$ corresponding to separation-related noise.

References

- [1] R. D. Sandberg, and D. S. Sandham and P. F. Joseph. Direct numerical simulations of trailing-edge noise generated by boundary-layer instabilities. *Journal of Sound and Vibration*, 304(3):677–690, 2007.
- [2] L. Lesshafft, O. Semeraro, V. Jaunet, A.V.G. Cavalieri and P. Jordan Resolvent-based modeling of coherent wave packets in a turbulent jet. *Phys. Rev. Fluids*, Vol 4, 063901, 2019.
- [3] L. Francheschini, D. Sipp and O. Marquet. Mean-flow data assimilation based on minimal correction of turbulence models: Application to turbulent high Reynolds number backward-facing step. *Phys. Rev. Fluids*, Vol 5, 094603, 2020.

NOISE-INDUCED TRANSITIONS AFTER A STEADY SYMMETRY-BREAKING BIFURCATION: THE CASE OF THE SUDDEN EXPANSION

Yves-Marie Ducimetière¹, Edouard Boujo² and François Gallaire²

¹*Courant Institute of Mathematical Sciences, New York University, New York, NY 10012, USA*

²*Laboratory of Fluid Mechanics and Instabilities, École Polytechnique Fédérale de Lausanne, Lausanne CH-1015, Switzerland*

Some nonlinear dynamical systems are metastable: subject to a weak noise, they randomly switch back and forth between two configurations, after long and unpredictable times. This is for instance occurring in the barotropic quasi-geostrophic equations, used to model quasi-stationary turbulent zonal jets [1]. However, precisely because the mean transition time to change from one attractor state to the other is extremely large, this situation will usually not be easily detected by simply running the numerical models. Instead, rare event algorithms based on the large-deviation theory are generally used.

Alternatively, to compute the flow statistics at a cheaper numerical cost, we propose to generalize the multiple-scale weakly nonlinear expansion technique typically deployed for the response of the Duffing oscillator, to the Navier-Stokes equations. Specifically, the Navier-Stokes equations are forced by a weak, narrow-band noise, which therefore acts on the same slow time scale τ as the amplitude of the dominant mode shortly after a bifurcation point Re_c (with neutral eigenmode $\mathbf{q}(x)$). Thereby, in the case of a steady symmetry-breaking bifurcation, we rigorously derive a stochastically forced Stuart-Landau equation for the slowly varying amplitude $A(\tau)$ premultiplying the dominant symmetry-breaking mode $\mathbf{q}(x)$

$$\frac{dA}{d\tau} = \lambda A(\tau) + \mu A(\tau)^3 + \eta \phi \xi(\tau), \quad (1)$$

where the coefficients λ , μ and η are all computed from scalar products of linearly computed fields, ϕ is the rescaled noise amplitude and $\xi(\tau)$ a rescaled band-limited white noise.

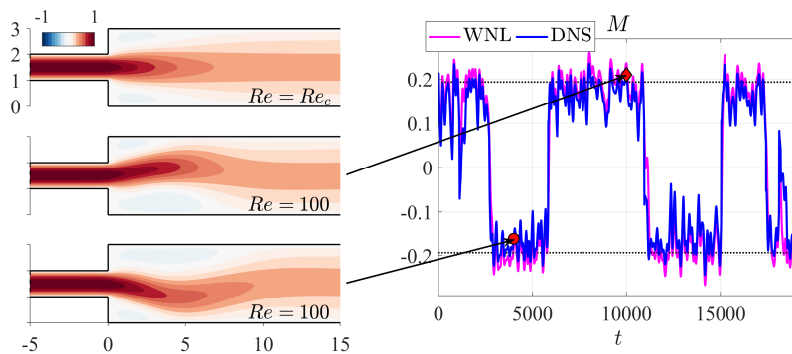


FIGURE 1. *The flow past a sudden expansion at $Re = 100 > Re_c$, beyond the symmetry-breaking bifurcation, and subject to a stochastic forcing. The flow switches from one attractor state to the other at random, extremely long times.*

The validity of this reduced order model (WNL) is tested on the flow past a sudden expansion after the symmetry-breaking bifurcation $Re > Re_c$ [2] (see figure 1). Given the nature of the amplitude equation (1), the dynamics of A derives from a potential and the probability density function of the solution is then easily determined by solving the Fokker-Planck equation. At a very low numerical cost, the statistics obtained by solving the Fokker-Planck equation accurately reproduce those of a long-time direct numerical simulation (DNS) of the unsteady forced Navier-Stokes equations, for different noise amplitudes ϕ .

References

- [1] E. Simonnet, J. Rolland and F. Bouchet. Multistability and Rare Spontaneous Transitions in Barotropic β -Plane Turbulence, Stability properties of the mean flow after a steady symmetry-breaking bifurcation and prediction of the nonlinear saturation. *J. Atmos. Sci.*, 78(6), 2021.
- [2] S. Camarri and G. Mengali. Stability properties of the mean flow after a steady symmetry-breaking bifurcation and prediction of the nonlinear saturation. *Acta Mechanica*, 230(5), 2019.



MODELING NONLINEAR DYNAMICS FROM DATA

David Fabre

IMFT, Université de Toulouse / CNRS, Toulouse, France

The transition to unsteadiness in the wake of fixed bodies is a classical problem in fluid mechanics which has received a large number of studies, since the first observations of the characteristic vortex alley structure by Bénard and Von Karman. This transition is now well explained through concepts of hydrodynamic instability theory. The modern explanation for this transition, built upon properties of the local velocity profiles and assuming a weakly nonparallel flow, was conceptualized by Chomaz and coworkers (see e.g. [1]). Accordingly, the global instability is due to the existence of a region of absolute instability of sufficient extent in the flow which acts as the "wavemaker". This scenario was first demonstrated for simple mathematical models such as the nonlinear Ginzburg-Landau equation. It was then shown to hold for the reference case a circular cylinder, and more generally 2D blunt bodies of other geometries. In such wakes, the region of absolute instability can be grossly identified with the recirculation region, which extends as the Reynolds number is increased until it reaches a sufficient size (the transition occurring for $Re \approx 47$ in the classical case of the circular cylinder). In this presentation, I will focus on the case of slender 2D bodies, such as a NACA0012 wing profile, for which the transition occurs for much higher values of the Reynolds number, of the order of 10000. A region of absolute instability is also present in such wakes and the weakly non-parallel hypothesis is much better approached than for slender bodies, so one would expect the whole scenario to remain valid. However, no available numerical study (using either DNS or Linear Stability analysis) has been able to give a precise value for the critical Reynolds number. For instance, Sabino [2] indicated a transition in the range $Re \in [6000 - 8000]$ and reported a significant dependence upon the size of the numerical domain, especially the position X_{out} of the downstream boundary. Sabino also reported that close to the onset, there exists a large number of near-neutral eigenmodes which are all spatially amplified up to the numerical boundary. This suggests that the transition observed in numerical simulations in a truncated domain could actually be dominated by spurious effects associated to the outlet boundary condition. By scrutinizing this problem using DNS, linear stability and sensitivity approaches, along with simplified mathematical models, it is demonstrated that two feedback mechanisms actually exist. The first one is local and related to the region of absolute instability, following the generally adopted view. The second is non-local, and involves a downstream propagating convective vortical perturbation and a pressure perturbation generated at the boundary condition (the latter being instantaneous in the strictly incompressible case and associated to a backward propagating acoustic wave in the compressible case). It is shown that the second mechanism dominates for thin profiles such as the NACA0012, and prevents from being able to locate the "true" critical Reynolds number in a domain of infinite size without proper care of the problem. Two methods (a complex mapping and a specifically designed sponge region) are eventually introduced to circumvent the problem by damping the vortical structures in the region away from the absolute instability region and preventing their spurious retroaction through the boundary condition. With these methods, along with the use of systematic mesh adaptation as explained in Fabre et al. [3], it is possible to localize the critical Reynolds for a NACA0012 profile in an infinite domain at $Re = 8550$. It is speculated that the identified phenomenon likely manifests in other classes of strongly convective flows, such as coaxial jets.

References

- [1] J. M. Chomaz, P. Huerre, and L. G. Redekopp. *Bifurcations to Local and Global Modes in Spatially Developing Flows*. Phys. Rev. Lett. 60, 25 (1988).
- [2] D. Sabino, *Aeroelastic instabilities of an airfoil in transitional flow regimes*. Doctoral dissertation, ONERA and University of Toulouse III - Paul Sabatier (2022).
- [3] Fabre. D. et al., *A Practical Review on Linear and Nonlinear Global Approaches to Flow Instabilities*. Applied Mechanics Reviews, 70(6), 2018.

IMPERFECT BIFURCATIONS IN A LAMINAR 3-D BLUFF BODY WAKE: EFFECT OF YAW AND PITCH

A. Lagwankar¹, A. Chiarini², F. Gallaire¹, E. Boujo¹

¹*École Polytechnique Fédérale de Lausanne, CH-1015 Lausanne, Switzerland*

²*Politecnico di Milano, 20156 Milano, Italy*

The laminar wake of a perfectly aligned Ahmed body undergoes pitchfork bifurcations, leading to a static symmetry-breaking deflection, either vertical or horizontal [1]. At slightly larger Re , the deflected wake undergoes a secondary Hopf bifurcation, leading to vertical or horizontal vortex shedding. Here, using 3-D linear and weakly nonlinear stability analysis, as well as DNS, we investigate how pitch and yaw modify these bifurcations, thus complementing existing turbulent studies [2, 3].

As typically observed for imperfect pitchfork bifurcations, at low Re a small misalignment selects one of the steady states: vertical deflection under pitch (Figure 1a), and horizontal deflection under yaw. Interestingly, pitch reduces the critical Re of the vertical Hopf bifurcation but also increases the critical Re at which the vertically deflected state loses stability (Figure 1b), resulting in a cross-over of the two bifurcations for $\alpha = 1^\circ$ (Figure 1c). The flow dynamics in the vicinity of this cross-over are strongly reminiscent of the very slow dynamics observed experimentally in ground proximity [4]: the wake first oscillates vertically, before transitioning to a steady horizontal deflection.

Finally, for small angles, the effect of combined yaw and pitch is studied efficiently via a weakly nonlinear analysis, unveiling complicated bifurcation diagrams.

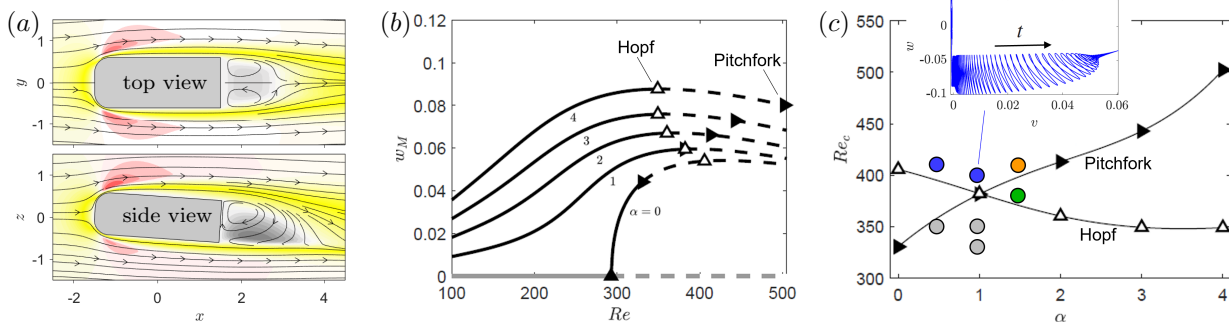


FIGURE 1. Effect of a small pitch angle α on the wake of an Ahmed body (width-to-height ratio $W/H = 1.2$, length-to-height ratio $L/H = 3$). (a) Base flow streamwise velocity u in the planes $z = 0$ (top view) and $y = 0$ (side view), for $\alpha = 4^\circ$, $Re = 360$. (b) Nonlinear base states (vertical velocity w measured in the wake on the axis $y = z = 0$) and their linear stability (solid/dashed lines: stable/unstable). (c) Stability diagram. Inset: slow transition from vertical vortex shedding ($v = 0$, $w \neq 0$) to steady horizontal deflection ($v \neq 0$) for $\alpha = 1^\circ$, $Re = 400$.

References

- [1] G. A. Zampogna and E. Boujo. From thin plates to Ahmed bodies: linear and weakly nonlinear stability of rectangular prisms. *J. Fluid Mech.*, 966:A19, 2023.
- [2] G. Bonnavion and O. Cadot. Unstable wake dynamics of rectangular flat-backed bluff bodies with inclination and ground proximity. *J. Fluid Mech.*, 854:196–232, 2018.
- [3] Y. Fan, V. Parezanović and O. Cadot. Wake transitions and steady z -instability of an Ahmed body in varying flow conditions. *J. Fluid Mech.*, 942:A22, 2022.
- [4] M. Grandemange, O. Cadot and M. Gohlke. Reflectional symmetry breaking of the separated flow over three-dimensional bluff bodies. *Phys. Rev. E*, 86(3):035302, 2012.

LOW-FREQUENCY UNSTEADINESS IN ROTATING PLANE COUETTE FLOW

Igor A. Maia¹, Carolina Cura², Julien Weiss², Ardeshir Hanifi³, André V. G. Cavalieri¹

¹*Divisão de Engenharia Aeronáutica, Instituto Tecnológico de Aeronáutica, São José dos Campos, Brazil*

²*Institut für Luft- und Raumfahrt, Technische Universität Berlin, Germany*

³*FLOW, Engineering Mechanics, KTH Royal Institute of Technology, Stockholm, Sweden*

Low-frequency unsteadiness is a common feature of separated flows, such as turbulent separation bubbles (TSBs), where they produce a characteristic “breathing” motion [1]. Centrifugal instabilities have been proposed as a possible mechanism for the observed unsteadiness in incompressible flows [2] and also in high-speed flows subject to shock wave/boundary layer interaction [3]. Here, we explore another possible mechanism for low-frequency unsteadiness in incompressible flows based on a destabilizing effect produced by a Coriolis force [4]. For that we consider a model problem wherein turbulent plane Couette flow is subject to constant rotation in the spanwise direction. Direct numerical simulations (DNS) of this flow have been performed at Reynolds number $Re = 1000$ and different rotation rates, Ω . It is found that low-frequency turbulent fluctuations increase substantially in the rotating system. This is illustrated in figure 1, which shows averaged pressure spectra on the lower wall for cases with and without rotation.

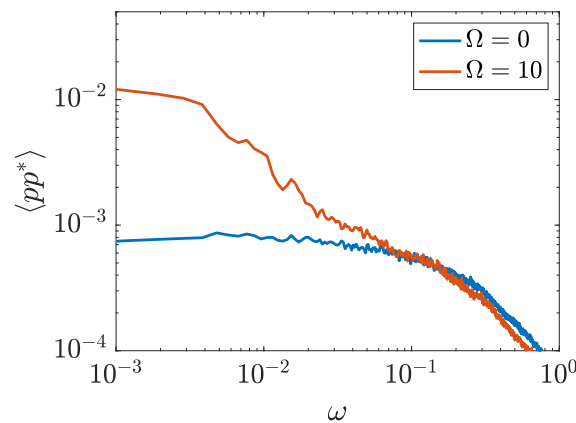


FIGURE 1. Pressure spectra computed from DNS of turbulent plane Couette flow at $Re = 1000$ and rotation rates $\Omega = 0, 10$. The spectra are computed at the lower wall and spatially-averaged.

The low-pass filter effect observed in rotating Couette flow is quite similar to that observed in TSBs [5], suggesting that this kind of rotational instability is a plausible physical mechanism for the generation of low-frequency motion in the latter (wherein rotation is induced by the concave streamline curvature of the mean flow). Furthermore, this low-pass filter effect is found to be correctly captured by a resolvent model based on the linearised Navier-Stokes system. We also investigate the link between low-frequency unsteadiness and the onset of superstructures that occupy the entire length of the domain.

References

- [1] A. Mohammed-Taifour and J. Weiss Unsteadiness in a large turbulent separation bubble *Journal of Fluid Mechanics*, 799, 383–412, 2016.
- [2] W. Wu, C. Meneveau and R. Mittal Spatio-temporal dynamics of turbulent separation bubbles *Journal of Fluid Mechanics*, 883, A45, 2020.
- [3] S. Priebe, J. Tu, C. Rowley and M. Martín Low-frequency dynamics in a shock-induced separated flow *Journal of Fluid Mechanics*, 807, 441–477, 2016.
- [4] T. Tsukahara, N. Tillmark and P. Alfredsson Flow regimes in a plane Couette flow with system rotation *Journal of Fluid Mechanics*, 648, 5–33, 2010.
- [5] C. Cura, A. Hanifi, A. Cavalieri and J. Weiss On the low-frequency dynamics of turbulent separation bubbles *Journal of Fluid Mechanics*, 991, A11, 2024.

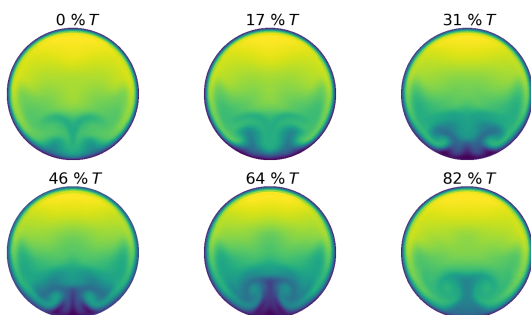
STABILITY OF LARGE-AMPLITUDE PULSATILE FLOW IN A TORUS

J. S. Kern [johann-simon.kern@ensam.eu], J.-C. Loiseau
DynFluid, Arts et Métiers Institute of Technology (ENSAM), Paris, France

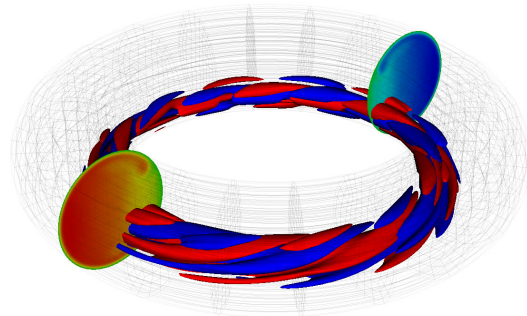
Pipe flows are ubiquitous in nature and technology, from the cardiovascular system to heat exchangers and hydraulic piping. This has led to a theoretical and practical interest in this geometry since the late 19th century in order to understand the flow behaviour, and its stability characteristics. While the linear stability of steady flow in a straight pipe up to very high Reynolds numbers is a well established result of stability theory, recent efforts by a number of research teams have extended the steady analysis to toroidal and helical pipes, showing that even small amounts of curvature and torsion lead to a linear instability at finite Reynolds numbers (e.g., [1, 3], among others).

However, many practical applications involving pipe flows in curved geometries are not subject to steady flow. A classic example is the blood flow in the aorta that is driven by periodic contractions of the heart. In cases without curvature, linear stability analyses of pulsatile channel flow have shown that time-periodic variations of the baseflow can lead to both stabilisation and destabilisation of the flow [6]. In order to assess the interaction of pulsations and curvature, a recent study has followed a similar approach to extend the linear stability results for steady flow in toroidal pipes to the pulsating case [4]. Progressively adding pulsations to a slightly supercritical steady state, the study showed that small-amplitude pulsations have an overwhelmingly stabilising effect. Unfortunately, in spite of its high accuracy, the use of a fully spectral matrix-forming approach severely limited the range of considered pulsation amplitudes.

In the present work, we revisit the case of pulsatile flow in the torus using a fully three-dimensional matrix-free time-stepper approach, thus eliminating the main restrictions of the previous analysis. The new implementation unlocks not only a considerably larger parameter range for the harmonically forced case, in particular to larger pulsation amplitudes in the highly nonlinear regime, but also opens up the perspective to include more complex geometries or pressure variations at modest extra development cost. Using a radically different numerical methodology, the new results for a curvature of $\delta = 0.3$ will allow us to cross-check and confirm the conclusions of the previous work. Furthermore, we fully map the space of laminar nonlinear periodic orbits with Womersley numbers and pulsation amplitudes in the ranges $Wo \in [15, 100]$ and $Q \in [0.0, 0.5]$, respectively, and track the leading unstable Floquet eigenvalue originating in the Hopf bifurcation of the steady flow for a larger range of pulsation amplitudes than before. The analysis is performed using `neklab`, a combination of the spectral element solver `Nek5000`[2] with the novel open-source toolbox `LightKrylov`[5] for linear algebra and stability calculations using Krylov-based methods written in modern Fortran making heavy use of abstract types for a highly adaptable, yet lightweight and portable implementation.



(a) Streamwise velocity of the nonlinear periodic orbit over the period T for $\delta = 0.3$, $Wo = 35$, $Q = 0.3$.



(b) Full torus geometry with steady baseflow (slices) and isocontour of the leading eigenmode (lower half).

References

- [1] J. Canton, P. Schlatter, and R. Örlü. Modal instability of the flow in a toroidal pipe. *J. Fluid Mech.*, 792:894–909, 2016.
- [2] P. F. Fischer, J. W. Lottes, and S. G. Kerkemeier. `Nek5000` web page, 2008.
- [3] A. Gelfgat. Instability of steady flows in helical pipes. *Phys. Rev. Fluids*, 5:103904, Oct 2020.
- [4] J. S. Kern, V. Lupi, and D. S. Henningson. Floquet stability analysis of pulsatile flow in toroidal pipes. *Phys. Rev. Fluids*, 9:043906, Apr 2024.
- [5] J.-C. Loiseau, J.S. Kern, and R.A.S. Frantz. `LightKrylov` repository, 2024.
- [6] B. Pier and P. J. Schmid. Linear and nonlinear dynamics of pulsatile channel flow. *J. Fluid Mech.*, 815:435–480, 2017.

STABILITY OF TURBINE DRAFT TUBE VORTEX

Eunok Yim¹

¹HEAD-lab. EPFL, Lausanne, Switzerland

For a given specific energy in hydraulic machines, there is a peak efficiency at a certain flow rate, known as the Best Efficiency Point (BEP). Beyond this point, efficiency decreases in an almost quadratic manner as flow rate deviates. This study aims to establish a connection between this phenomenon and the flow stability properties at two different operating points. The base flow vortex considered here is based on the experimental data by [1, 2]. Based on experimental measurement at a location of turbine outlet (upstream of draft tube), Susan-Resiga *et al.* [1] proposed a mathematical fitting of the turbine vortex into one rigid body motion and two batchelor vortices with two different core radii $\mathbf{U}_b = [0, V_\theta, V_z]$:

$$V_\theta = \Omega_0 r + \frac{\Omega_1 R_1}{r/R_1} (1 - \exp(-r^2/R_1^2)) + \frac{\Omega_2 R_2}{r/R_2} (1 - \exp(-r^2/R_2^2)), \quad (1)$$

$$V_z = W_0 + W_1 \exp(-r^2/R_1^2) + W_2 \exp(-r^2/R_2^2), \quad (2)$$

where W_0 is the free stream velocity (positive for downward direction). The subscription $0,1,2$ are fitting parameters which vary with the operation points and by construction $R_1 > R_2$. The values are nondimensionalized by turbine outlet radius $R_0 = 20$ cm and the turbine velocity at this radius ($V_{outlet} = 1000 \text{ rpm} \times 2\pi/60 \times R_0$). A local stability analysis ($u' = u(r) \exp(-i\omega t + im\theta + ikz) + c.c.$) is performed for two different operating points (two different baseflows). Following [5], the turbulent viscosity ($\nabla \cdot [(\nu + \nu_T)(\nabla \hat{\mathbf{u}} + (\nabla \hat{\mathbf{u}})^T)]$) is taken into account and ν_T is derived from the experimental data [2]. The first operating point (OP1) corresponds to the part-load regime, where the flow rate is approximately 97% of that at the BEP. The second operating point (OP2) corresponds to the BEP itself. For OP1, the most unstable mode is associated with an azimuthal wavenumber of $m = 2$. In contrast, for OP2, the dominant instability is an axisymmetric mode for all axial wavenumber k . These findings align with previous observations [4], as shown in Figure 1a for a similar discharge coefficient. In the experiment, a vortical structure with a small radius is observed and visualized through cavitation. Figure 1b illustrates the vorticity distribution of the most unstable mode for OP1 (marked as a circle in Figure 1c), exhibiting five axial wavenumber cycles. The large grey circle represents the draft tube radius, indicating that the instability mode is concentrated near the center. The mode shape and its localization near the axis further support this interpretation. At the BEP (OP2), experimental observations reveal no distinct vortical structures (not shown).

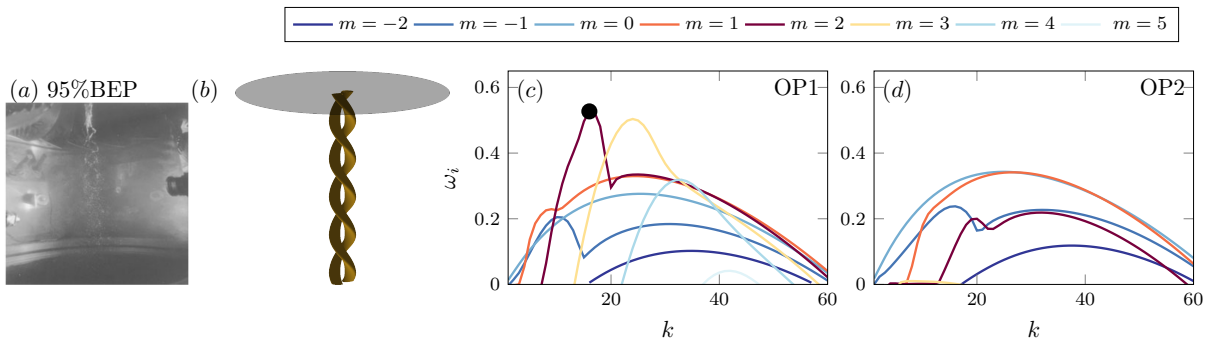


FIGURE 1. (a) Experimental observation [4]. (b) Three dimensional view of vorticity ($\zeta = 0.3 \max(\zeta)$) of the most unstable mode of $m = 2$, $\zeta(r) \exp(im\theta + ikz)$, (marked as \bullet in (c)). The growth rate as functions of axial wavenumber k and azimuthal wavenumber m for (c) OP1 (97 % BEP) and (d) OP2 (BEP).

References

- [1] R. Susan-Resiga, D. Ciocan, I. Anton, and F. Avellan. *Analysis of the swirling flow downstream a francis turbine runner. J. Fluids Eng.*, 128:177–189, 2006.
- [2] R. Susan-Resiga, S. Muntean, V. Hasmatuchi, I. Anton, and F. Avellan. *Analysis and prevention of vortex breakdown in the simplified discharge cone of a francis turbine. J. Fluids Eng.*, 132:051102, 2010.
- [3] P. Billant, and F. Gallaire. *A unified criterion for the centrifugal instabilities of vortices and swirling jets. J. Fluid Mech.*, 734:5–35, 2013.
- [4] S. Mauri. *Numerical simulation and flow analysis of an elbow diffuser. Ph.D. thesis*, EPFL, Lausanne (2002).
- [5] F. Viola, G. V. Iungo, S. Camarri, F. Porté-Agel, and F. Gallaire. *Prediction of the hub vortex instability in a wind turbine wake: stability analysis with eddy-viscosity models calibrated on wind tunnel data. J. Fluid Mech.*, 750:R1, 2014.

DETUNED STREAK INSTABILITIES ORIGINATE LARGE-SCALE FLOWS IN TRANSITIONAL CHANNEL

N. Ciola^{1,3}, Y. Duguet², J.-C. Robinet³, S. Cherubini¹, P. De Palma¹

¹*DMMM, Politecnico di Bari, Via Re David 200, 70125 Bari, Italy*

²*LISN-CNRS, Université Paris-Saclay, 507 Rue du Belvédère, 91405 Orsay, France*

³*DynFluid, Arts et Métiers Paris /CNAM, 151 Bd de l'Hôpital, 75013 Paris, France*

Plane shear flows at low Reynolds number are characterized by the coexistence of laminar and turbulent flow. As the Reynolds number is decreased, initially homogeneous turbulence becomes modulated in the streamwise and spanwise directions resulting in oblique patterns referred to as turbulent bands [1]. Recently, it was shown that such modulation arises as a linear instability of the homogeneous turbulent flow [2]. Several direct numerical simulations of a perturbed turbulent channel flow were performed and ensemble averaged in order to extract a statistical dispersion relation. With this technique, it was possible to obtain a growth rate for the large-scale component of the perturbation. This growth rate becomes positive as the Reynolds number is decreased, giving the critical Reynolds number for the appearance of the pattern. Nevertheless, using this approach, it was not possible to retrieve the unstable mode. On the other hand, a recent work [3] employed the block-circulant matrix method [4] to show that a detuned instability of near-wall streaks can generate large-scale motions in the turbulent channel flow at moderately high Reynolds number. Although this second approach needs some modelling assumptions, it allows the formulation of a classical stability problem with eigenvalues and eigenmodes. The idea of the present work is to perform a similar analysis on the transitional channel flow and recover the unstable mode that brings the large-scale modulation of the turbulent flow. With this aim, near-wall streaks are computed from the linear optimal forcing of the mean flow with the typical spanwise spacing of 100 wall units. Then, a secondary stability analysis is performed over an array of streaks plus the mean flow. If the amplitude of the streaks is large enough and if an eddy viscosity is included in the linear operator to model unresolved turbulent motions, the streaky base flow becomes unstable as the Reynolds number is decreased. The instability is found over a range of wavenumbers compatible with those reported in [2]. Nonlinear simulations initialized with the unstable mode and the base flow are performed in order to observe the saturation of the mode. The outcome is portrayed in figure 1 where it can be seen a large-scale wall-parallel flow developing around an oblique band. This represents the first stage of the pattern development. Key takeaways and limitations of the modelling approach will be discussed.

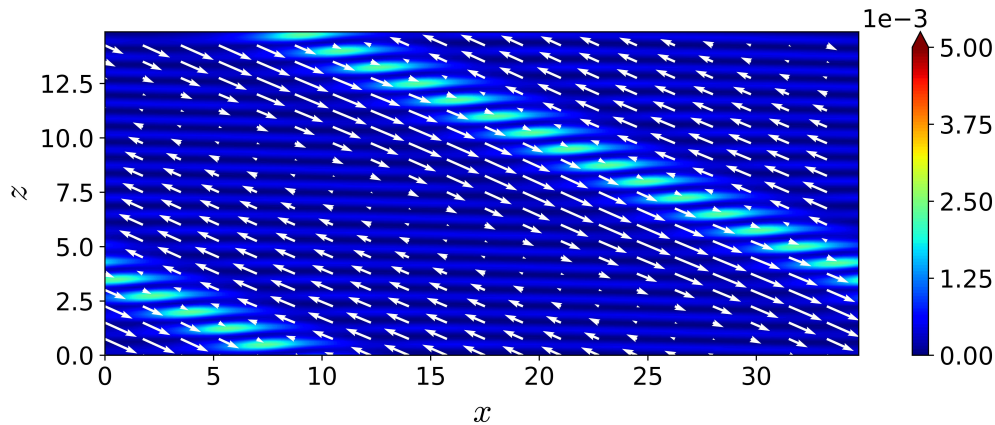


FIGURE 1. Large-scale flow developed by the nonlinearly saturated unstable mode over the streaky base flow. The figure shows the wall-normal integrated wall-normal velocity kinetic energy (shaded contours) and the wall-normal integrated wall-parallel large-scale flow (arrows). Flow from left to right.

References

- [1] M. Shimizu, and P. Manneville. Bifurcations to turbulence in transitional channel flow. *Physial Reviv Fluids*, 4(11):113903, 2019.
- [2] P. V. Kashyap, Y. Duguet, and O. Dauchot. Linear instability of turbulent channel flow. *Physical Review Letters*, 129(24):244501, 2022.
- [3] N. Ciola, P. De Palma, J.-C. Robinet, and S. Cherubini. Large-scale coherent structures in turbulent channel flow: a detuned instability of wall streaks. *Journal of Fluid Mechanics*, 997:A18, 2024.
- [4] P. J. Schmid, M. F. De Pando, and N. Peake. Stability analysis for n-periodic arrays of fluid systems. *Physial Reviv Fluids*, 2(11):113902, 2017.

STABILITY OF THE FLOW PAST A FLEXIBLE CYLINDER

Simone Cruciani^{1,2}, Riccardo Bertonecello¹, Alessandro Chiarini¹, Michel Fournié², Franco Auteri¹

¹*Dipartimento di Scienze e Tecnologie Aerospaziali, Politecnico di Milano, via La Masa 34, Milano, Italy*

²*Fédération ENAC ISAE-SUPAERO ONERA, Université de Toulouse, Département d'Ingénierie des Systèmes Complexes (DISC), 10 avenue Edouard-Belin, 31055 Toulouse, France*

The present work investigates the two-dimensional (2D) and three-dimensional (3D) linear stability of the fluid-structure interaction (FSI) problem composed of an incompressible fluid flowing past an infinite and flexible circular cylinder at low Reynolds number (see figure 1). The flexible cylinder is free to oscillate in the x and y direction, with a characteristic wavelength of $\lambda_z = 2\pi/\beta$ in the spanwise direction z , and its dynamics is governed by the Euler-Bernoulli beam equation. By varying the bending stiffness of the cylinder over more than two orders of magnitude we characterise the bifurcation scenario ranging from the (well-known) rigid case to the (here considered for the first time) extremely flexible one.

The FSI problem is formulated using an Arbitrary Lagrangian Eulerian (ALE) approach. At the interface between the fluid and the deformable structure the continuity of the velocity, which is in the x - y plane at leading order, and of the normal component of the stress tensor are enforced. For both the fluid and the structure we solve the equations in an initial, fixed reference system, similarly to what has been done in previous works [1]. We use the finite element, open source library GetFEM [2] to implement the ALE scheme and run the simulations.

Our preliminary results show that the flexibility of the cylinder influences the primary bifurcation of the FSI problem in a non trivial way. At low values of the bending stiffness, the primary instability consists of a Hopf bifurcation towards the classical von Kármán unsteady wake, as for a rigid cylinder [3]. In contrast, when the cylinder is flexible enough, the primary bifurcation consists of a regular bifurcation towards a 3D steady state. This bifurcation is due to an anti-symmetric mode that, to the best of our knowledge, has never been observed so far.

At the conference we will characterise the bifurcation scenario in the complete parameter space, and shed light on the role of the flexibility of the cylinder on the stability of this FSI system.

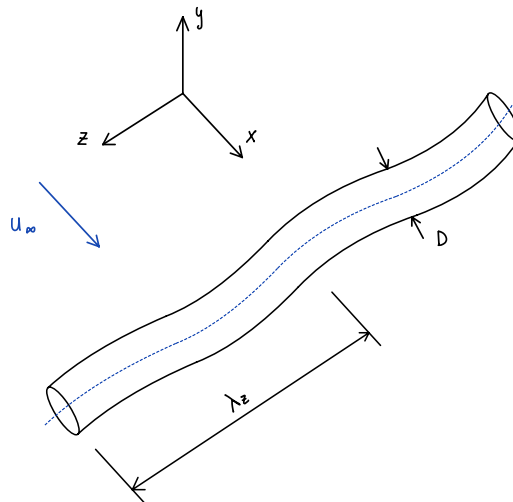


FIGURE 1. Sketch of the FSI system. An incompressible fluid with unperturbed velocity $\mathbf{u} = U_\infty \hat{\mathbf{e}}_x$ flows past an infinite flexible cylinder of diameter D having axis aligned with $\hat{\mathbf{e}}_z$.

References

- [1] J.-L. Pfister, O. Marquet, and M. Carini. Linear stability analysis of strongly coupled fluid–structure problems with the Arbitrary-Lagrangian–Eulerian method. *Comput. Methods Appl. Mech. Eng.*, 355: 663–689, 2019.
- [2] Y. Renard, and K. Poullos. Getfem: Automated FE modeling of multiphysics problems based on a generic weak form language. *ACM Transactions on Mathematical Software*, 47 (1), 2020.
- [3] M. Provansal, C. Mathis, and L. Boyer. Bénard-von Kármán instability: transient and forced regimes. *J. Fluid Mech.*, 182: 1–22, 1897.

WIDOM-LINE EFFECT ON THE BOUNDARY-LAYER TRANSITION WITH A HIGHLY NON-IDEAL FLUID

P. C. Boldini¹, B. Bugeat², J. W. R. Peeters¹, M. Kloker³, R. Pecnik¹

¹Process and Energy Department, Delft University of Technology, Leeghwaterstraat 39, 2628 CB Delft, the Netherlands

²School of Engineering, University of Leicester, University Road, Leicester, LE1 7RH, United Kingdom

³Institute of Aerodynamics and Gas Dynamics, University of Stuttgart, Pfaffenwaldring 21, 70569 Stuttgart, Germany

Research on the hydrodynamic stability of boundary layers with fluids exhibiting non-ideal thermodynamic behaviour has made notable progress in recent years. The newly identified Mode-II instability [1] in the transcritical-heating regime – linked to the kinematic viscosity minimum at the Widom line – arises from the interaction between shear and baroclinic waves [2]. Non-modal stability analysis has shown that Mode II alters the streamwise invariance of optimal streamwise streaks [3]. More recently, the first controlled laminar-to-turbulent transition of a transcritical boundary layer with a fluid at supercritical pressure was performed by means of direct numerical simulation (DNS) [4]. Nevertheless, the role of the Widom line in the non-linear stages of boundary-layer breakdown remains an open question.

In this talk, we consider a transitional zero-pressure-gradient flat-plate boundary layer at a Mach number of 0.2 and reduced pressure of $p^*/p_c^* = 1.10$, with p_c^* being the critical pressure, using the open-source DNS solver CUBENS (CUBic Equation of state Navier-Stokes) [5]. To investigate the Widom-line effect, a strongly stratified transcritical (pseudo-boiling) temperature profile with slightly heated wall is selected. First, we compare linearly and non-linearly forced two-dimensional (2-D) boundary-layers. The latter is characterised by a train of billow structures resembling the Kelvin-Helmholtz instability in shear layers, along with localised flow reversal, which is typical of an adverse streamwise pressure gradient (see Fig. 1). Second, we analyse the three-dimensional (3-D) breakup of the spanwise-oriented billows under high-amplitude 2-D forcing. The near-wall downstream-convected local separation bubbles further destabilise the dominant 2-D mode, amplifying it to high amplitude levels and triggering a rapid fill-up of the spectrum of all 3-D modes. The breakdown of each spanwise roller into fine-scale 3-D structures occurs over an extended streamwise distance before the boundary layer becomes fully turbulent. A detailed analysis of this 3-D transition mechanism will be presented, alongside additional controlled transitional scenarios under varying wall blowing–suction conditions.

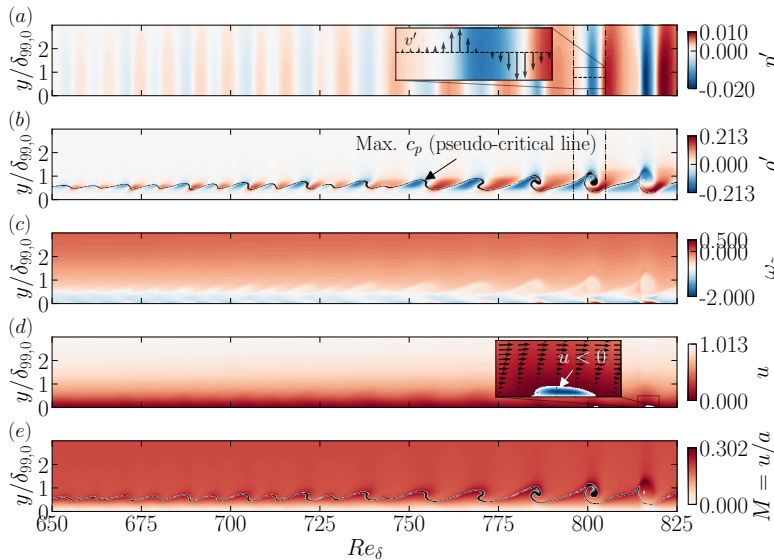


Figure 1: Instantaneous contours of transcritical-heated case with $A_{2-D}^{(1,0)} = 7.5 \times 10^{-3}$: (a) pressure fluctuation p' , (b) density fluctuation ρ' , (c) spanwise vorticity ω_z , (d) streamwise velocity u , and (e) Mach number $M = u/a$. The Widom line $y = y_{WL}$ lies in the black region, i.e. between 95% $\max\{c_p\}$ and $\max\{c_p\}$. In the inset of (a), wall-normal velocity fluctuation v' . In the inset of (d), velocity vectors $|\vec{V}| = \sqrt{u^2 + v^2}$ with separation bubble.

References

- [1] J. Ren, O. Marxen, and R. Pecnik. Boundary-layer stability of supercritical fluids in the vicinity of the Widom line. *J. Fluid Mech.*, 871, 831–864, 2019.
- [2] B. Bugeat, P. C. Boldini, A. M. Hasan, R. Pecnik. Instability in strongly stratified plane Couette flow with application to supercritical fluids. *J. Fluid Mech.*, 984, A31, 2024.
- [3] P. C. Boldini, B. Bugeat, J. W. R. Peeters, M. Kloker, and R. Pecnik. Transient growth in diabatic boundary layers with fluids at supercritical pressure. *Phys. Rev. Fluids*, 9, 083901, 2024.
- [4] P. C. Boldini, R. Gaspar, B. Bugeat, P. Costa, J. W. R. Peeters, and R. Pecnik. Direct numerical simulation of H-type transition in a flat-plate boundary layer with supercritical fluids. *14th International ERCOFTAC Symposium on Engineering Turbulence Modelling and Measurements (ETMM14)*, Barcelona, Spain, September 6-8, 2023.
- [5] P. C. Boldini, R. Hirai, P. Costa, J. W. R. Peeters, and R. Pecnik. CUBENS: A GPU-accelerated high-order solver for wall-bounded flows with non-ideal fluids. *Comput. Phys. Commun.*, 309, 109507, 2025.



FLOW TRANSITION OVER GAPS

Víctor Ballester Ribó¹, Jeffrey Crouch², Yongyun Hwang¹, Spencer Sherwin¹

¹*Department of Aeronautics, Imperial College London, UK*

²*The Boeing Company, USA*

Aircraft wings are not perfectly smooth; they often feature spanwise gaps due to manufacturing tolerances, structural components, or control surface discontinuities. These geometric discontinuities can significantly influence boundary layer transition, potentially affecting aerodynamic performance and efficiency. In this study, we investigate the interaction between such gaps and the transition process, with a particular emphasis on the enhanced amplification of Tollmien-Schlichting (TS) waves and by-pass mechanisms. Specifically, we examine the role of gap-induced modes in triggering or enhancing natural boundary layer instabilities [1]. The analysis is conducted at low Mach number under incompressible flow conditions at a Reynolds number of $Re_{\delta^*} = 1000$, where δ^* denotes the displacement thickness measured at the upstream edge of the gap on a smooth surface that is free of discontinuities. The depth of the gap considered is $d/\delta^* = 4$, while the width is varied within the range $w/\delta^* \in \{10, \dots, 30\}$ to assess the onset of global instability. High-fidelity numerical simulations are performed using the spectral/hp element method implemented in the open-source framework Nektar++ [2]. The results provide new insights into the transition mechanisms induced by geometric discontinuities, contributing to the design of more aerodynamically efficient wings. Future work will extend the study to compressible flow regimes and three-dimensional configurations to account for sweeping effects.

References

- [1] P. J. Schmid, and D. S. Henningson. *Stability and Transition in Shear Flows*. Springer, Berlin, 2001.
- [2] Nektar++. <https://www.nektar.info/>. Accessed: 24/02/2025.

A FAST AND ACCURATE METHOD TO SIMULATE THE EFFECT OF A BUMP ON A TS WAVE

Fernando H. T. Himeno¹, Marcello A. F. Medeiros¹

¹University of Sao Paulo, Sao Carlos, Sao Paulo, Brazil, 13566-590.

The simulation cost can be greatly increased due to the mesh spacing when dealing with very small bumps ($h \lesssim 10\%$ of the local displacement thickness, δ_R^*). Using a high-fidelity simulation code, we were inspired by a similar approach used in receptivity studies [1] but here used in the context in which the bump affects the evolution of a propagating Tollmien-Schlichting (TS) [2]. For the method, the boundary layer profile distorted by a sufficiently small irregularity is modelled by including a non-homogeneous velocity boundary condition at the wall. For the steady flow, the magnitude of the wall velocity components is estimated via Taylor expansion of the smooth case profiles. An unsteady term must be added in the wall velocity condition to cancel out the amplitude of the travelling TS wave at the bump contour. One may also need to consider that the unsteady correction is damped along the normal direction and also takes a time interval to reach the bump top. Based on the solution of well known second Stokes problem we added a correction term in the wall velocity components that finally becomes expressed as,

$$u_{wall}(x, t) = -h_R \underbrace{\frac{\partial \bar{u}_S}{\partial y} \Big|_{y=0}}_{\text{('T')}} - \Re \left\{ \underbrace{\hat{u}'_S \Big|_{TS, y=h_R}}_{\text{('A')}} \underbrace{\exp \left[(1+i) h_R \sqrt{\frac{\omega_{TS} Re_{\delta^*}}{2}} \right]}_{\text{('S')}} \right\}, \quad (1)$$

$$v_{wall}(x, t) = -h_R \frac{\partial \bar{v}_S}{\partial y} \Big|_{y=0} - \Re \left\{ \hat{v}'_S \Big|_{TS, y=h_R} \right\},$$

where ‘T’ indicates the steady term, ‘A’ is the unsteady term needed to cancel out the TS wave amplitude at the bump contour, and ‘S’ the term related to the Stokes problem used to correct the amplitude damping and delay time. Figure 1 compares the approximate approach with the body-fitted bump solution. We also considered repeating the calculation in a second iteration of the method. The agreement of the second iteration case with the body-fitted is remarkable (relative error below 1%). The computational cost was also considerably reduced since the minimum mesh spacing could be increased by a factor of 5 relative to that required to simulate the body-fitted bump.

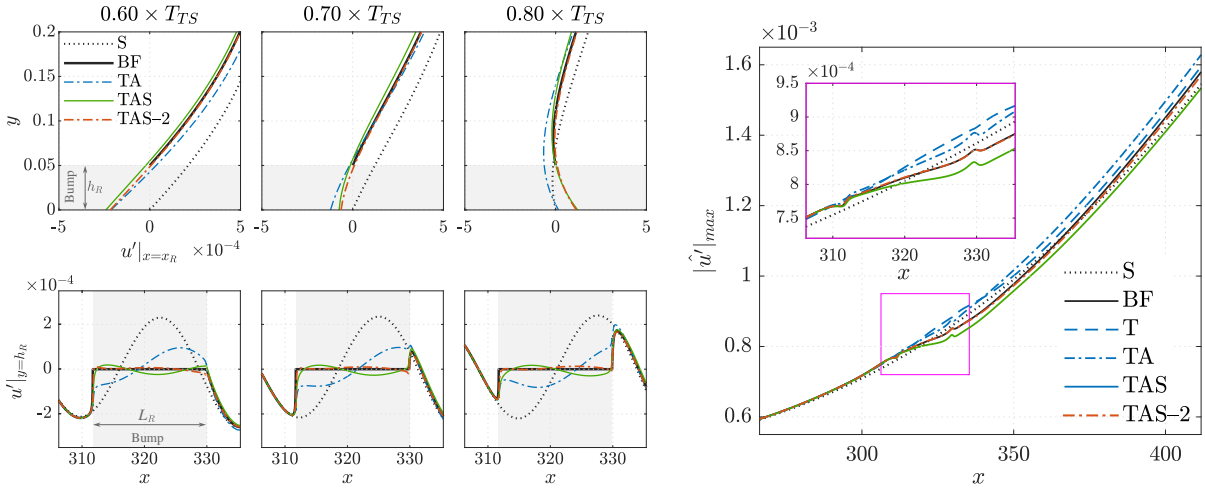


FIGURE 1. Approximated bump compared with body-fitted solution showing the contribution of each term of equation 1. The Reynolds number at the bump center was $Re_{\delta^*} = 950$ and the Mach number was set to $M_\infty = 0.1$. The bump was centered at $x_R = 320.82$ with height $h_R = 0.05$ and length of $L_R = 18.18$, all normalised by δ_R^* . T_{TS} denotes a period of the TS wave which had a non-dimensional frequency of $F = 2\pi f^* \nu^* / U_\infty^2 = 90 \times 10^{-6}$. ‘S’: Smooth, ‘BF’: Body-fitted, while ‘T’, ‘A’ and ‘S’ denote the terms of eq. (1), ‘TAS-2’: ‘TAS’-2nd iteration.

References

- [1] L.-U. Schrader, and L. Brandt, and D. S. Henningson. *Receptivity mechanisms in three-dimensional boundary-layer flows*. *J. Fluid Mech.*, 618:209–241, 2009.
- [2] F. H. T. Himeno, and A. E. B. Carvalho, and M. A. F. Medeiros. *Analyses of Reynolds and Mach number effects on Tollmien-Schlichting wave-bump interaction in subsonic flows*. *J. Fluid Mech.*, 998:A11, 2024.

CROSSFLOW-DOMINATED LAMINAR-TURBULENT TRANSITION DOWNSTREAM OF AN ISOLATED ROUGHNESS ELEMENT OF SMALL HEIGHT

Hans Peter Barth¹, Stefan Hein¹

¹German Aerospace Center, Institute of Aerodynamics and Flow Technology, Department of High Speed Configurations

The effect of an isolated roughness element on laminar-turbulent transition has been thoroughly investigated in the range of roughness Reynolds numbers Re_k for which the laminar-turbulent transition front advances to the immediate vicinity of the isolated roughness, a behaviour often referred to as direct tripping. Experimental studies for this range have been conducted in both two-dimensional (e.g. [1]) and three-dimensional boundary layers (e.g. [2]). Radeztsky et al. [3] showed that roughness elements with Re_k values orders of magnitude smaller can already have a significant impact on the location of laminar-turbulent transition. In this investigation, the effect of an isolated roughness element with a particularly low roughness Reynolds number of $Re_k = 0.55$ (compared to typical critical values for direct tripping of $Re_k \gg 100$ [3]) is studied experimentally in a three-dimensional boundary layer. Detailed spatially scanned hot-wire anemometry measurements are performed in the SPECTRA-B configuration (shown in Fig. 1a, see [4]). The development of steady and unsteady instabilities is characterized in comparison to a reference case without artificial roughness and a case with spanwise-periodic forcing. In Fig. 1b, isocontours of the nondimensional main velocity component u_s in the coordinate system locally aligned with the boundary-layer edge streamline visualize an overview of the three-dimensional steady boundary-layer flow field. The local boundary-layer edge velocity is denoted by q_e . The red curve follows the flow direction at the wall-normal distance of the inflection point in the crossflow velocity component v_s , starting from the chordwise and spanwise location of the isolated roughness element (represented as a black circle). The artificially excited wave packet can be traced downstream across a large portion of the model chord up to the location of the final turbulent breakdown. The final breakdown is significantly advanced relative to the reference case without roughness.

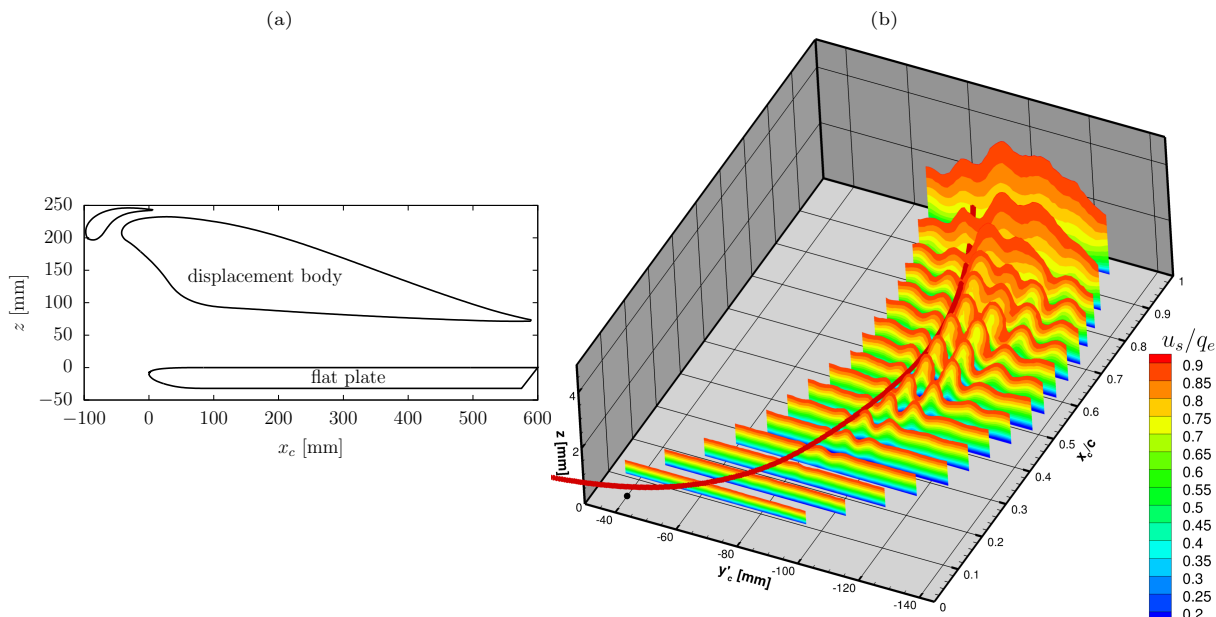


Figure 1: (a) Cross-section of the SPECTRA-B configuration (b) Overview of the steady boundary-layer flow field downstream of the isolated roughness element

References

- [1] P. S. Klebanoff, W. G. Cleveland, and K. D. Tidstrom. On the evolution of a turbulent boundary layer induced by a three-dimensional roughness element. *Journal of Fluid Mechanics*, 237, 101–187, 1992
- [2] G. Zoppini, D. Ragni, and M. Kotsonis. Experimental Investigation of Isolated Roughness Induced Transition in a Swept Wing Boundary Layer. *AIAA SCITECH 2022 Forum*, 2022
- [3] R. H. Radeztsky, M. S. Reibert, and W. S. Saric. Effect of Isolated Micron-Sized Roughness on Transition in Swept-Wing Flows. *AIAA Journal*, 37(11), 1370–1377, 1999
- [4] H. P. Barth, S. Hein, and H. Rosemann. Redesigned Swept Flat-Plate Experiment for Crossflow-Induced Transition Studies. *Notes on Numerical Fluid Mechanics and Multidisciplinary Design*, 155–165, 2017

OPTIMAL PERTURBATIONS IN A BLASIUS BOUNDARY LAYER

Riccardo Bertoncello¹, Alessandro Chiarini¹ and Franco Auteri¹

¹*Dipartimento di Scienze e Tecnologie Aerospaziali, Politecnico di Milano, via La Masa 34, Milano, Italy*

Non-normal growth may induce a transient amplification of finite amplitude perturbations in boundary layers, eventually favouring the bypass transition towards a turbulent regime [1]. Among all the velocity disturbances, the Optimal Perturbations (OP) are able to maximize the energy growth over a finite time horizon and they represent the most threatening flow state which can lead to bypass transition.

The aim of this work is to assess the ability of a spanwise motion of the wall to influence the growth of both linear and non-linear OP in a Blasius boundary layer. Indeed, apart from reducing skin friction drag in turbulent wall-bounded flows [2], the spanwise motion of the wall has also proven the ability to delay the onset of bypass transition in laminar boundary layer flows [3, 4]. However, the physical mechanism for which the wall-forcing is effective at postponing transition is still under debate.

In this work we study how the growth of OP is affected by streamwise travelling waves of spanwise wall velocity i.e. $w(t, x) = A \cos(\kappa x - \omega t)$, where κ and ω are the spatial wavenumber and temporal frequency of the wave, respectively. After fixing a suitable time horizon T , we compare the energy gain $G(T) = E(T)/E(0)$ (where $E(t) = \int_{\Omega} u(t)^2 + v(t)^2 + w(t)^2 d\Omega$; Ω is the volume domain) experienced by the OP with and without the control. Unlike previous studies, we consider a wide portion of the parameter space, varying κ and ω in the range $0 < \kappa \delta^* \leq 2.5$ and $-2 \leq \omega \delta^*/U_{\infty} \leq 2$, where δ^* is the displacement thickness at the inlet section and U_{∞} is the external velocity of the boundary layer. We search for the shape of the OP with an optimization loop consisting of a sequence of direct-adjoint iterations [5]. The employed code is fully three-dimensional and no assumptions on the shape of the perturbations are necessary. As an example of our results, figure 1 shows how the energy gain G and the shape of the linear OP are influenced by κ , when $\omega = 0$. We clearly see that for a suitable choice of κ the energy gain G decreases with respect to the uncontrolled case. Finally, we use Direct Numerical Simulations to describe how OP evolve in a fully non-linear framework. This passage is crucial to observe how the coherent flow structures which are the main characters of the non-normal growth phenomena (i.e. streamwise vortices, streaks and hairpin-like eddies) are altered by the wall actuation.

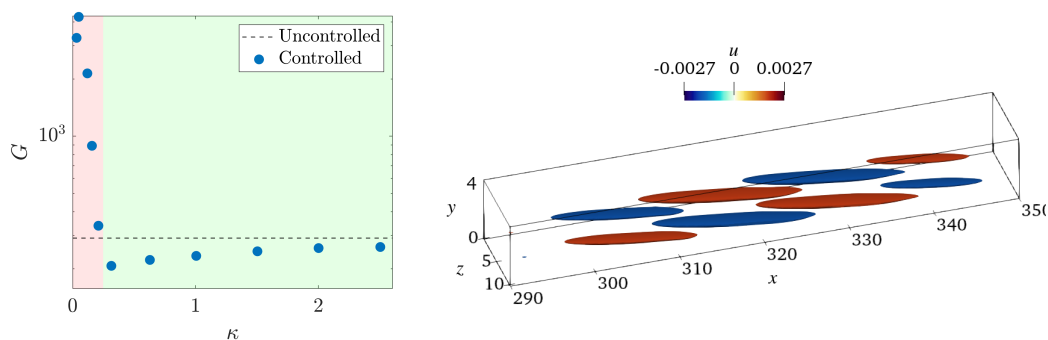


FIGURE 1. Left: Energy gain G of linear optimal perturbations controlled by a steady wall motion, i.e. $\kappa \neq 0$ and $\omega = 0$. Red region: $G(T; \kappa) > G_{uncontrolled}$. Green region: $G(T; \kappa) < G_{uncontrolled}$. Right: Shape of the linear optimal perturbation with $\kappa \approx 1$. Isosurfaces of streamwise perturbation velocity $u = \pm 0.018$.

Acknowledgments: This project has received funding from the European Union's Horizon Europe research and Innovation programme under grant agreement N°101129952.

References

- [1] P. J. Schmid, and D. S. Henningson. *Stability and Transition in Shear Flows*. Springer, Berlin, 2001.
- [2] M. Quadrio, P. Ricco, and C. Viotti. Streamwise-travelling waves of spanwise wall velocity for turbulent drag reduction. *J. Fluid Mech.*, 627:161–178, 2009.
- [3] M. J. P. Hack, and T. A. Zaki. The influence of harmonic wall motion on transitional boundary layers. *J. Fluid Mech.*, 760:63–94, 2014.
- [4] M. J. P. Hack, and T. A. Zaki. Modal and non-modal stability of boundary layers forced by spanwise wall oscillations. *J. Fluid Mech.*, 778:389–427, 2015.
- [5] S. Cherubini, P. De Palma, J.-C. Robinet, and A. Bottaro. The minimal seed of turbulent transition in the boundary layer. *J. Fluid Mech.*, 689:221–253, 2011.

LINEAR STABILITY ANALYSIS OF FREELY FALLING ANNULAR DISKS

P.G. Ledda¹, G. Corsi², G. Vagnoli³, F. Gallaire⁴, A. De Simone^{2,5}

¹DICAAR, University of Cagliari, Cagliari, Italy

²The Biorobotics Institute, Scuola Superiore Sant'Anna, 56127 Pisa, Italy,

³Gran Sasso Science Institute, L'Aquila, 67100, Italy,

⁴LFMI, EPFL, CH-1015 Lausanne, Switzerland,

⁵ MathLab SISSA-International School for Advanced Studies, 34136 Trieste, Italy

We examine the stability of the steady vertical descent and the resulting trajectories of a buoyancy-driven annular disk as the diameter of its central hole varies (Fig. 1a). For small hole diameters, the steady and axisymmetric wake resembles that of a permeable disk, where vortex ring detachment occurs due to flow bleeding through the hole. As the hole enlarges, a secondary vortex ring with opposite vorticity forms at the annulus's inner edge. Further increases in hole size lead to the shrinkage and eventual disappearance of these recirculating regions. These flow modifications influence the stability characteristics of the steady, axisymmetric descent (Fig. 1b).

The coupled fluid-solid problem exhibits a nonmonotonic trend in the critical Reynolds number for destabilization of the steady vertical path, particularly for low disk moment of inertia. However, when the hole diameter exceeds approximately half of the outer disk diameter, the neutral stability threshold rises significantly. The primary instability also changes in nature with hole size, resulting in large (small) amplitude oscillations at intermediate (very small and large) hole diameters (Fig. 1c).

We further present fully nonlinear simulations of the time-dependent dynamics and compare them with linear stability analysis results. Various falling styles—such as steady descent, hula-hoop, fluttering, chaotic motion, and tumbling—emerge as attractors in the nonlinear coupled fluid-structure system. Interestingly, the presence of a central hole does not always decrease the falling Reynolds number; instead, it can drive transitions from tumbling to fluttering, fluttering to hula-hoop, and hula-hoop to steady descent, effectively reducing lateral deviations from the vertical. The observed trajectories and flow patterns align well with predictions from linear stability analysis near the instability threshold (Fig. 1c).

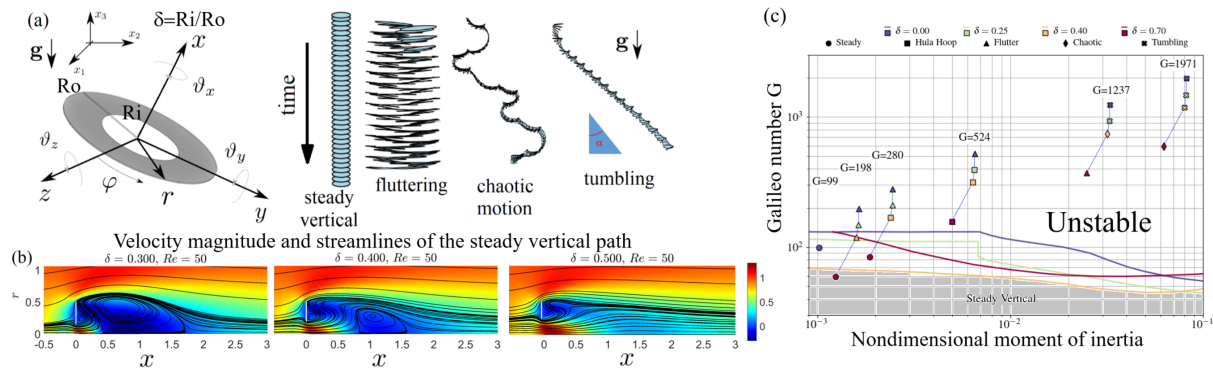


FIGURE 1. (a) Sketch of the freely falling annular disk and trajectories. (b) Velocity magnitude colormaps overlaid with streamlines for increasing values of the hole size and fixed falling velocity. (c) Stability diagram with marginal stability curves for various internal hole sizes (colors) overlaid with results of nonlinear simulations in terms of falling trajectories: steady vertical (circles), hula hoop (squares), flutter (triangles), chaotic (squares), tumbling (crosses).

INTERFACE STABILITY OF A FERROFLUID COATED CHANNEL FLOW SUBJECT TO COLLINEAR MAGNETIC FIELD

Usama M. Zahid¹, Marco Mazzuoli¹, Stefano Brizzolara², Markus Holzner³

¹DICCA, University of Genoa, 16145 Genoa, Italy

²Institute of Science and Technology Austria (ISTA), Klosterneuburg 3400, Austria

³Institute of Hydraulic Engineering and River Research, BOKU University, 1180 Vienna, Austria

Predicting the interfacial stability of a channel flow with the walls coated by a ferrofluid layer is essential for achieving significant drag reduction in applications that encompass a variety of applications from mechanical seals to biomedical devices. More precisely, identifying the conditions that cause interface instabilities can lead to more efficient flow control techniques. In the laminar regime, it was demonstrated by linear stability analysis that interfacial disturbances are suppressed in the presence of a collinear magnetic field [1, 2]. Experimental results of turbulent channel flow with a ferrofluid layer showed that, in the presence of a collinear magnetic field, the interface can also be stable under high-shear conditions and that the interface waves formed, which propagated in the flow direction [3, 4]. These results motivate an extension of the linear stability analysis to turbulent-flow conditions with the objective of reliably predicting the ferrofluid interface stability across laminar and turbulent flow regimes. We carry out the linear stability analysis in the laminar flow conditions by perturbing the Navier-Stokes equations, in order to predict the stability regions of the parameter space and derive dispersion relations for the evolving interface instabilities. Our formulation of the problem in the turbulent flow regime is obtained by replacing the incompressible Navier-Stokes equations with the RANS equations, where an eddy viscosity that varies with the distance from the boundaries is considered. We complement the theory with experiments using an experimental facility that consists of a closed-loop water circulation system in a Plexiglas channel facility, which is equipped with a magnetic field and a two-dimensional particle tracking velocimetry (PTV) system [3, 4]. Accurate flow measurements allowed the exploration of the parameter space and the characterization of the ferrofluid interface dynamics under controlled magnetic field conditions (cf. figure 1). The experimental observations were compared with the predictions of the linear stability analysis, constituting a novel approach that has not been performed in the literature yet, which is ultimately expected to provide new insights into magnetically controlled interfacial dynamics and pave the way for the development of drag reduction and optimised flow control systems.

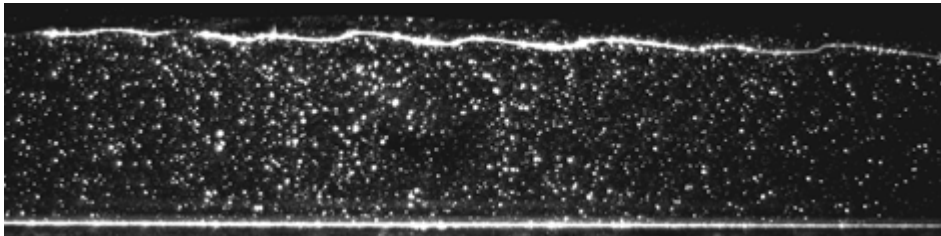


FIGURE 1. Raw image from the PTV recordings showing travelling waves of the interface between ferrofluid (above) and main flow. The bright dots are tracer particles seeded into the diamagnetic fluid (water).

References

- [1] Yecko, P., Stability of layered channel flow of magnetic fluids. *Physics of Fluids*, (21): 034102, 2009.
- [2] Yecko, P., Effect of normal and parallel magnetic fields on the stability of interfacial flows of magnetic fluids in channels. *Physics of Fluids*, (22): 022103, 2010.
- [3] Neamtu-Halic, M. M., Holzner, M., & Stancanelli, L. M., Drag reduction utilizing a wall-attached ferrofluid film in turbulent channel flow. *Journal of Fluid Mechanics*, (7):A35, 2024.
- [4] Stancanelli, L. M., Secchi, E., & Holzner, M., Magnetic fluid film enables almost complete drag reduction across laminar and turbulent flow regimes. *Communications Physics*, 7(1):30, 2024.

COMPETITION BETWEEN DEFORMATION AND DRIFT IN UNIAXIAL STRAINING FLOWS

Aliénor Rivière¹, François Gallaire¹

¹LFMI, Ecole Polytechnique Fédérale de Lausanne, CH-1015, Lausanne, Switzerland

The equilibrium positions of a bubble centered at the stagnation point of an axi-symmetric uniaxial straining flow have been first described by Miksis in 1981 [1], for an inviscid flow. He showed that bubble dynamics undergoes a saddle-node bifurcation, controlled by the ratio between inertial and capillary forces, namely the Weber number We . Below a critical Weber number, We_c , there exist one stable and one unstable equilibrium position. While, above We_c , there is no stable solution anymore and the bubble unconditionally breaks. This transition remains valid in finite Reynolds number flows [2]. However, in practice, the dynamics is richer: first, bubbles can break at sub-critical Weber due to finite amplitude perturbations [4] or random fluctuations of the velocity field, second, bubbles can escape from the stagnation point and avoid breakup. Indeed, Sierra-Ausin et al. [3] showed recently that there exist additional unstable drift modes along the azimuthal and radial directions which will compete with the deformation modes. An illustration of these two behaviors is given in figure 1 (pictures from D. Ruth) which shows a bubble in a turbulent flow, encountering a local flow geometry similar to a uniaxial straining flow. The bubble can either break (1a) or escape (1b) from the uniaxial straining flow.

In this work, we investigate the non-linear bubble deformations and focus on the competition between deformation and drift. To do so, we generalize the recently developed linearized Arbitrary Lagrangian-Eulerian (ALE) approach of Sierra-Ausin et al. [3] to derive amplitude equations controlling bubble fate. These equations help to predict breakup or escape given an initial bubble shape or location. They also help computing breakup statistics under stochastic excitations.

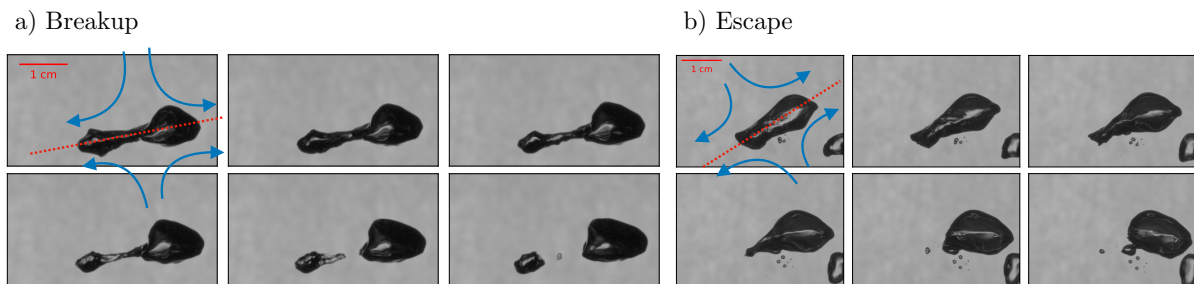


FIGURE 1. *Experimental picture from D.Ruth illustrating the two possible behaviors of a bubble in a local flow similar to a uniaxial straining flow. a) Breakup. b) Escape, here along the straining direction.*

References

- [1] M. Miksis. A bubble in an axially symmetric shear flow *Phys. of Fluids*, (24):1229, 1981.
- [2] I. Kang and L. Leal. Small-amplitude perturbations of shape for a nearly spherical bubble in an inviscid straining flow (steady shapes and oscillatory motion) *J. Fluid Mech.*, 148, 37, 1984.
- [3] J. Sierra-Ausin, P. Bonnefis, A. Tirri, D. Fabre, and J. Magnaudet. Dynamics of a gas bubble in a straining flow: Deformation, oscillations, self-propulsion. *Phys. Rev. Fluids* 7, 113603, 2022.
- [4] A. Rivière, L. Duchemin, C. Josserand, and S. Perrard. Bubble breakup reduced to a one-dimensional nonlinear oscillator *Phys. Rev. Fluids* 8 (9), 094004, 2023.

STABILITY OF QUANTUM FLUIDS WAKES

Niccolò Geracitano¹, Francesco Viola¹, Paolo Antonelli¹, Paolo Luchini², Vincenzo Citro²

¹Gran Sasso Science Institute, Viale Francesco Crispi 7, 67100 L'Aquila, Italy

²Dipartimento di Ingegneria (DIIN), Università degli Studi di Salerno, 84084 Fisciano, Italy

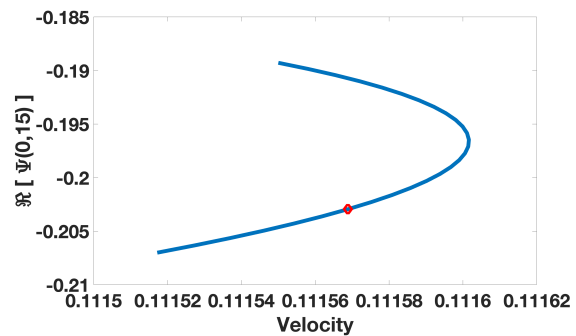
In 1938, it was observed for the first time that Helium II was able to flow without viscosity, a property that led to the choice of the name *superfluid*. The macroscopic behaviour of a superfluid can be described using the Gross-Pitaevskii equation (GPE), where the unknown field is the complex wavefunction $\Psi(\mathbf{x}, t)$. The GPE can be written in a fluid dynamics fashion by seeing the squared modulus of the wave function as the density of the fluid, whereas the gradient of the phase represents its velocity.

The effect of an obstacle moving with constant horizontal velocity inside a superfluid has been the subject of extensive research, both through experimental [1] and numerical [2] means. In the existing literature, the dynamics of the transition from stationary profiles to periodic and then irregular vortex wakes occurring when the velocity is increased has been investigated through direct numerical simulations (DNSs). Based on direct observation of temporal evolution, a preliminary classification of the parameter space has been proposed [2], the most significant parameters being the dimensionless velocity of the system and the diameter of the obstacle. The question of whether this transition can be attributed to an underlying instability is still debated.

In this talk, we propose a novel approach in addressing this challenge by extending stability analysis tools from classical to superfluids. To this aim, firstly a coordinate change from the laboratory frame to the one moving with the obstacle is applied. The system is thus rewritten as a scattering problem, where an incoming carrier wave interacts with the obstacle, and the subsequent wave reflections are collected. Afterwards, having subtracted the incoming wave to the system, we implement an arclength continuation technique to follow the behaviour of the basestate varying the obstacle velocity. We identify a fold in the velocity-basestate curve and we study the structure of the different bifurcations happening along the curve, investigating the effect of the symmetries of the system on it. The evolution of the leading eigenfunctions (see Figure 1) and eigenvalues along the bifurcation diagram will be presented, and a discussion on the limits of the linear analysis near the fold will be given, with comparison to the DNSs results. If time allows, we will share some insight concerning the structural sensitivity of the system.



(a) Density of the unstable mode after the fold.



(b) Fold plot. The red dot indicates the parameters value for the lefthand side plot.

Figure 1: Linear unstable modes.

References

- [1] Y. Lim, Y. Lee, J. Goo, D. Bae and Y. Shin. *Vortex shedding frequency of a moving obstacle in a Bose-Einstein condensate*. *New J. Phys.*, 24 083020, 2022.
- [2] K. Sasaki, N. Suzuki and H. Saito. *Bénard-von Kármán Vortex Street in a Bose-Einstein Condensate*. *Phys. Rev. Lett.*, 104, 150404, 2010.

Author Index

- Alferez, N., 30, 39
Antonelli, P., 58
Antonuzzi, L.D., 29
Auffred, D., 32
Auteri, F., 49, 54
Avanci, M., 30
Ayoub, R., 19
Ballester Ribó, V., 51
Barth, H.P., 53
Beck, P., 22
Ben Hassan Saïdi, I., 25
Bertoncello, R., 49, 54
Bodony, D., 34
Boldini, P.C., 50
Boscagli, L., 24
Boujo, E., 42, 44
Brizzolara, S., 56
Bruce, P., 24
Bugeat, B., 50
Caillaud, C., 26, 27
Cavalleri, A.V.G., 31, 32, 45
Chassaing, J.-C., 33
Chen, Y., 13
Cherubini, S., 48
Chiarini, A., 44, 49, 54
Cinnella, P., 23
Ciola, N., 48
Citra, V., 58
Corsi, G., 55
Cotté, B., 41
Crouch, J., 51
Cruciani, S., 49
Cura, C., 45
d'Eprémesnil, N., 27
David, F., 43
De Palma, P., 48
De Simone, A., 55
Demange, S., 10
Desai, A., 11
Ducimetière, Y.-M., 42
Duguet, Y., 21, 48
Esquieu, S., 26
Forte, M., 16
Fournié, M., 49
Franchini, A., 30, 39
Fuchs, L.M., 35
Gallaire, F., 42, 44, 55, 57
Gaylard, A., 36
Geracitano, N., 58
Gesla, A., 21
Giannetti, F., 28, 29
Glazkov, A., 8
Gowree, E.R., 16
Haller, G., 17
Hanifi, A., 14, 31, 45
Hao, J., 25
Hein, S., 53
Himeno, F.H.T., 52
Holzner, M., 56
Hwang, Y., 51
Janczuk, K., 36
Jaunet, V., 31
Jordan, P., 27, 31, 32
Jouin, A., 41
Kern, J.S., 46
Kloker, M., 50
Knechtel, S.J., 10, 12
Kotsonis, M., 13, 14, 38
Kourta, A., 37
Lagwankar, A., 44
Le Quéré, P., 21
Lebedev, A., 32
Ledda, P.G., 55
Lehnasch, G., 27
Lesshafft, L., 40, 41
Loiseau, J.-C., 46
Luchini, P., 58
Lugrin, M., 26
Lusseyran, F., 11
Maia, I.A., 45
Mancinelli, M., 29, 32
Mantravadi, B., 8
Maranelli, R., 33
Marbona, H., 9
Marquet, O., 40, 41
Martínez-Cava, A., 9
Martini, E., 32
Marxen, O., 24
Mazzuoli, M., 56
Medeiros, M.A.F., 52
Michelis, T., 38
Modesti, D., 13
Moniripiri, M., 14
Mons, V., 33, 41
Morgans, A.S., 36
Müller, J.S., 10, 12
Murthy, S., 34
Oberleithner, K., 10, 12, 35
Olazabal, M., 27
Oulghelou, M., 19
Padovan, A., 34
Pastur, L., 11
Pecnik, R., 50
Peeters, J.W.R., 50
Penet, P., 40
Petrosino, F., 29
Prieto, V., 16
Raibaud, C., 37
Reumerschüssel, J.M., 10
Rigas, G., 24
Ringebach, J.-C., 20
Rist, U., 15
Rius-Vidales, A.F., 14
Rivière, A., 57
Robinet, J.-C., 25, 30, 39, 48
Rodríguez, D., 9
Sayadi, T., 33
Schmid, P.J., 7, 8, 19
Schmidt, O.T., 18
Schneider, T.M., 20, 22
Semeraro, O., 11
Sherwin, S., 51
Sierra-Ausin, J., 28
Song, Z., 25
Steinfurth, B., 35
Synodinos, A.L., 38
Tobias, S.M., 20
Tocquer, M., 37
Vagnoli, G., 55
Valero, E., 9
Viola, F., 58
von Saldern, J.G.R., 35
Weiss, J., 35, 45
Wenzel, C., 15
Witkowski, L.M., 21
Wu, Y., 15
Yim, E., 47
Yuan, Z., 31
Zahid, U.M., 56

